Characterization of the cholinergic system in macaque lateral intraparietal area: An investigation of neuromodulatory compartments in cortex

By

Jennifer Coppola

Dissertation

Submitted to the Faculty of the

Graduate School of Vanderbilt University

in partial fulfillment of the requirements

for the degree of

DOCTOR OF PHILOSOPHY

in

Psychology

August 9, 2019

Nashville, Tennessee

Approved:

Sohee Park, Ph.D.

Anita Disney, Ph.D.

Jon Kaas, Ph.D.

Christine Konradi, Ph.D.

Dedication

This dissertation is dedicated to Dr. Anita Disney, who taught me so much more than good science.

Acknowledgements

I am indebted to the many animal subjects who gave their life to research, without whom this work would not be possible. These include animals over the entirety of my research career, but notably those macaque monkeys who were a part of this dissertation. They are Voxel, Taylor, MTAA7, Aussie, and Bandicoot.

This work was supported through various funding and institutional resources, including NIH grant MH093567 (Anita Disney), the Lisa M. Quesenberry Foundation Scholarship Fund, the Vanderbilt Cell Imaging Shared Resource (supported by NIH grants CA68485, DK20593, DK58404, DK59637 and EY08126), and the Duke Proteomics and Metabolomics Shared Resource.

To my committee, Dr. Sohee Park, Dr. Jon Kaas, and Dr. Christine Konradi, I am thankful for the many years of guidance and support. I have genuinely enjoyed each of my committee meetings and very much appreciate the challenges, thoughtful questions, and interesting insights they have provided.

Many other trainees have contributed in no small part to my research and wellbeing throughout graduate school. Dr. Nick Ward has been a constant source of support and friendship since my first day in the Disney Lab. Dr. Ward never grew tired of my (countless) questions and helped me to navigate the many aspects of graduate student life. I am thankful for his expertise and, importantly, for his kindness. Dr. Juliane Krueger has continuously offered generous support, assistances, and friendship. I am thankful to her for the many conversations she has helped me through and for her constant encouragement and optimism. Corey Roach has been an ideal lab mate and a true friend. Corey openly shares his knowledge and resources—diligently supporting those around him. I am fortunate to have shared my time in graduate school with Corey, and I am thankful for his ongoing friendship. Dr. Kacie Dougherty has been a source of motivation, encouragement, and friendship. Dr. Dougherty has made my time in grad school not only more manageable, but much more enjoyable. It has been a true pleasure to share an office with her.

Finally, I am grateful to Dr. Anita Disney, who has provided me with unending support and encouragement. Dr. Disney has worked meticulously and intentionally to create a space in which her trainees can ask questions, make mistakes, be curious, be wrong, be human beings, and follow their intuitions. Importantly, she has taught me—and continues to teach me—the importance of empiricism, the preciousness of our resources, and the value in having grit. Dr. Disney's ongoing mentorship and guidance have provided me with the curiosity to ask good questions and the confidence to pursue the answers. To her, I am endlessly thankful.

Table of Contents

List of Tables

List of Figures

Chapter 1

Introduction

1.1 Neuromodulation

All nervous systems are subject to neuromodulation. Neuromodulation describes diverse processes by which neuronal activity is regulated through molecular action on neurons and/or their synapses. The result of such processes is alteration of functional circuits. The term neuromodulation broadly encompasses a range of non-classical neural regulation, lending to the complicated nature of defining it. Katz (1999) has described neuromodulation, instead, by what it is not. According to Katz, neuromodulation is any neural communication that is either not fast, not point-to-point, or not simply excitatory or inhibitory. In these ways, neuromodulation provides flexibility to neural networks not possible through classical neurotransmission alone. As such, neuromodulation can be considered a subset—or even along a dynamic spectrum—of neural plasticity, but specifically acting on a short-term timescale and via chemical action onto a neuron. This is opposed to longer term and/or structural changes such as synaptic facilitation and receptor sprouting, commonly associated with the more traditional definition of plasticity.

Understanding neuromodulation is important because it dynamically affects the outputs of behavioral circuitry. The anatomical connectome provides the basic framework for communication through "wired" neural circuits, and evidence from simple model systems demonstrates various ways in which neuromodulatory environments can shape the functional circuits that yield behavior. For example, research from invertebrate systems demonstrates that even the simplest and best-characterized circuits can exhibit complex variation in behavioral outputs through neuromodulatory actions. Neuromodulation can profoundly alter neural communication by modifying such things as intrinsic firing properties and effective synaptic strength between neurons. An example of output alteration by neuromodulators is demonstrated in the crab stomatogastric ganglion. The stomatogastric ganglion is a nervous system within the stomach of crustaceans that produces feeding behaviors and its circuitry is well characterized. Modulatory neurons in this circuit can signal using more than one transmitter, meaning they use a "cotransmitter." In the crab stomatogastric ganglion, three proctolin (a modulatory neuropeptide found in insects and crustaceans)-containing neurons each use a different cotransmitter, and stimulation of each neuron elicits a different motor pattern/rhythm within the same circuit. This demonstrates the ability of neuromodulators to modify behavior, producing different outcomes all within the same circuit described by the connectome. In these ways, neuromodulators dynamically alter how circuit neurons communicate (Marder, 2012).

Beyond invertebrate systems, neuromodulatory signaling has been hypothesized to function broadly, creating a "tone" across large swaths of cortex (e.g. arousal: Jasper and Tessier, 1971). Major neuromodulatory systems include the cholinergic system, the noradrenergic system, the dopaminergic system, and the serotonergic system. Importantly, these systems are believed to participate in non-synaptic "wireless" transmission because their signaling molecules are often released from axonal varicosities that are not associated with any synaptic specialization (Umbriaco et al., 1994; Mrzljak et al., 1995 but see Turrini et al., 2001). Classical synaptic transmission provides one mechanism for chemical signaling between neurons. Non-synaptic transmission, often termed volume transmission, is another method by which cells communicate. This term, introduced by Fuxe and Agnati (1991), describes the diffusion of signaling molecules throughout the extracellular space, beyond the confines of a synapse (Figure 1). This type of communication differs from classical synaptic (point-to-point) transmission (Figure 1A) in that molecules are released from varicosities that are not apposed to a specialized receptive surface (Figure 1B). Under these circumstances, it is often thought

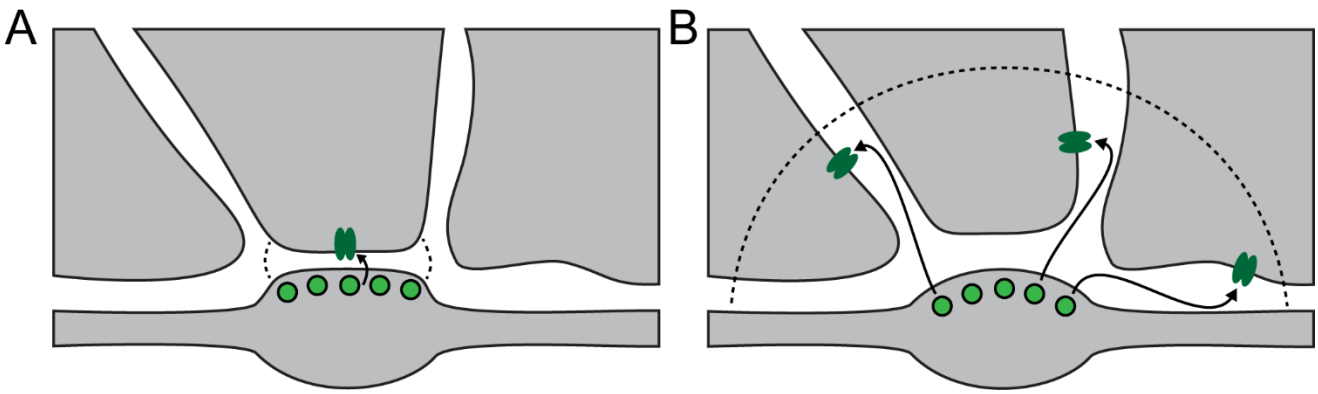

Figure 1: Synaptic versus non-synaptic "volume" transmission
Examples show an axonal varicosity releasing singling molecules. A depicts classical synaptic transmission, in which molecules (light green) released from the varicosity cross the synapse and bind to a receptor (dark green). B depicts the release of molecules into a volume of tissue that diffuse away to bind to nearby receptors. Dashed lines indicate the extent to which molecules will diffuse in each type of transmission. Arrows indicate possible paths of molecular diffusion through the extracellular space toward receptors. Coppola et al., 2016.

that the resulting signal will be both slow and homogeneous over large regions of cortex. This is in contrast to classical synaptic transmission, in which signals are generally assumed to be fast and precise. I have focused my research on neuromodulation imparted by the cholinergic system, as such, the following sections will describe the anatomical and functional characteristics of acetylcholine.

1.2 Acetylcholine: anatomy

Acetylcholine (ACh) is a ubiquitous and well-studied neurotransmitter, best characterized in the peripheral nervous system where it acts as the signaling molecule at the neuromuscular junction. ACh is also present in non-neural tissue such as the heart and the placenta. In fact, ACh likely evolved well before the nervous system itself, as its synthetic and degradative machinery is present even in bacteria, fungi, protozoa, and plants (Semba, 2004). Despite being among the first discovered and presently best studied neurotransmitters, ACh's role in the central nervous system is less well understood, although it is believed to act as a neuromodulator in cortical circuits that support cognition. Specifically, ACh has been implicated in many cognitive processes including learning and memory consolidation (reviewed by Hasselmo and McGaughy, 2004), reward and addiction (Maskos et al., 2005), and the sleep/wake cycle and arousal (Jasper and Tessier, 1971). More commonly, cholinergic modulation is associated with attention (reviewed by Everitt and Robbins, 1997, Sarter et al., 2005). For example, increases in ACh have been shown to preferentially enhance the signal of thalamic inputs to sensory cortices, while also suppressing intracortical retrieval and processing (described below; Hasselmo and Bower, 1992). More simply, ACh enhances sensory input relative to cortical feedback—a circuit effect that has been linked to attention (Hasselmo and McGaughy, 2004).

In all mammalian species studied to date, the cell bodies of cholinergic projection neurons are located in subcortical nuclei of the brainstem and forebrain. Two major clusters of nuclei exist: the brainstem cholinergic system and the basal forebrain. The brainstem system is comprised of the pedunculopontine tegmental nucleus and the laterodorsal pontine tegmentum, which project to the basal ganglia, the thalamus, and the basal forebrain. Alternatively, the basal forebrain provides ACh to all of cortex.

In primates, the basal forebrain is made up of the medial septal nucleus that projects to the hippocampus and entorhinal cortex, the diagonal band of Broca that projects to the hippocampus, entorhinal cortex, and olfactory cortex, and the nucleus basalis/substantia innominata that provides ACh to the rest of cortex and to the amygdala (Mesulam et al., 1983). Neurons whose cell bodies reside in the basal forebrain are the only source of cortical ACh in adult non-human primates (Mesulam et al., 1983). However, cell bodies immunoreactive for the synthetic enzyme choline acetyltransferase have been reported in the cortex of rats (Houser et al., 1983); (Ichikawa and Hirata, 1986), cats (Avendano et al., 1996), and fetal monkeys (Hendry et al., 1987). In primates, the cholinergic projection neurons in the basal forebrain nuclei correspond to partially overlapping cell groups termed Ch1-Ch4 (Rye et al., 1984). The medial septal nucleus corresponds to Ch1, the vertical limb of the diagonal band of Broca to Ch2, the horizontal limb of the diagonal band of Broca to Ch3, and the nucleus basalis/substantia innominata to Ch4. Similarly, the pedunculopontine tegmental nucleus and the laterodorsal pontine tegmentum of the brainstem projection system correspond to Ch5 and Ch6, respectively (Mesulam et al., 1983). There has been some debate regarding the extent to which the "Ch" nomenclature can extend to species beyond primates (i.e. to rodents and carnivores; Butcher and Semba, 1989), as the differentiation of cholinergic nuclei may be more subtle in other species (Gorry, 1963). Generally, however, the Ch1-Ch4 schema is considered applicable across species (Mesulam et al., 1983).

While the "Ch" nomenclature refers exclusively to the cholinergic neurons within the basal forebrain nuclei, it is important to note that other neuron types are present and intermingled with the cholinergic cells. These other populations include γ-aminobutyric acid (GABA)-ergic and glutamatergic neurons (Mesulam et al., 1983; Gritti et al., 1997; Gritti et al., 2006). Interestingly, the proportions of the total neuronal population that each of these subpopulations represents is species-specific and differs between cholinergic nuclei within

species. Mesulam et al. (1983) report the proportion of cholinergic neurons in each of the macaque Ch1-4 nuclei. The variation is striking: 1% cholinergic in Ch3, through ~10% in Ch1, up to 70% and 90% in Ch2 and Ch4, respectively.

In humans, the nucleus basalis (Ch4) alone contains approximately 220,000 neurons per hemisphere (Arendt et al., 1985). When we consider that Ch4 is one of two large nuclei in the basal forebrain (the other being Ch2) this leads to the prediction that there are well over half a million neurons in the human basal forebrain total. Interestingly, Raghanti et al. (2011) report the number of cholinergic neurons in the human nucleus basalis to be between 200,000 and 230,000 per hemisphere, strikingly similar to the estimates for the total neuron number in human nucleus basalis. Accounting for individual variation, this estimate for cholinergic neurons may reflect a finding that in humans—as in macaques—90% of nucleus basalis neurons are cholinergic. The macaque nucleus basalis is estimated to have 90,000 to 120,000 cholinergic neurons (Raghanti et al., 2011).

Cortical projections to the nucleus basalis of the macaque originate in the orbitofrontal cortex, temporal pole, prepyriform cortex, entorhinal cortex, inferotemporal cortex, insula, and prefrontal cortex (Mesulam and Mufson, 1984). Subcortical projections to the nucleus basalis originate in the medial hypothalamus, septal nuclei, nucleus accumbens-ventral pallidum, and the amygdala (Mesulam and Mufson, 1984; Price and Amaral, 1981). Importantly, the nucleus basalis is also the target of extensive input from other neuromodulatory systems—the serotonergic, dopaminergic, and noradrenergic systems (reviewed by Mesulam, 2004a).

Cholinergic projection neurons from the nucleus basalis innervate cortex almost exclusively via unmyelinated axons (Mrzljak et al., 1995) and have been shown to demonstrate a somewhat crude topography in cortex. For instance, Pearson et al. (1983) shows bands of cells within the nucleus basalis correspond to distinct lobes in primates; the frontal, parietal, temporal, and occipital cortices correspond to anterior, posterior, postero-lateral and posterior extension portions of the nucleus basalis, respectively. Further, the projection of individual neurons within the nucleus basalis is limited to no more than 1.5 millimeters in diameter within the rodent cortex (Price and Stern, 1983).

Within these projections, ACh is synthesized in the axon terminals of cholinergic neurons by an enzyme called choline acetyltransferase. Choline acetyltransferase catalyzes the transfer of an acetyl group from acetyl coenzyme A (made in the mitochondria) to choline (from the diet). Once packaged into vesicles by the vesicular ACh transporter, ACh can be released from the cell. Following release, it can bind to a cholinergic receptor, or it can be broken down by acetylcholinesterase. Acetylcholinesterase is an enzyme—membrane bound or freely soluble—that rapidly metabolizes ACh into acetate and choline. The acetate enters the blood and the choline is taken up into the cell via high-affinity choline transporters to be used for further ACh production or to support the turnover of phosphatidylcholine (a phospholipid).

Once ACh is released, the cholinergic system transduces signals through two families of receptors: nicotinic and muscarinic, named for the exogenous ligands to which they are particularly responsive—nicotine and muscarine, respectively. Nicotinic receptors are cation (ionotropic) channels, which mediate a fast depolarization of the receiving cellular membrane. As pentamers (i.e. containing five subunits), they can be characterized by their subunit composition and their relative affinity for nicotine. Heteropentameric nicotinic receptors contain two obligatory α subunits in addition to other subunits, usually β2 in cortex (Gotti et al., 2006; Albuquerque et al., 2009). The only homopentameric nicotinic receptors described so far in mammals comprise five α7 subunits. Homomeric α7 subunit-containing receptors have a low affinity for nicotine, bind the antagonist α-bungarotoxin, and desensitize rapidly. Conversely, heteromeric β2 subunit-containing receptors have a high affinity for nicotine, do not bind α-bungarotoxin, and desensitize slowly.

The muscarinic receptors are metabotropic. They can act via direct channel coupling or through coupling to various intracellular second messenger systems. Five muscarinic receptor subtypes have been identified (m1-m5) and are characterized according to the class of G protein to which they are coupled (reviewed by Gilsbach and Hein, 2008). The m2 and m4 receptors are preferentially coupled to the Gi/o signaling pathway and correspond to the M2 pharmacological class (i.e. they are insensitive to the antagonist pirenzepine; MacIntosh, 1984). These receptors are typically expressed presynaptically and act as autoreceptors—inhibiting adenylyl cyclase activity (Bonner et al., 1988). The m1, m3, and m5 receptors are preferentially coupled to the Gq signaling pathway and correspond to the M1 pharmacological class, although sensitivity to pirenzepine varies within this class. These receptors are more often expressed postsynaptically and activate phospholipase C (Bonner et al., 1988). Importantly, muscarinic receptors vary in their affinity for ACh, with m2 and m4 receptors exhibiting higher affinity for ACh than do m1, m3, and m5 receptors (Kuczewski et al., 2005).

1.3 Acetylcholine: function

The basal forebrain cholinergic system has long been implicated in modulating cognitive processes and brain states through its widespread cortical projections (described above). Early studies in rats that used excitotoxic lesions of basal forebrain nuclei were interpreted as indicating that the cholinergic system is particularly involved in learning and memory (Hepler et al., 1985; Dubois et al., 1985). However, excitotoxic lesions eliminate all cells types within the basal forebrain, and interestingly, cholinergic neurons in the rat—unlike in the primate—represent a minority of basal forebrain neurons (Gritti et al., 2006). Thus, it was realized that attributions of these effects to the cholinergic system had to be treated with caution. The development and use of the cholinergic-specific toxin 192 IgG-saporin (Wiley et al., 1991) revealed that, in rats, lesions that leave non-cholinergic cells intact result in a somewhat different pattern of cognitive deficits. For instance, performance in learning and memory tasks following cholinergic-specific lesions was either unimpaired or not as severely impaired compared to non-specific lesions (Berger-Sweeney et al., 1994; Wenk et al., 1994). This indicates that non-cholinergic cell types within the basal forebrain of rats may contribute more to some processes, such as learning and memory, than do the cholinergic neurons.

While learning and memory appear to be less sensitive to cholinergic depletion, attentional processes are impaired following cholinergic-specific lesions in rats (reviewed by McGaughy et al., 2000). In one study by Waite et al. (1999), the multiple choice reaction time task was used to challenge sustained attention (also referred to as vigilance). Briefly, rats received a food reward by selecting one out of a number of available ports, the correct port having been indicated by brief illumination of a light. Some manipulations to the task were used to increase the "attentional demand" such as changing the time between trials (inter-trial interval variability) and increasing the number of response ports (e.g. from five active ports to nine), making the task more difficult. During times of increased demand, task performance was impaired following cholinergic depletion in rats. This indicates that ACh may have a role in vigilance, especially when the task load is greater. Another study by Bucci et al. (1998) reports depletion of cholinergic innervation to posterior parietal cortex in rats (an area thought to be involved in attentive regulation, discussed below) impairs the ability to increase processing capacity to meet task demands. Here, processing of a visual stimulus (a light) was assessed following manipulation of the predictive relationship between the light and an auditory stimulus (a tone) in relation to a food reward. Rats with depleted cholinergic innervation were impaired at appropriately shifting attention based on the predictive relationships between stimuli compared to control rats. In fact, many studies in rats have demonstrated impairments in vigilance tasks following cholinergic-selective depletion (Turchi and Sarter, 1997; McGaughy and Sarter, 1998; McGaughy et al., 2002). It is important to note here that attention is not a unitary phenomenon and these lesion studies explore a different process (vigilance) than do traditional studies of attention in humans and non-human primates.

In mammals other than rats and mice, ME20.4 IgG-saporin is used to selectively eliminate cholinergic cells. In the marmoset, both excitotoxic and cholinergic-specific lesions to the nucleus basalis resulted in learning impairments (Ridley et al., 1986; Fine et al., 1997). In these studies, subjects were trained to perform a simple visual discrimination task in which the location of a food reward was signified by one of two objects; the object marking the reward location had to be learned over a series of trials. Marmosets with both lesion types were impaired at this task relative to controls. Given that the primate nucleus basalis is at least 90% cholinergic, discussed above, it is not surprising that the two lesion methodologies do not differ in this species as profoundly as they do in rats, where a smaller proportion of basal forebrain cells are cholinergic (5% of all basal forebrain neurons; Gritti et al., 2006). In macaques, a study by Browning et al. (2009) assessed learning and memory following specific cholinergic depletion of the inferotemporal cortex. Here, macaques were trained to identify one of two objects in a complex scene. Identification of the correct object was rewarded with a food pellet (object-in-place scene learning). To assess memory, macaques were trained in a delayed nonmatch-to-sample task. In this task, a sample object is presented briefly then two objects appear, one being the sample object and one being a novel object. Subjects are rewarded with a food pellet for identifying the novel object. Cholinergic depletion did not result in impairments in either task (but see Turchi et al., 2005). Croxson et al. (2011) report no impairment in decision-making or in the object-in-place scene learning task described above, however, spatial working memory was impaired following cholinergic depletion of the prefrontal cortex. The latter was assessed using a spatial delayed response task, which requires subjects to remember the location of a food reward after a delay period. Thus, cholinergic depletion in macaques impairs spatial working memory. Macaques who have undergone non-selective excitotoxic lesions showed impaired memory in the delayed nonmatch-to-sample task (described above as unimpaired by selective cholinotoxic lesions of cortex), however, the impairment follows combined lesions to the nucleus basalis, medial septal nuclei, and diagonal band of Broca (Aigner et al., 1991). Lesions to the nucleus basalis alone (or any of the cholinergic nuclei in isolation) did not result in any impairment.

It has also extensively been proposed that ACh facilitates attentive processes in sensory cortices. A suggested model for this facilitation is the simultaneous enhancement of a sensory input and suppression of intrinsic cortical activation (Hasselmo and Giocomo, 2006), which is based primarily on pharmacological studies in rodent sensory cortex (Hasselmo and Bower, 1992; Gil et al., 1997; Kimura et al., 1999; Hsieh et al., 2000). Nicotinic receptors expressed presynaptically by thalamic terminals are thought to increase the gain of incoming sensory data (Disney et al., 2007). Many studies have described a population of nicotinic receptors in the input layer of a number of thalamic recipient cortical areas across species including rat, cat, and primate (Clarke et al., 1984; London et al., 1985; Prusky et al., 1987; Lavine et al., 1997; Disney et al., 2007; Eickhoff et al., 2007). These receptors were found located on terminals from thalamic nuclei innervating sensory (Prusky et al., 1987; Lavine et al., 1997; Disney et al., 2007), motor (Lavine et al., 1997), and association (Lavine et al., 1997) cortical areas. The suppression of intracortical pathways in the rodent studies listed above has been attributed to a reduction in glutamate release through activation of m2 muscarinic receptors expressed on the axons of excitatory neurons (Hasselmo and McGaughy, 2004). However, another suppressive mechanism has been proposed for primates. In macaque primary visual area V1, cholinergic suppression of visual responses was shown to be mediated by a strengthening of inhibition (Disney et al., 2012). Here, suppression by ACh is mediated by an increase in GABA release (as opposed to the reduction in glutamate release observed in rats).

Interestingly, Soma et al. (2012) report a predominant enhancement by ACh (in contrast to the dominant suppression observed by Disney et al., 2012) mediated by muscarinic receptor activation, although both studies report both suppression and enhancement. The difference between these studies is not clear but may be attributable to the concentration dependence of ACh effects or sampling bias in recording. Concentration-dependent effects can result from differing affinities of muscarinic receptor subtypes (discussed above; Kuczewski et al., 2005; Disney et al., 2012). Both of these studies were conducted under anesthesia and basal levels of ACh in cortex may differ if the maintained depth of anesthesia differed. Further, differences in ejection barrel geometry and applied iontophoretic currents will yield different levels of delivered drug above that basal

level. These factors can combine to activate different populations of receptors for subtly different experimental conditions. Neither study reported the proportion of interneurons in their recorded population, but given the anatomy of macaque primary visual area V1, a recording bias towards excitatory neurons will also yield a higher proportion of suppression, and a recording bias towards interneurons would yield more apparent enhancement. It is important to note that across the population of neurons in V1, in all species studied, both enhancement and suppression are observed with cholinergic activation *in vivo*. What may differ between species and with methodology is the proportion of excitatory versus suppressive effects, and perhaps the mechanism underlying the suppression, when observed (Sillito and Kemp, 1983; Sato et al., 1987; Muller and Singer, 1989; Murphy and Sillito, 1991; Zinke et al., 2006; Disney et al., 2007; Herrero et al., 2008; Disney et al., 2012; Soma et al., 2012).

In macaques and humans, there have been functional demonstrations of ACh enhancing sensory input relative to intrinsic cortical activity. One study in macaque V1 shows that administration of nicotine (a ligand for nicotinic receptors) improves contrast sensitivity (Disney et al., 2007) for V1 neurons. Here, anesthetized macaques were presented drift-grating stimuli of multiple contrasts with or without iontophoretic application of nicotine in V1. Physiological recordings reveal that in the presence of nicotine, cells in the input layer 4c produced reliable responses to lower-contrast stimuli, indicating that low-contrast detection is improved with nicotine. Similarly, in humans, cholinergic enhancement has been shown to increase signal detection. In a study by Boucart et al. (2015), participants engaged in a two alternative forced choice task in which they are shown two pictures of natural scenes, one of which contains an animal (the target). Participants must indicate which picture contains the target under varying levels of contrast. Before the task, participants were given either a placebo or the drug donepezil. Donepezil limits ACh degradation by inhibiting the ACh metabolizing enzyme acetylcholinesterase, thereby enhancing cholinergic transmission. In the presence of donepezil, signal detection of the target was facilitated. Of course, with systemic drug delivery such as this, there is no way to determine where in the brain the nicotine is acting to produce this behavioral effect. Further data would be needed to assign nicotine's actions to the increased gain at the input to cortex.

Beyond the input layer, a decrease in receptive field size and a reduced spread of excitation have been proposed as measurable consequence of suppressing lateral cortical interaction. This is because the size of a receptive field center is thought to be largely determined by inputs arising from the thalamus, while the receptive field surround is provided by lateral and feedback connectivity within cortex (Angelucci and Bressloff, 2006). Silver et al. (2008) report cholinergic enhancement suppresses the spread of excitation in human V1. In this study, subjects passively viewed high-contrast/contrast-reversing checkerboards interspersed with a blank gray screen, while maintaining fixation on a central point. Positive blood-oxygen-level dependent (BOLD) responses to the checkerboard stimulus relative to baseline (the gray screen) were observed by functional magnetic resonance imaging (fMRI). Prior to fMRI sessions, subjects ingested either a placebo or donepezil (described above). Donepezil administration resulted in a positive BOLD response to stimuli that occupied less cortical surface area compared to placebo. This indicates cholinergic enhancement reduces the spatial spread of excitation. Similar effects have been observed in non-human primates. In a study by Roberts et al. (2005), length tuning of V1 neurons to bar stimuli was studied with and without iontophoretic application of ACh. In the presence of ACh, the neurons' preferred stimulus length shifted toward shorter bars. This phenomenon was modeled as a reduction in the summation area of the neurons' receptive fields, again consistent with a suppressive effect of cortical ACh release.

As described earlier, the suggested mechanism for ACh's facilitation of vigilance is the simultaneous enhancement of a sensory input and suppression of intrinsic cortical activation. To date, only one study has used a true focal attention task to investigate the local effects of ACh in the cortex of an awake, behaving primate (Herrero et al., 2008). Here, recordings were made in macaque V1 during performance of a cued contrast change detection task. In the task, macaques must maintain fixation at a central point and detect a luminance change at a cued location (target) while ignoring a luminance change in a non-cued location (distractor). The

results showed the expected increase in the firing rate of V1 neurons when a target is detected in their receptive fields, that is, when the target is "attended to." Further, they demonstrate that V1 neurons showed a greater attentional modulation during application of ACh. These effects were also shown to be the result of muscarinic receptor activation, as the muscarinic antagonist scopolamine reduced the attentional enhancement, while nicotinic antagonists had no effect on attentional modulation. This study provides clear evidence that ACh is involved in some form of attentive processing that goes beyond vigilance in showing differences in the attend-to versus attend-away conditions.

While much of the cholinergic research discussed so far has been focused in visual cortex, my own research aims to understand ACh's actions beyond the striate cortex in the lateral intraparietal area (LIP). LIP is located in the intraparietal sulcus of the parietal lobe and is thought to play a role in attentional prioritization by guiding visual attention and saccadic eye movements; however, it is relatively unstudied in terms of anatomy and of dynamic and modulatory influences. The cholinergic basal forebrain innervates the posterior parietal cortex, and thus LIP (Mesulam et al., 1983; Kitt et al., 1987). Cholinergic modulation is particularly interesting in this context because LIP has been implicated in visual attention and because, as discussed above, many studies link ACh with attentive processes.

1.4 Lateral intraparietal area

Considered a visuomotor area, LIP is defined by its connections with visual, oculomotor, and prefrontal areas (Blatt et al., 1990; Lewis and Van Essen, 2000a). Specifically, it receives visual input from a number of areas including visual areas V2, V3, V3a, V4, and middle temporal area MT. Likewise, it maintains reciprocal connections with the frontal eye fields of the frontal lobe as well as projections to the superior colliculus (Blatt et al., 1990; Lewis and Van Essen, 2000a). This region also receives thalamic inputs from both the lateral and medial pulvinar nucleus (Hardy and Lynch, 1992) and the mediodorsal nuclei (Schmahmann and Pandya, 1990). LIP is retinotopic in organization, with visual receptive fields typically confined to one contralateral quadrant of the visual field (Hamed et al., 2001). Contrary to its common designation as a single region, LIP is made up of two subregions: LIP dorsal (LIPd) and LIP ventral (LIPv). These regions can be distinguished—from each other and from surrounding cortical areas—based on myelination, connectivity, and immunohistochemistry. LIPd is lightly myelinated with two distinct inner and outer bands of Baillarger, with light to medium reactivity to SMI-32 (the nonphosphorylated neurofilament H protein); LIPv is densely myelinated with more ambiguous inner and outer bands of Baillarger and denser SMI-32 reactivity. LIPd has stronger connections to visual area V4, area TEa, and the temporal parietal occipital area (among others), while LIPv has stronger connections to visual area V3, posterior intraparietal area, and the parietal-occipital area (Lewis and Van Essen, 2000b).

While anatomically distinct, it remains to be determined the extent to which LIP subregions are functionally separate, although evidence suggests they have distinct roles. In a study by Liu et al. (2010) the GABAa agonist muscimol was injected into different portions of LIP to characterize the reversible effects of inactivation. They found that LIPd may be responsible for oculomotor planning (specifically restricted to guiding saccadic eye movements), while LIPv may be more broadly responsible for both oculomotor planning and mechanisms of visual attention, such as visual search. LIP as a whole has been argued to act as a "priority map" using bottom-up stimulus information and top-down input—such as stimulus importance and expected reward—to guide attention. In macaques engaged in a visual search task, three distinct signals were observed in the activity of LIP neurons. The first was a visual response to the onset of a stimulus, indiscriminate of whether the stimulus was a target or a distractor in the task. This was followed by a pre-saccadic signal (i.e. the choice of a saccadic goal), and finally by a cognitive signal. The cognitive signal was greater in response to a target than to a distractor, indicating it was not simply an undifferentiated visual response and was also not found to be a pre-saccadic signal. Thus, it was considered a top-down signal associated with task-relevant information. By summing these sensory, motor, and cognitive signals, LIP is hypothesized to prioritize different parts of the

visual field. Visual and oculomotor areas—which exhibit strong connections to LIP—may then access the map created by LIP to plan saccades and allocate visual attention (Ipata et al., 2009). Consistent with this idea, the responses of LIP are not stereotyped and seem to depend on task relevant information (Gottlieb and Snyder, 2010).

1.5 Dissertation outline

In the preceding sections, I have introduced the broad concept of neuromodulation, discussed one such neuromodulator (ACh), and described the anatomy and function of the cholinergic system. Beyond that, I have introduced an interesting—especially in the context of attentional modulation—cortical area (LIP) in which ACh can be studied as a foundation for the experiments described in the coming chapters. This dissertation characterizes the cholinergic system in macaque LIP by exploring four key features: receptor expression, synthesis, degradation, and extracellular ACh levels *in vivo*. In Chapter 2, I will describe ACh receptor expression and distribution across cortical layers in macaque LIPd and LIPv by cell type. In Chapter 3, I will discuss the density and expression of the cholinergic synthetic and break-down enzymes. In Chapter 4, I will provide measurements of the local cholinergic tone in posterior parietal cortex of an awake, behaving macaque. Following the presentation of these data, I will introduce our hypothesis of neuromodulatory compartments in primate cortex (Chapter 5). It is my goal to provide evidence for the existence of compartments based on extant literature as well as my own data presented herein. Finally, this dissertation will conclude with a discussion (Chapter 6) providing a general summary, describing caveats and future directions, and touching upon the broader impacts of this research.

An important component of this work is the comparison of the cholinergic system across cortical areas. In particular, V1 of the macaque has been studied extensively and there are rich data to describe its circuitry. Importantly, similar methods have been deployed to characterize V1 (Disney et al., 2006; Disney and Reynolds, 2014) as are described here. Beyond this, the LIP/V1 comparison is also interesting because a recent study from our lab—Ward et al. (in preparation)—suggests visual (occipital) and sensorimotor (parietal) areas comprise separate neurochemical groupings. As such, having comparable anatomical data as well as *in vivo* microdialysis from two possibly distinct regions could provide insight to the functional roles carried out by ACh in primate cortex.

Chapter 2

Quantification of acetylcholine receptor expression and distribution in macaque LIP

2.1 Introduction

In a system that signals mostly through non-synaptic, volume transmission (see Chapter 1), a detailed mapping of receptors and the cell types by which they are expressed is a critical step in understanding the subsequent circuit effects in cortex. One means of characterizing cell types is through their primary neurotransmitter substance, usually either GABA (inhibitory)—which accounts for 25% of the neuronal population in cortex (Hendry et al., 1987)—or glutamate (excitatory; DeFelipe, 1993). Indeed, the downstream effects of a signaling molecule binding to an inhibitory neuron would likely be very different from that same molecule binding to an excitatory neuron. As such, knowing the proportions of excitatory and inhibitory neurons that express cholinergic receptors is an important starting point in gaining insight to ACh's actions across cortex.

As mentioned above, the cholinergic system transduces signals through the nicotinic and muscarinic receptor families, with the nicotinic receptors being ionotropic and muscarinic being metabotropic. My research focuses on the muscarinic receptors. In the mammalian cortex, the m1 muscarinic subtype is the most commonly expressed of all cholinergic receptors (Mesulam, 2004a). In humans, anywhere from 35-60% of all cholinergic receptors is m1; in the parietal cortex in particular—where LIP is located—that number is approximately 40%, with the other muscarinic receptors combined making up ~60% (Flynn et al., 1995). The m1 subtype is preferentially coupled to the Gq signaling pathway and corresponds to the M1 pharmacological class. These receptors are more often expressed postsynaptically and their activation results in an increase in spike rate. Being metabotropic, m1 receptors (m1AChRs) can activate a broad range of signaling pathways. These can include activation of phospholipase C and mitogen-activated protein kinases (MAPKs), as well as direct modulation of ion channels (reviewed by Volpicelli and Levey, 2004). As the predominant muscarinic cholinergic receptor in the primate brain, I have investigated expression of the m1 receptor in macaque LIP.

Specifically, I used immunofluorescence to localize and quantify the distribution of m1AChRs across cell type and laminar position in macaque LIP. To distinguish receptor expression by cell type, I dual-labeled neurons for both the m1AChR and for GABA. Using this method, receptors that are labeled on somata immunoreactive for GABA will provide a measure of the proportion of those receptors that are expressed by inhibitory cells. Those receptor-expressing neurons that are not immunoreactive for GABA I have assumed to be not inhibitory, and therefore excitatory. In the reverse, I have measured the proportion of GABAergic cells that expressed an m1 receptor, providing the degree to which inhibitory cells are receptive to the cholinergic system. I have quantified and localized these cells separately for LIPd and LIPv and for each of the six cortical layers, such that laminar patterns of expression can also be observed. Following these quantifications, I compare my results to data from macaque V1, as those data are detailed and have been obtained using similar methods to those described here.

2.2 Materials and methods

2.2a Animals

Three adult, male, rhesus macaque monkeys (*Macaca mullata*) were used in this study. Appendix A provides details for all animals used throughout this dissertation and each animal has been numbered using a uniform schema. Those used in this study were Animals 2, 4, and 5. All procedures were approved by the Institutional Animal Care Committee and performed in accordance with National Institutes of Health and institutional guidelines for the care and use of animals.

2.2b Histological preparations

Animals were euthanized by intravenous injection of sodium pentobarbital (60 mg/kg). Following the abolition of the pedal and corneal reflexes, animals were transcardially perfused with 0.01 M phosphate-buffered saline (PBS, pH 7.4) followed by 4 L of chilled 4% paraformaldehyde (PFA) with 0.15% glutaraldehyde in 0.1 M phosphate buffer (PB, pH 7.4). For two of the three animals (Animals 4 and 5), 5-20% sucrose in PB was perfused following the fixative. The addition of sucrose in these steps was to reduce the time needed between brain removal and tissue sectioning. Following perfusions, for all animals, the brain was then removed and blocked as necessary to provide donor laboratories with tissue for their needs. The remaining tissue was postfixed 4 hours-overnight at 4°C in 4% PFA. Following the postfix, the brain was transferred to 30% sucrose in PB and stored at 4º C until it sank.

Hemispheres to be sectioned from these brains were blocked in approximately the coronal plane just posterior to the central sulcus. The tissue from these blocks was sectioned at a thickness of 50 μm on a freezing microtome and reacted for 30 minutes in 1% sodium borohydride in PB. Sections were then rinsed in PB. Two 1-in-6 series of sections were set aside to provide reference sections for determining laminar and areal boundaries (Nissl and Gallyas silver stains). Remaining sections were stored at 4°C in PBS with 0.05% sodium azide.

For this experiment, I used three tissue sections, each containing LIPd and LIPv, from each of the three animals (nine sections total). I used systematic random sampling to select the tissue sections and aimed to collect sections that spanned the full extent of LIP. Before immunolabeling, I improved tissue permeability using a "freeze-thaw" method (Wouterlood and Jorritsma-Byham, 1993). First, I cryoprotected the tissue in 10-minute washes of 5-20% dimethylsulfoxide (DMSO). Then, I moved the tissue through eight quick cycles of repeated freezing (with cooled 2-Methylbutane) and thawing (with fresh 20% DMSO). Following these cycles, I rinsed the tissue in PBS. To immunolabel, I blocked the tissue in 1% IgG-free bovine serum albumin (BSA, Jackson ImmunoResearch) in PBS with 0.1% Tween 20 (PBSt, Sigma) for 1 hour on a shaker at room temperature. Following the block, I diluted both primary antibodies (anti-GABA and anti-m1) in the blocking solution and incubated the tissue for 3 days on a shaker at room temperature. Detailed antibody information for all experiments in this dissertation is provided in Appendix B. All primary antibodies have been previously characterized and have passed controls for use in macaques by Western blotting and/or preadsorption. Following the primary antibody incubation, I rinsed sections in PBSt 3 x 15 minutes. Then, I diluted fluorophore-conjugated secondary antibodies in blocking solution and incubated tissue for 4 hours on a shaker at room temperature with minimal exposure to light. Again, secondary antibody information is provided in Appendix B. All secondary antibodies underwent and passed a "no primary control" in which sections were processed according to this protocol, but without the addition of any primary antibody. This procedure revealed a detectable background but that was sufficiently distinguishable from the primary-produced signal. Following the secondary incubation, I rinsed the sections in PBSt 5 x 15 minutes with minimal exposure to light. Then, I mounted the sections on subbed slides to dry overnight in the dark before dehydrating and coverslipping.

2.2c Confocal microscopy

I imaged dual-immunolabeled tissue using a Zeiss LSM 880 confocal microscope driven by Zeiss ZEN imaging software (Carl Zeiss AG, Oberkochen, Germany). For fluorophore excitation, I used the 405 and 633 nm laser lines corresponding to the 405 and 647 fluorescent labels, respectively (the secondary fluorophores, Appendix B). The 405 laser power was 2%, and the 633 laser power was 20%. I used a pinhole of 66.1 µm to collect data from both channels concurrently. To determine the appropriate imaging depth within the tissue, I collected "z-stacks" spanning the entire section thickness just below the pial surface (i.e. in the upper portion of cortical layer 2) and above the white matter (i.e. in the lower portion of cortical layer 6) in the same cortical column at 63x magnification (oil immersion). Using these z-stacks, I chose a single imaging plane at which to capture a "tilescan." Each tilescan represents an approximately 270 µm-wide column of tissue that spans the cortex from pia to white matter collected at 63x (oil immersion) with 4x averaging. I collected two tilescans per tissue section (one for LIPd and one for LIPv) and stored images for offline analysis.

2.2d Defining architectonic boundaries

To identify area LIP, I used reference sections (adjacent to each immunolabeled section) that had been stained to visualize myelin according to the Gallyas (silver) method (Gallyas, 1970). LIP is located on the lateral bank of the intraparietal sulcus of the posterior parietal cortex and is characterized by heavy myelination that has a matted appearance (LIPv) and a lighter degree of myelination in which two distinct bands are present (LIPd) (Figure 2-1). I referred to atlases (Paxinos et al., 2000a; Saleem and Logothetis, 2012) and published data (Pandya and Seltzer, 1980; Blatt et al., 1990; Lewis and Van Essen, 2000b) alongside the Gallyas reference sections to identify areal borders. For each immunolabeled section, I referred to an adjacent Nissl (cresyl violet) reference section to identify laminar boundaries (Figure 2-2A and 2-2D). I captured Nissl reference images using a Carl Zeiss Axio Imager M2 light microscope with a 63x objective (oil immersion). I coregistered the light and fluorescence images using fiduciary marks such as pial surface shape, structural morphology, blood vessels, and cutting artifacts. To correct for differences in tissue shrinkage arising from differences in the Nissl and immunofluorescent tissue processing protocols, I measured the distance from the pial surface to the layer 2/3 border (defined by a sharp increase in cell density) and compared between each Nissl and tilescan image using Adobe Photoshop CS6 (San Jose, CA). I evaluated distances from the pial surface to each layer boundary on the Nissl section and converted to the distance for the corresponding tilescan. I added laminar boundaries to tilescan images before quantification.

2.2e Cell counting

My goal was to determine the proportion of GABA-immunoreactive (ir) neurons that express the m1AChR and the proportion of m1-expressing neurons that is GABAergic. Because I am interested in investigating proportional data, and not in estimating absolute cell numbers, I used a non-stereological counting method. I quantified immunolabeled cell bodies manually using Adobe Photoshop. First, I isolated each data channel (blue for m1 and red for GABA) and counted labeled cell bodies from each population in grayscale. My counting criterion included wholly visible cell bodies with roughly 75% of the membrane in focus (determined qualitatively). I did not count cell bodies that touched the left boundary of the image or a laminar boundary line. In each isolated channel, I marked immunolabeled cells that met these counting criteria with shapes that

Figure 2-1: Lateral intraparietal area location
Gallyas-stained coronal sections from macaque right hemisphere. Black bars mark approximate areal boundaries for ventral lateral intraparietal area (closest to the fundus) and dorsal lateral intraparietal area (closest to the brain surface). Sections are ordered from posterior (left) to anterior (right). Scale bar = 1 mm.

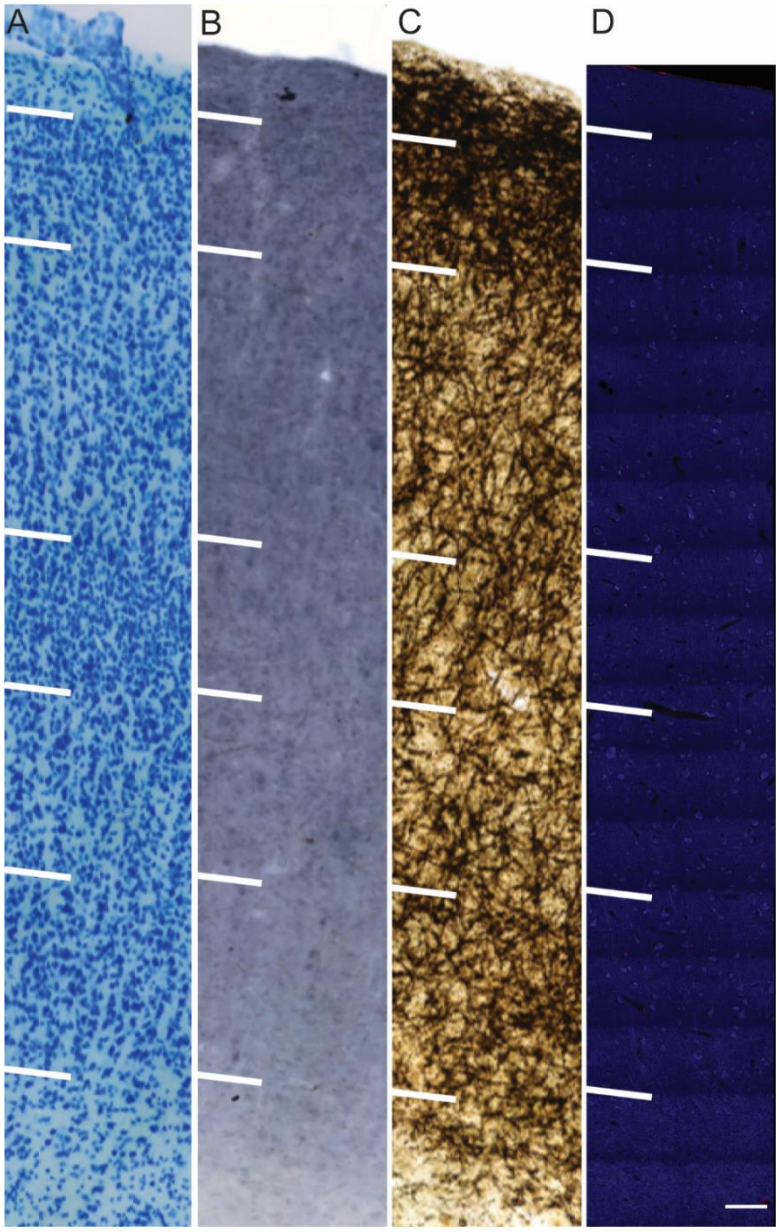

Figure 2-2: Laminar boundaries
Panels of macaque tissue stained for Nissl (A), choline acetyltransferase (B), acetylcholinesterase (C), and the m1 acetylcholine receptor and γ-aminobutyric acid (GABA; D) from pial surface (top) to white matter (bottom). White bars mark layer boundaries. Scale bar = 50 μm.

reflected the size of the cell body in a separate Photoshop image layer. To quantify dual-labeled cells, I marked the overlap of their shape markers (Figure 2-3).

2.2f Analysis

I used ANOVAs and t-tests as appropriate to assess the significance of observed differences in my cell quantification data. Comparisons between animals, layers, and subregions (LIPd versus LIPv) revealed no significant differences proportions of receptor expression ($p > 0.05$). As such, analyses are collapsed across all data.

2.3 Results

I quantified dual-immunofluorescence to determine the extent to which coexpression occurs within the m1AChR and GABA populations. Altogether, I counted 4,880 cells in an approximate area of 9.7 mm^2 across three animals. Most of the immunoreactive cells were located in the middle layers, specifically layer 3 (which is also the largest layer in LIP), and sometimes layers 2 and 4 as well. The fewest number of immunoreactive cells was located in layer 1, usually followed by layer 6.

2.3a m1AChR expression by GABAergic cells

In LIPd, 76% of GABAergic cells expresses the m1AChR (Figure 2-4). Similarly, 74% of GABAergic cells in LIPv expresses the m1AChR (Figure 2-5). Because we know that GABAergic neurons account for 25% of the total neuronal population in cortex (Hendry et al., 1987), we can calculate that the m1AChR-expressing GABAergic neurons account for approximately 19% of all neurons in LIP. The smallest proportion of dual-labeled cells in both LIPd and LIPv was found in layer 1. Cell expression in this layer in particular is quite variable due to the small number of cells present here. For example, in some cases there may be as few as two cells in layer 1, but both are dual-labeled resulting in a proportion of 100% m1AChR/GABA coexpression for that layer. On the other hand, two cells may be present, but neither of them is dual-labeled, resulting in 0% coexpression. As such, the averaged proportions for dual-labeled cells in layer 1 is generally lower with a higher degree of variability. The remaining layers are more uniformly distributed.

2.3b GABA expression by m1AChR-ir cells

In LIPd, 48% of m1AChR-ir neurons was GABAergic (Figure 2-6). This is similar to LIPv, where that number is 52% (Figure 2-7). As such, about half of the neurons expressing the m1AChR is inhibitory, the other half being putatively excitatory. Because, as discussed in the preceding section, we determined that 19% of cells in LIP were m1-expressing inhibitory cells, and because we see here that this proportion makes up half of the 40% of neurons in LIP expresses m1, half being inhibitory and half being excitatory. It follows, then, that about 25% of excitatory neurons in LIP expresses m1AChR.

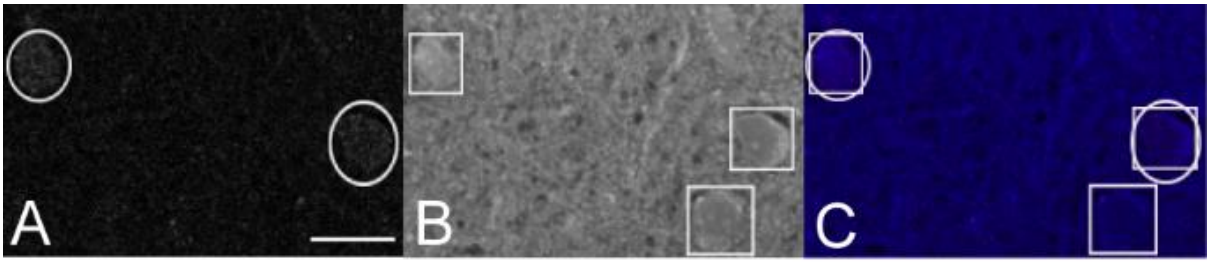

Figure 2-3: Dual-immunofluorescence quantification
Immunofluorescent tissue imaged at 63x magnification (oil immersion) for GABA (A, red), m1 acetylcholine receptor (B, blue), and merged (C). Circles mark cells counted as being immunoreactive for GABA. Squares mark cells counted as being immunoreactive for m1. The overlap of circles and squares marks cells counted as being dual-labeled. Scale bar = 10 μm.

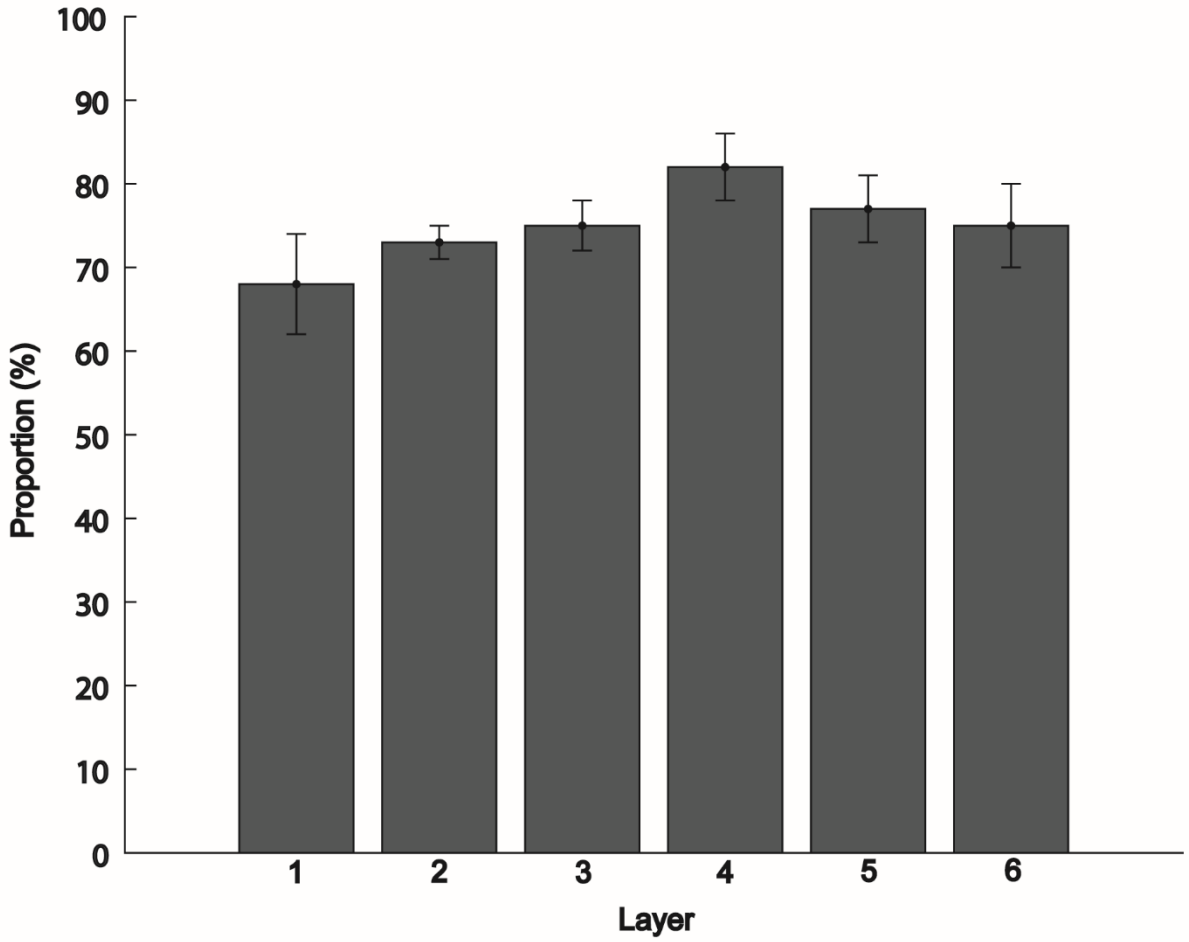

Figure 2-4: m1AChR expression by GABAergic cells in LIPd
Proportion (%) of GABAergic cells that expresses the m1 acetylcholine receptor across cortical layers 1-6 in dorsal lateral intraparietal area. An average of 76% of GABAergic cells expresses the m1 receptor. Error bars = 2x standard error of the mean.

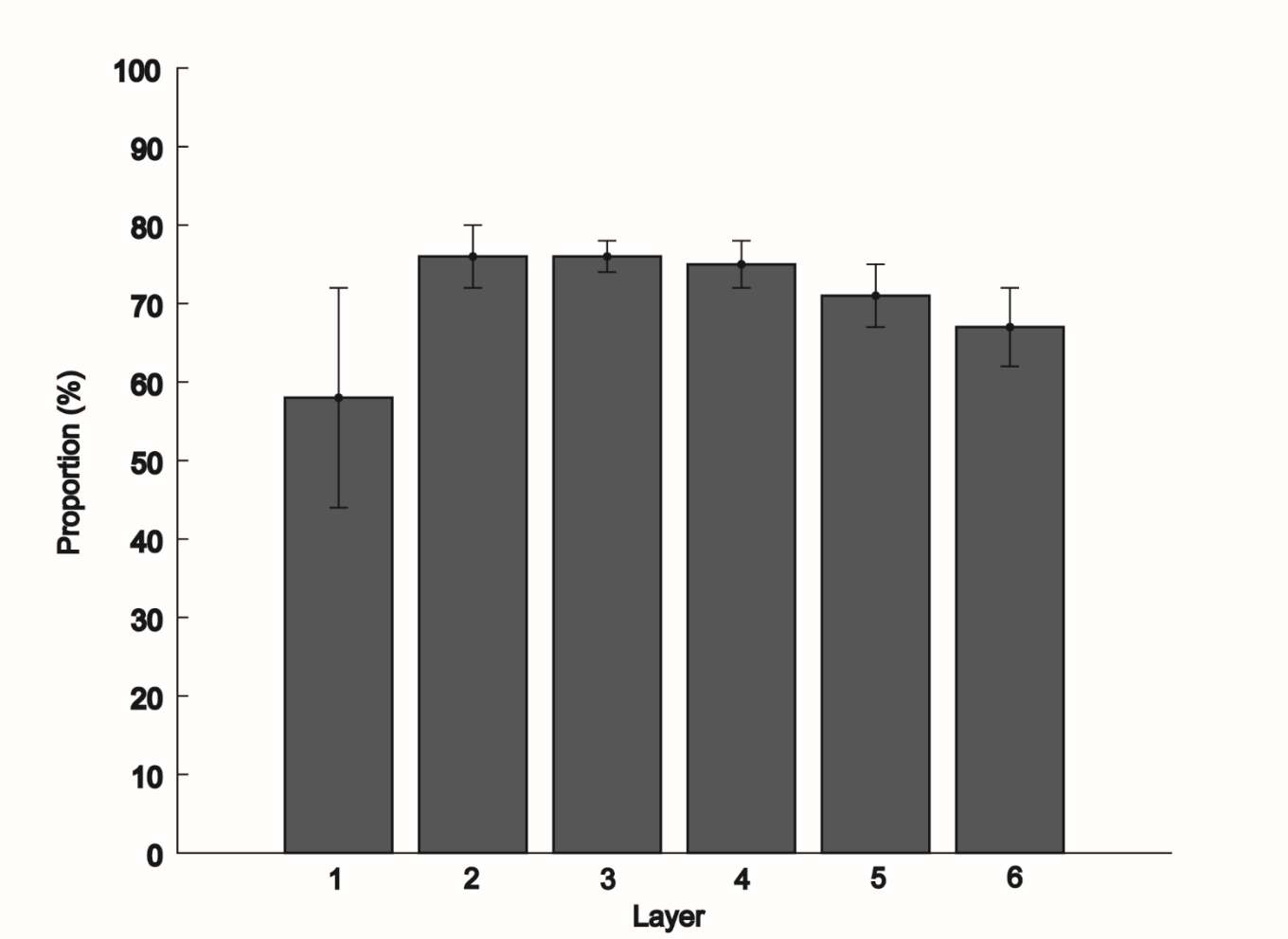

Figure 2-5: m1AChR expression by GABAergic cells in LIPv
Proportion (%) of GABAergic cells that expresses the m1 acetylcholine receptor across cortical layers 1-6 in ventral lateral intraparietal area. An average of 74% of GABAergic cells expresses the m1 receptor. Error bars = 2x standard error of the mean.

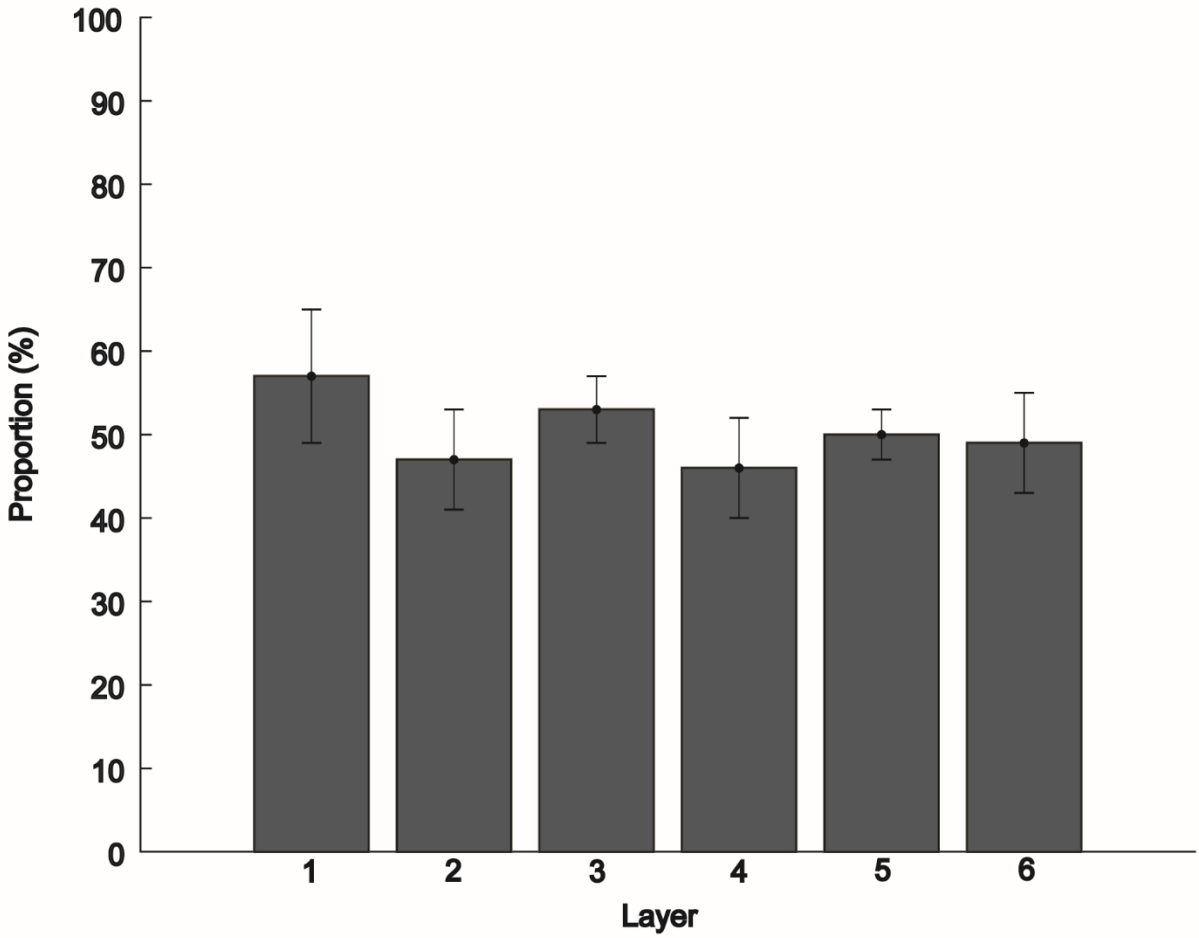

Figure 2-6: GABA expression by m1AChR-ir cells in LIPd
Proportion (%) of m1 acetylcholine receptor-expressing cells that is immunoreactive for GABA across cortical layers 1-6 in dorsal lateral intraparietal area. An average of 48% of m1-expressing cells is immunoreactive for GABA. Error bars = 2x standard error of the mean.

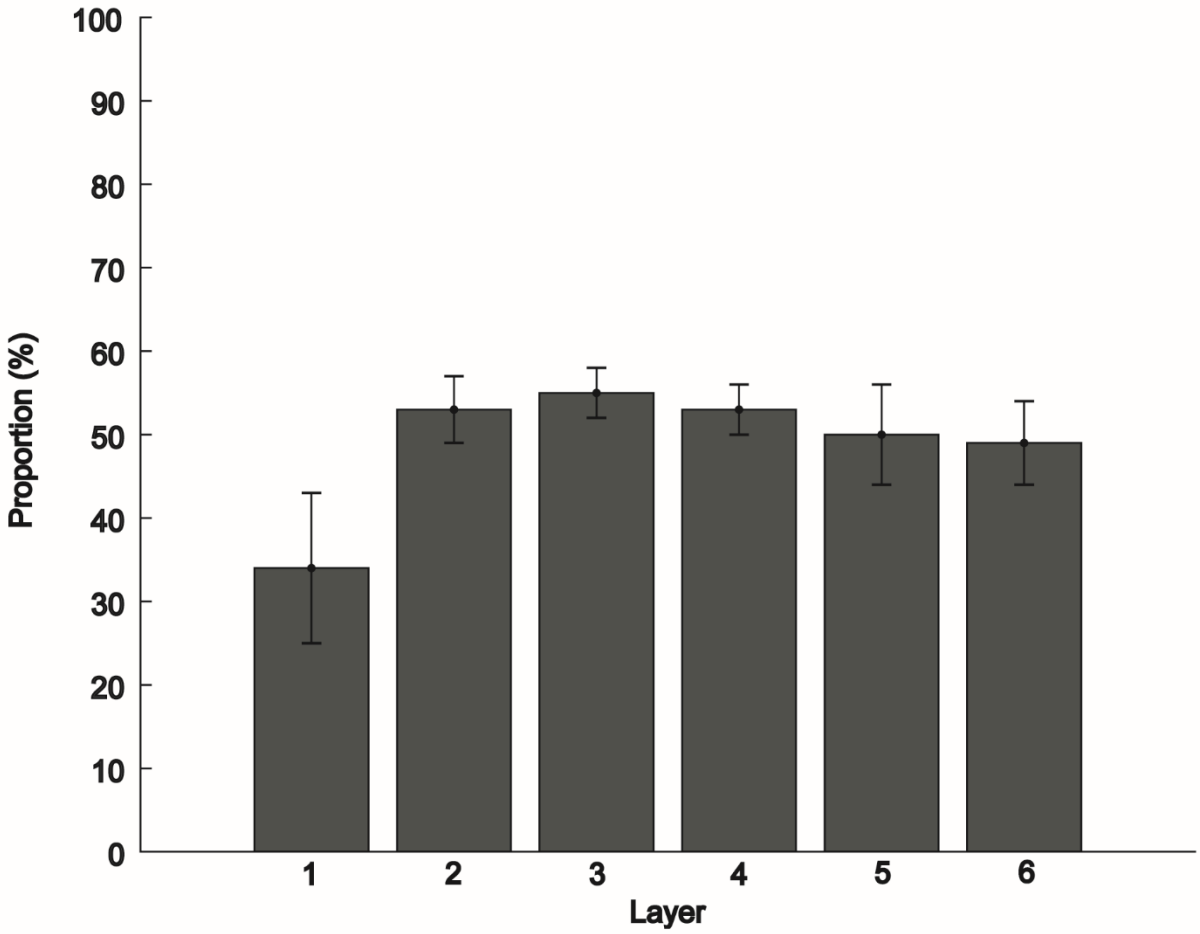

Figure 2-7: GABA expression by m1AChR-ir cells in LIPv
Proportion (%) of m1 acetylcholine receptor-expressing cells that is immunoreactive for GABA across cortical layers 1-6 in ventral lateral intraparietal area. An average of 52% of m1-expressing cells is immunoreactive for GABA. Error bars = 2x standard error of the mean.

2.3c m1AChR immunoreactivity

The m1AChR-ir cells are present in all layers. Their label most often appears in the entire somata, but with a brighter cytoplasmic ring near the border and what appears to be an equally bright nucleolus-type center (Figure 2-8). Some neuropil staining is present, however only very proximal processes are identifiable extending beyond the soma (if at all). Some smaller cells, usually in layer 4, appeared to form tight clusters of 2-4 cell bodies (Figure 2-9). These general characteristics seem to be consistent with previous reports of the m1 immunoreactivity profile (Disney et al., 2006; Disney and Aoki, 2008; Disney and Reynolds, 2014; Coppola and Disney, 2018b).

2.3d GABA immunoreactivity

GABAergic immunoreactivity labels the entirety of the cell body, which is equally bright throughout (Figure 2-10). Few processes connected to the somata were present, but some nicely labeled axons exhibiting the typical "beads-on-a-string" appearance were observed. GABAergic cells were also present in all cortical layers and were consistent with previous reports for GABAergic immunoreactivity profiles (Disney et al., 2006).

2.3e Dual m1/GABA immunoreactivity

Interestingly, many cells that were labeled for m1AChR appeared to be pyramidal in shape, putatively excitatory. However, these cells often appeared to be immunoreactive for GABA as well, making them inhibitory. Many of these cells were also quite large (Figure 2-11). This characteristic has previously been described (Disney et al., 2006) and leads to the interpretation that cell morphology alone should not be used to identify interneuron populations. Some cells exhibited a degree of brightly-labeled dots or puncta around the cell body (Figure 2-12). These puncta were not used as an inclusion or exclusion criterion; instead, I evaluated cell labeling regardless of these features. It is possible the puncta-like labeling represents terminals, perisomatic baskets, synaptic points, or some degree of autofluorescence, et cetera. The presence of the puncta, though, was not restricted to only dual-labeled cells and did appear to some degree in both populations.

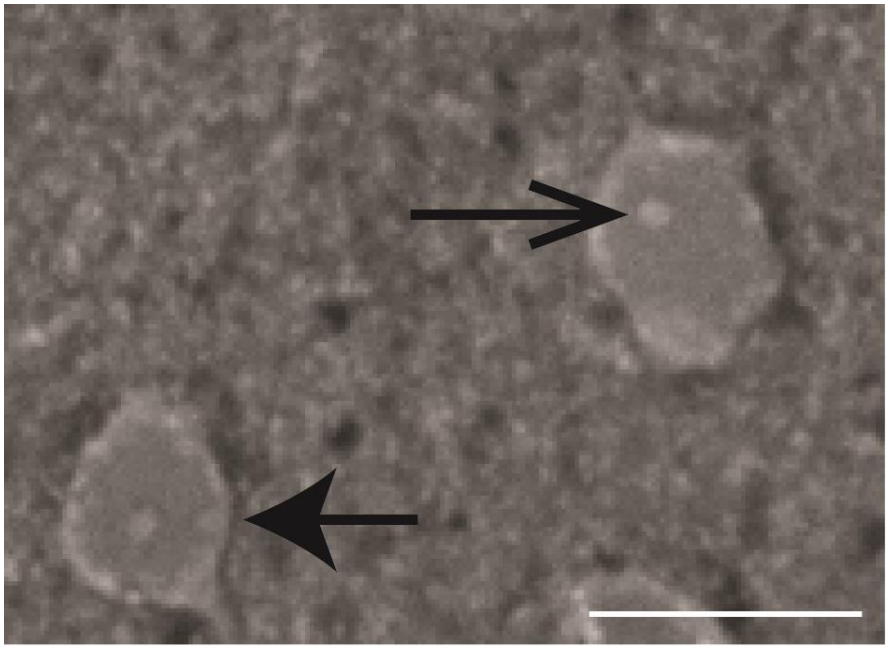

Figure 2-8: m1 acetylcholine receptor-expressing cell immunoreactivity profile
Two cells expressing the m1 acetylcholine receptor in dorsal lateral intraparietal area imaged at 63x magnification (oil immersion). Closed arrow marks a brightly-fluorescent cytoplasmic ring. Open arrow marks a bright-fluorescent center with a nucleolus appearance. Scale bar = 10 µm.

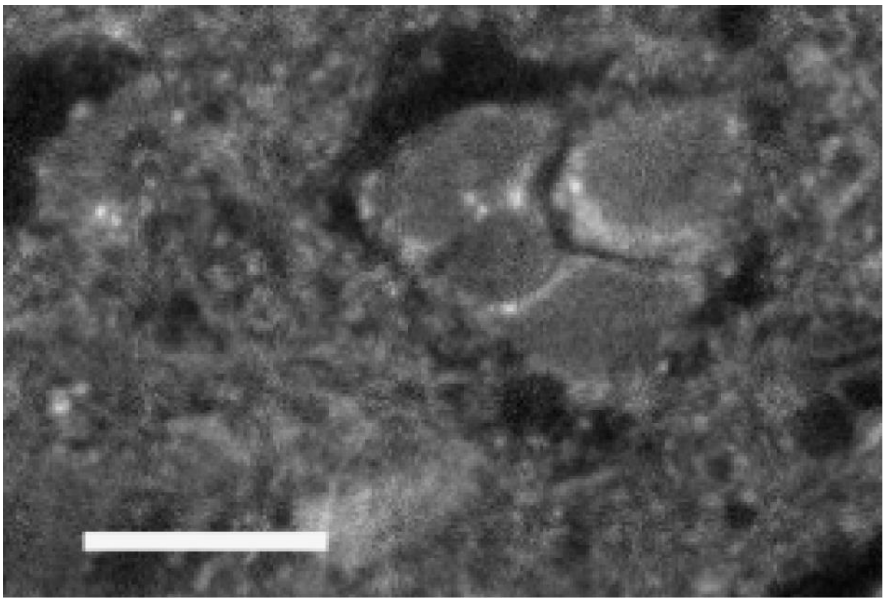

Figure 2-9: m1 acetylcholine receptor-expressing cell cluster
Four cells expressing the m1 acetylcholine receptor clustered together in layer 4 of ventral lateral intraparietal area imaged at 63x magnification (oil immersion). Scale bar = 10 µm.

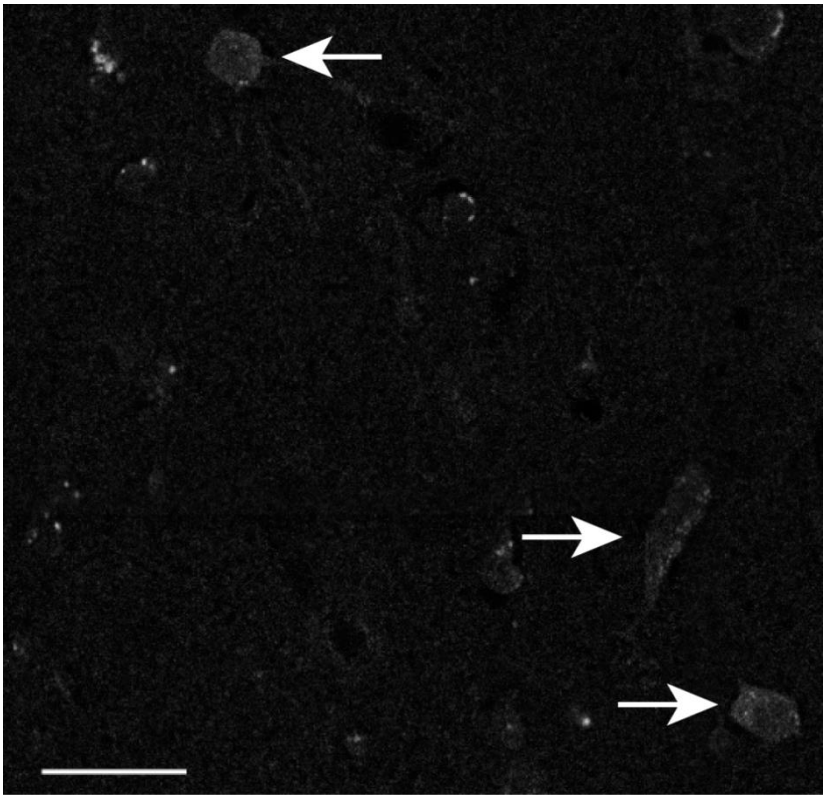

Figure 2-10: GABA-expressing cell immunoreactivity profile
Three cells (marked by arrows) immunoreactive for GABA in layer 3 of dorsal lateral intraparietal area imaged at 63x magnification (oil immersion). Scale bar = 25 μm.

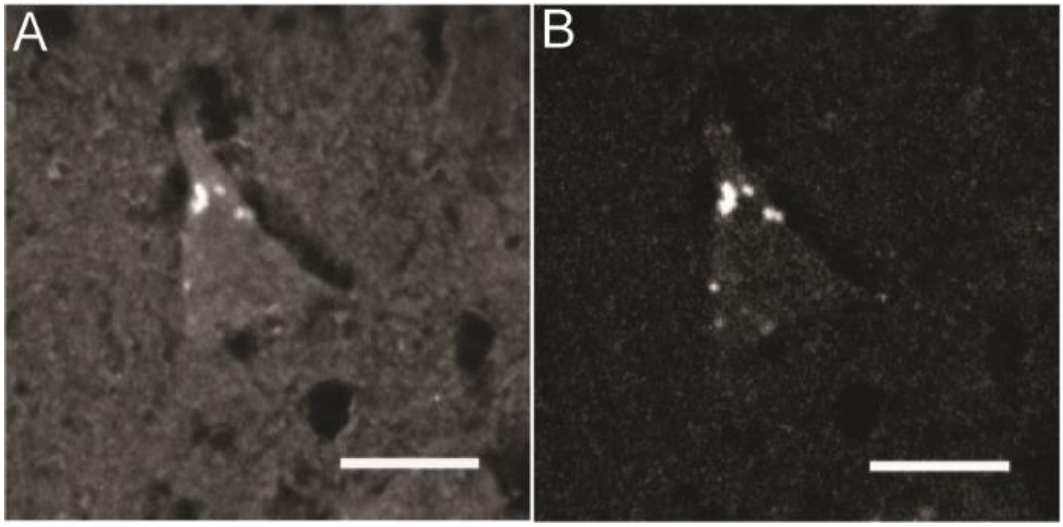

Figure 2-11: Dual labeled pyramid-like cell
Cell in layer 3 of ventral lateral intraparietal area imaged at 63x magnification (oil immersion) that has a pyramid-like morphology but that is dual-labeled for both the m1 receptor (A) and GABA (B). Scale bar = 10 µm.

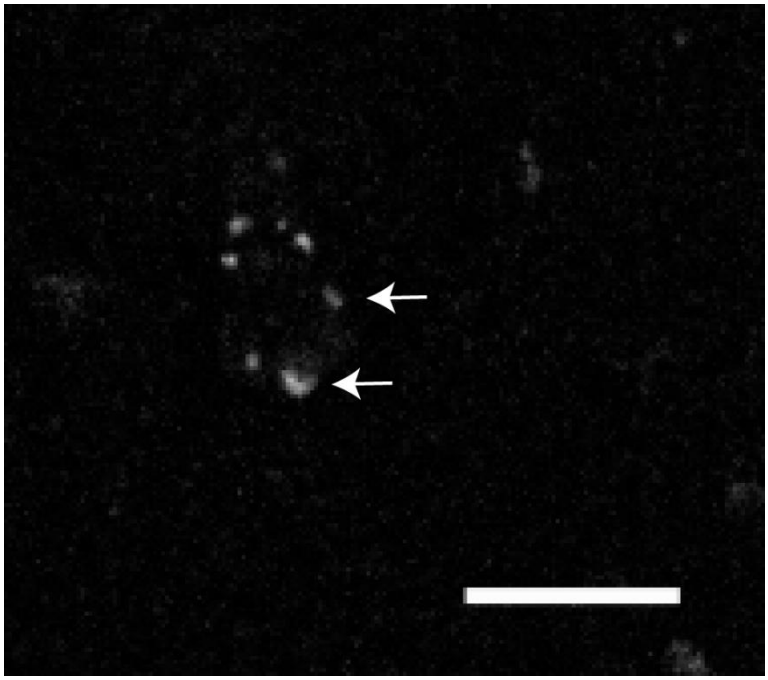

Figure 2-12: Punctate labeling
Example of puncta-like labeling around what appears to be a cell body in layer 2 of dorsal lateral intraparietal area imaged at 63x magnification (oil immersion) in the red (GABA) fluorescent channel. Scale bar = 10 µm.

2.4 Discussion

Here, I show that in LIP, approximately 75% of inhibitory neurons expresses m1AChR and that approximately 50% of m1AChR-expressing neurons is inhibitory. As discussed above, this means that of all neurons in LIP, roughly 40% express the m1AChR, with half being inhibitory and half being excitatory. Because I did not find any significant differences across animal, tissue section, layer, or between LIPd and LIPv, it seems that m1AChR expression is relatively uniform throughout the region and does not differ based on individual, location, or subregion (at least in this sample). Interestingly, however, these results are much different than those reported for other cortical areas.

Autoradiographical studies provide information on the general distribution of m1AChRs across primate cortices (Mash et al., 1988; Lidow et al., 1989; Zilles et al., 1995), but our most detailed accounts of receptor expression and distribution by cell type come from work in the visual cortex (Disney et al., 2006; Disney and Aoki, 2008; Disney and Reynolds, 2014). In macaque V1, the m1 receptor is expressed by over 60% of inhibitory neurons and by less than 10% of excitatory neurons (Disney et al., 2006). In V2, m1 receptor expression by inhibitory neurons is similar to that in V1. However, receptor expression by excitatory neurons differs sharply between V1 and V2, with at least double the proportion of excitatory neurons expressing these receptors in V2 compared to V1 (Disney et al., 2006). In fact, across the visual pathway—from V1, through V2, V3a, V4d, to MT—m1 receptor expression by inhibitory neurons remains roughly constant at 50-60%, while m1 receptor expression by excitatory neurons differs with an increasing m1AChR-ir excitatory population moving "up" through the visual pathway (Disney et al., 2006; Disney et al., 2014; unpublished data). Specifically, in MT, it has been reported that a little more than half of the m1AChR-expressing population is putatively excitatory (Disney et al., 2014), similar to what I report here for LIP (~50%). It may be the case, then, that as we continue to move through the brain from posterior to anterior, there may be a trend for an increase in m1 expression by excitatory neurons. It could also be the case that this trend plateaus at the level of LIP, or even that it falls off again as we move toward frontal cortex. Data are needed in the more anterior cortices to determine what, if any, trends exist moving forward.

LIP also shows an increase in m1AChR expression by inhibitory neurons compared to occipital lobe—50-60% in visual cortices versus 75% here in LIP, highlighting the degree to which inhibitory cells are a target of the cholinergic system. In LIP, a higher proportion of GABAergic cells is being modulated by ACh (at least through the m1 receptors) than in more posterior visual cortices. This, paired with an increase in expression by excitatory cells could indicate an overall increase in the "cholinoceptivity" of LIP neurons compared to previously described visual cortices. Importantly, however, this study only quantifies a single—albeit the most predominantly expressed—cholinergic receptor. Other receptor types are certainly expressed in LIP, most likely the m2 receptor (discussed above) as well as nicotinic receptors. While I have shown an increase in expression of the m1 receptor, we do not know the degree to which cells express these other receptors. This is especially important to investigate given that a single cell can express more than one type of cholinergic receptor. An experiment quantifying m2 expression is underway and will be included in the final manuscript for publication of this study.

If there is a true increase in the cholinoceptive nature of the tissue in LIP compared to more posterior regions, one possible interpretation is that this trend is correlated with increases in the strength of attentional modulation in cortex. For example, an fMRI study in humans has shown increased attentional affects from V1 up through V4. Specifically, humans focused attention to specific visual field locations, and the attentional affects were measured across visual areas. The activation in those areas during "attend to" trials increased from each visual area to the next (V1, to V2, to V3, and so on; Tootell et al., 1998). A possible feature of the mechanism responsible for increased attentional modulation could be an increase in m1AChR expression, especially by the excitatory population. Given that LIP is thought to be heavily involved in attentive

processes—acting as a map to guide visual attention (see Chapter 1)—it could be hypothesized that the strength of attentional modulation might be increased in this area compared to others.

Patterns and proportions of receptor expression by cell type provide insight to the receptiveness of a circuit to a molecule and the ability to broadly predict the type of activity that will result from the binding of that molecule. This is one important aspect of cholinergic circuitry in cortex, but equally important is the degree to which ACh can be delivered to and cleared from an area. The cholinergic innervation and degradation capabilities are the subject of the following chapter. In the Discussion section of this dissertation (Chapter 6), data describing receptor expression by cell type as well as innervation and degradation will be reviewed together in order to provide a description of the overall cholinergic environment in LIP.

Chapter 3

Characterization of the expression of cholinergic synthesizing and degradation enzymes in macaque LIP

3.1 Introduction

Similar to the importance of receptor expression by cell type in a diffuse neuromodulatory system, an understanding of the synthesis and termination of a signaling molecule is likely critical to understanding the functional capabilities of that molecule in cortex. ACh is synthesized in the cholinergic cell terminal by an enzyme called choline acetyltransferase (ChAT). ChAT catalyzes the transfer of an acetyl group from acetyl coenzyme A to choline. As a molecular marker for cholinergic cells and processes, ChAT is often used to measure the cholinergic innervation density from the basal forebrain to the cortex (Campbell et al., 1987; Mesulam and Geula, 1988; Lewis, 1991; Raghanti et al., 2008). This provides a measure for the relative amount of ACh that can be delivered to any area, especially given that in the cortex of adult non-human primates, there are no intrinsic cholinergic neurons in cortex.

Acetylcholinesterase (AChE) is an enzyme—membrane bound or freely soluble—that rapidly metabolizes ACh into acetate and choline. AChE is so fast and efficient that one molecule can hydrolize 5,000 molecules of ACh per second (Lawler, 1961; Cooper et al., 2003). This is remarkable considering ACh release occurs in quanta containing only several thousand molecules (Katz, 1969). AChE has been extensively characterized at the neuromuscular junction, where it terminates the action of ACh on nicotinic receptors found in muscle (Descarries et al. 1997, Gašperšič et al. 1999). Within the central nervous system, however, less is known about the expression, regulation, and function of AChE (Sarter et al. 2009, Fass and Hamill 1984). Likewise, the extent to which cholinergic signaling is fully terminated by AChE is difficult to characterize (see Chapter 6). Before the use of antibodies directed against ChAT in the 1980s, AChE histochemistry was used to identify cholinergic cells and processes. However, this enzyme was found to be present in non-cholinergic cell elements as well, including those of dopaminergic and noradrenergic cells (Butcher et al., 1975; Albanese and Butcher, 1979 but see Mesulam and Geula, 1992). As such, this enzyme is generally not used to classify cholinergic processes, but it still provides important insight to the cholinergic signaling in an area. Specifically, AChE intensity provides a measure of the relative ability of an area to "clean up" ACh, thus terminating the cholinergic signal.

In macaque LIPd and LIPv, I used immunohistochemistry to characterize and quantify expression of ChAT across layers. This provides a measure of the relative degree to which cholinergic axons originating in the basal forebrain innervate LIP, thus providing ACh. Similarly, I used histochemistry to characterize and quantify expression of AChE across layers in macaque LIPd and LIPv. While this does not provide a direct measure for cholinergic processes, it does provide measures for the relative degree to which an area can break down ACh, terminating the signal. These two measures (ChAT and AChE) together provide insight to the capabilities of the cholinergic system to signal in LIP.

3.2 Methods and materials

3.2a Animals

All five animals listed in Appendix A were used in this study. All procedures were approved by the Institutional Animal Care Committee and performed in accordance with National Institutes of Health and institutional guidelines for the care and use of animals.

3.2b Histological preparations

Refer to Chapter 2, section 2.2b for detailed descriptions of histological preparations. Briefly, animals were euthanized by intravenous injection of sodium pentobarbital. Following the abolition of the pedal and corneal reflexes, animals were transcardially perfused with PBS followed by 4% PFA and with 0.15% glutaraldehyde (for Animals 2, 4, and 5) in PB. For two of the five animals (4 and 5), 5-20% sucrose in PB was perfused following the fixative. Following perfusions, for all animals, the brain was removed and blocked as necessary. The remaining tissue was post-fixed 4 hours-overnight at 4°C in 4% PFA. Following the post-fix, the brain was transferred to 30% sucrose in PB and stored at 4º C until it sank.

Hemispheres to be sectioned were blocked in approximately the coronal plane just posterior to the central sulcus. The tissue from these blocks was sectioned at a thickness of 50 μm on a freezing microtome and reacted for 30 minutes in 1% sodium borohydride in PB. Sections were then rinsed in PB. Two 1-in-6 series of sections were set aside to provide reference sections for determining laminar and areal boundaries. Remaining sections were stored at 4°C in PBS with 0.05% sodium azide. Similar to the tissue selection method from Chapter 2, I used three sections from each of the five animals, selected using systematic random sampling and aiming to sample the full extent of area LIP.

I performed ChAT immunohistochemistry using the protocol from Stephenson et al. (2017). First, I washed tissue for 10 x 5 minutes in PBS. Then, I pretreated sections for antigen retrieval by incubating in 0.01% citraconic acid (pH 7.4) for 30 minutes at 86°C. I allowed the tissue to cool in the same solution for 20 minutes before 6 x 5 minutes of washing in PBS. Following washes, I quenched endogenous peroxidase in 75% methanol with 2.5% hydrogen peroxide for 20 minutes at room temperature on a shaker. Following another 30 minutes of PBS washes, I preblocked the tissue in 4% normal donkey serum (NDS, Jackson ImmunoResearch, Inc.), 0.6% Triton X-100 (Sigma), and 5% BSA for 1 hour on a shaker at room temperature. Following washes, I incubated tissue in PBS with the primary antibody for 24 hours at room temperature on a shaker, followed immediately by another 24 hours at 4°C (not shaking). The primary antibody used here has been previously characterized (Stephenson et al., 2017) and all antibody information for this experiment is listed in Appendix B. After the primary incubation, I washed tissue 6 x 5 minutes in PBS then incubated sections in the secondary antibody diluted in 2% NDS in PBS for 1 hour at room temperature on a shaker. After another 30 minutes of washing, I incubated sections in the Avidin-peroxidase Complex (ABC, Vector Laboratories PK-100) solution for 1 hour at room temperature on a shaker. Following washes, I reacted the sections in a 3,3'-diaminobenzidine-peroxidase (DAB, Vector Laboratories SK-4100) substrate with nickel solution enhancement. Finally, I washed sections and mounted them on subbed slides to dry overnight before dehydrating and coverslipping.

For AChE histochemistry, I used the protocol listed in Geneser-Jensen and Blackstad, (1971) and Stepniewska et al. (1994). First, I rinsed tissue sections for 3 x 10 minutes in PB before incubating the sections in a solution containing 17.5% sodium acetate, 7.5% acetic acid, 1.15% acetylthiocholine iodide, .075% copper sulfate, and .05% glycine (pH 5.0). The incubation lasted between 21 hours and 10 days. The large variations in processing times were correlated with the amount of time each animal's tissue had been stored following

perfusion, with the most recently perfused animals having the shortest incubation time and the animal perfused longest ago having the longest incubation time. To determine when an animal's tissue was finished being incubated, I performed this protocol on a number of test sections from each animal, choosing the incubation time that produced the best signal to background ratio, aiming for all tissue sections to have a similarly stained appearance. Following incubation, I rinsed the tissue for 3 x 30 seconds in distilled water, followed by a 45-60 second rinse in 1.25% sodium sulfide. I then rinsed the tissue again in water, followed by a 20-60 second rinse in 0.5% silver nitrate. After another water rinse, I incubated the tissue for 10 minutes in 5% sodium thiosulfate. Following another set of water rinses, I mounted the tissue onto subbed slides out of PB and dried overnight before dehydrating and coverslipping.

3.2c Light microscopy

For both ChAT and AChE labeled tissue, I used a Zeiss Axio Imager M2 light microscope with AxioCam MRc camera (Carl Zeiss AG, Oberkochen, Germany) driven by Stereo Investigator software (MBF Bioscience, Williston, VT) with a 40x objective. I determined settings for the contrast and brightness to match the image as it appeared through the ocular lenses. For each tissue section, I captured a montage of stitched images (slide scanning workflow in Stereo Investigator) covering either the entirety of LIP, or covering only LIPd or LIPv in the case that the entire sulcus was too large to contain both subregions in a single image. I adjusted the plane of focus every 7-10 images (as the stitched montage was being captured) aiming to keep the top of the tissue in clear focus. For Nissl reference images (discussed below), I captured images using the methods described here.

3.2d Defining architectonic boundaries

I used the same methods to define areal and laminar boundaries as described in Chapter 2. Briefly, I used Gallyas reference alongside macaque atlases and published data to determine LIP areal boundaries. I then referred to Nissl reference sections to identify laminar boundaries (Figure 2-2A-C). I captured Nissl reference images at 40x magnification and I coregistered the light images using fiduciary marks such as pial surface shape, structural morphology, blood vessels, and cutting artifacts. To correct for differences in tissue shrinkage arising from differences in the Nissl and ChAT/AChE tissue processing protocols, I measured the distance from the pial surface to the layer 1/2 border (defined by a sharp increase in cell density) and compared between each Nissl and tilescan image using Adobe Photoshop. I evaluated distances from the pial surface to each layer boundary on the Nissl section and converted to the distance for the corresponding data section.

3.2e Quantification

For both ChAT and AChE quantification, I converted images to grayscale in Adobe Photoshop. For ChAT, I first added laminar boundaries (using the Nissl reference sets described above) in ImageJ (National Institutes of Health, Bethesda, MD). Once laminar boundaries were in place, in Photoshop, I overlaid an image layer onto the data images that consisted of a straight line made up of individual circles. Each circle had a diameter of 200 pixels (approximately 50 μm), and the circles were separated by a space of approximately 20 pixels. I placed this "circle line" over the tissue such that the line would be perpendicular to the pial surface and span all cortical layers (Figure 3-1). With the circles in place, I counted the number of ChAT-ir axons that crossed any part of the circle. In order to count an axon crossing, it had to be clearly visible both inside and

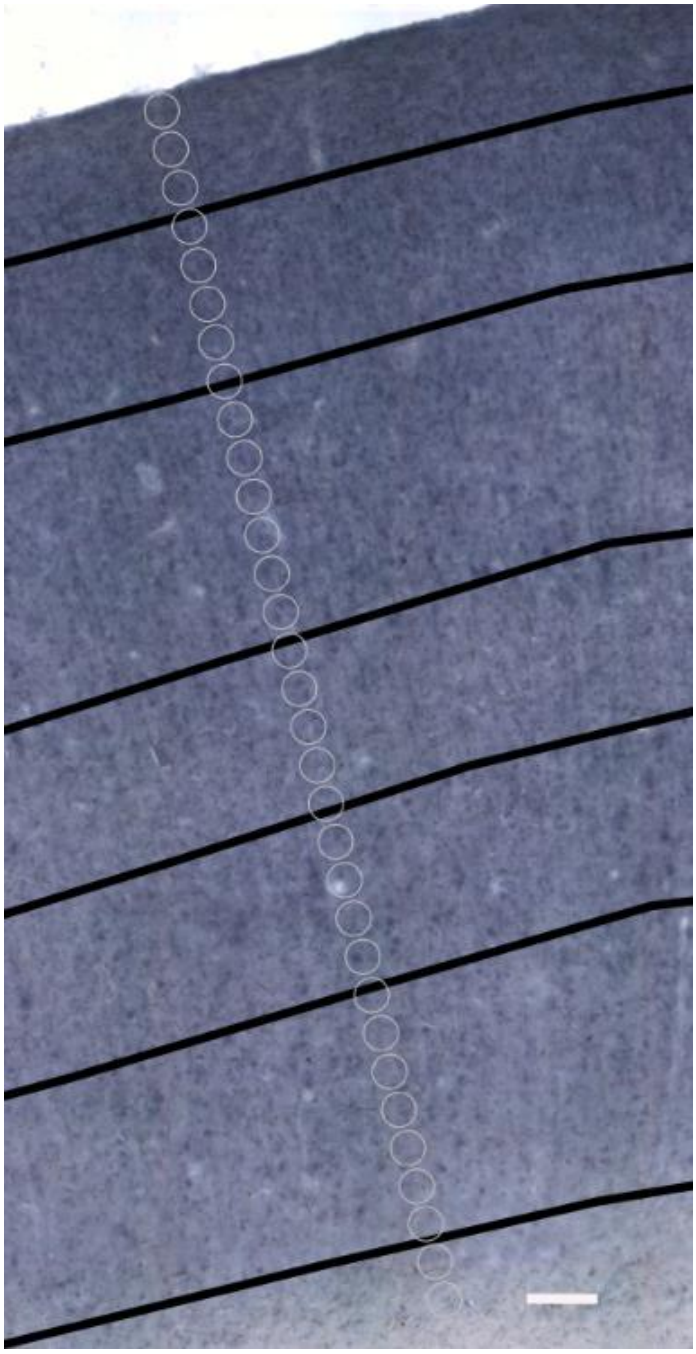

Figure 3-1: ChAT-ir axon quantification
Cortical tissue stained to visual choline acetyltransferase-ir axons in dorsal lateral intraparietal area. Black lines mark laminar borders with the pial surface at the top of the image. The "line" of circles is placed perpendicular to the pial surface and traverses all 6 cortical layers. Axons are counted as they cross from outside to inside of each circle. Scale bar = 100 μm.

outside of the circle. I marked axon crossings with a shape marker in Photoshop and then counted the number of markers per circle. I quantified one circle line per section per animal. This method provides a quantification of the density of ChAT-ir axons in an area.

For AChE, in ImageJ, I first drew a data line perpendicular to the pial surface that spanned all cortical layers (Figure 3-2). I then used the "plot profile" tool to generate a grayscale value for each pixel along the line. Once I had recorded those values, I then drew on all of the laminar boundaries (black lines, 50 pixels wide) onto the image, flattened the image such that the laminar boundaries were now imbedded in the image, and then plotted to same data line again to record the new grayscale values. The only difference in the two lists of values (pre- and post-laminar boundaries) was that the laminar boundary lines now generated values of "0" (black) for the pixels they covered. The purpose of pre- and post-laminar data collection was to know precisely where on each data line the laminar boundaries were located, such that I could still have the values that existed "beneath" the laminar lines—so as to not lose any data and to preserve the ability to analyze the data in specific ways (e.g., to be able to create a curve showing the increases and decreases of AChE intensity throughout cortex, without having laminar lines affecting the shape of the curves). This method provides an indication of AChE intensity within an area.

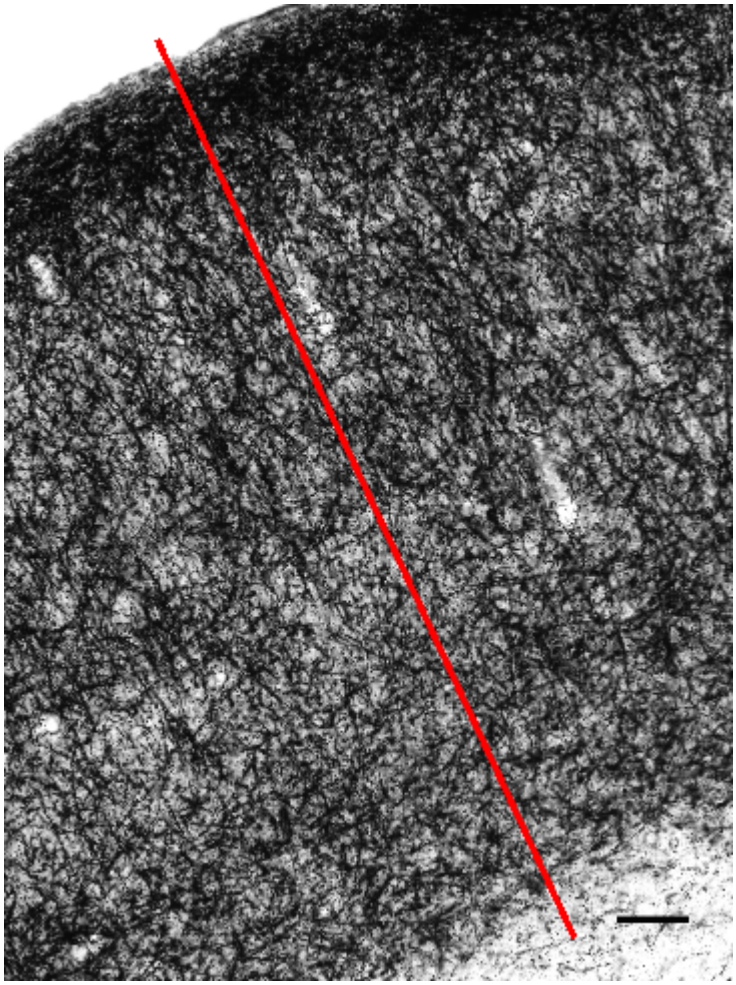

Figure 3-2: AChE expression quantification
Cortical tissue stained to visual expression of acetylcholinesterase in dorsal lateral intraparietal area. The red line runs perpendicular from the pial surface (top) to the white matter (bottom). Grayscale values are generated for each pixel along the line. The stained fibers have a matted appearance, with the most intense staining occurring in layer 1 near the pial surface. Scale bar = 100 µm.

3.2f Analysis

For AChE, I first used a custom MATLAB (MathWorks, Natick, MA) script to invert the grayscale values such that a value for black (0) would now be equal to 255 (white) and a value of 255 would now equal 0. The purpose of this was to make interpretation of results more intuitive such that a more darkly stained location would have a higher grayscale value, indicating "more," and a more lightly stained area would have a lower grayscale value, indicating "less." To interpret relative differences across layers and subregions, I used custom MATLAB script to normalize the values for AChE histochemistry using a scale from 0 to 1, with 1 being the highest grayscale pixel value (greatest amount of stain), and 0 being the lowest grayscale pixel value (the least amount of stain). Following normalization, I used custom MATLAB script to smooth the data. Many of the AChE data lines were more than 10,000 pixels long, and the raw plots were difficult to interpret because the value for each of those 10,000 pixels was displayed. To smooth the appearance of these lines, I used a "moving mean" function to take the sliding average across 999 pixels. Beyond the inverting, normalization, and smoothing, I did not manipulate the data in any way, including averaging/collapsing data. This was because the intensity of the stains could appear different for a number of reasons, including reaction time in the AChE incubation and the degree to which the tissue could "take up" the stain that differed for each animal and microscope/camera settings during imaging, which could be different across animals that were not imaged at the same time. Because of these factors, I analyzed each plot individually.

For ChAT analysis, I averaged the number of counts across all animals and sections for LIPd and for LIPv. Because the methodology I used to quantify ChAT axon crossings was by counting them—unlike a pixel intensity value along a line for AChE—I was able to collapse the data since difference in intensity and brightness did not affect quantification. Once I combined all LIPd data and all LIPv data, I normalized those values in the same way I did for AChE values (0 being the lowest number of axons and 1 being the highest number of axons).

For both AChE and ChAT, I also obtained sublaminar measures for layers 2, 3, 4, and 6. For AChE, I averaged the first and last 100 pixels of each layer and then turned those two values into a ratio so as to get a sense of "slope" or progression of the line as it moves through the layers. Similarly, for ChAT, I divided the layers into an upper and a lower half and averaged values from each portion. I did not perform these operations on layers 1 or 5 because these tended to be smaller in area compared to the other layers and have less degree of variation within. For layers 1 and 5, I instead provide an average for the entire layer.

3.3 Results

I used immunohistochemistry to characterize and quantify expression of ChAT and histochemistry to characterize and quantify expression of AChE across layers in macaque LIPd and LIPv. I find that overall, ChAT and AChE have specific laminar profiles such that superficial layers exhibit "higher" (i.e. more intense staining in terms of AChE or a higher number of axons crossings for ChAT) levels than do the deeper layers. These findings were mostly consistent across dorsal and ventral subregions.

3.3a ChAT density

The number of ChAT axon crossings is usually highest in layer 1, sometimes being equal to layer 2 (points, Figure 3-3 and Figure 3-4). There is a slight decrease from upper layer 2 to lower layer 2, then the number continues to fall into layers 3 and 4. Layer 5 values remain at about the same level as layer 4, then there is a final decrease where the crossings reach their lowest points in layer 6. This trend is similar for dorsal and for ventral subregions, although ventral values tend to be lower than dorsal values.

3.3b AChE intensity

AChE intensity values also exhibit a specific laminar profile (lines, Figure 3-3 and Figure 3-4). Intensity is highest in layer 1, with a decline toward layer 2, continuing to the lower portion of layer 3. At or near the layer 3/4 border is a drop in intensity that then ramps back up from layer 4 to layer 5. The intensity remains steady at this level until it begins to fall in layer 6 toward the white matter border. Based on the ratio data (Table 1), the steepest declines within layers occur at upper layer 2 to lower layer 2 and at upper layer 6 to lower layer 6. The only incline within a layer occurs from upper layer 4 to lower layer 4. These results are consistent between dorsal and ventral subregions.

3.3c ChAT immunoreactivity

ChAT staining yielded nicely labeled axons and varicosities. In the supraficial layers, especially layer 1, axons seemed to be oriented in a more horizontal fashion, traversing the width of the layer. Layer 1 and upper layer 2 seemed to be more varicose as well (Figure 3-5). In the deeper layers, the axons appeared more vertically oriented, traveling the length of the layers (Figure 3-6). Consistent with other reports (Mesulam et al., 1983; Mesulam et al., 1986; Raghanti et al., 2008), I did not find perisomatic staining (found in some species of macaques, but not rhesus), "clusters" of ChAT-ir fibers (found in chimpanzees and humans, but not in macaques), or intrinsic perikarya immunoreactive for ChAT (reported in rodents but not in primates) (Raghanti et al., 2008). Both axons and visible varicosities were present in all cortical layers.

3.3d AChE reactivity

Contrary to the fine structural integrity and clearly visible varicose axons immunoreactive for ChAT, AChE labeling appeared instead as mesh of intermediate to dark fiber staining (Figure 3-2). I was unable to get a sense of fiber orientation and directionality, but the upper layers appeared especially matted. In many cases, I was able to see distinct bands of intensity that were unobservable in the ChAT stain. Overall, this staining appears to be consistent with previous AChE labeling described in macaque cortex (Mesulam et al., 1984; Hackett et al., 2001). Similarly, I did not encounter identifiable AChE-ir cell bodies that have been described in chimpanzee and human cortex (Hackett et al., 2001; Mesulam and Geula, 1992).

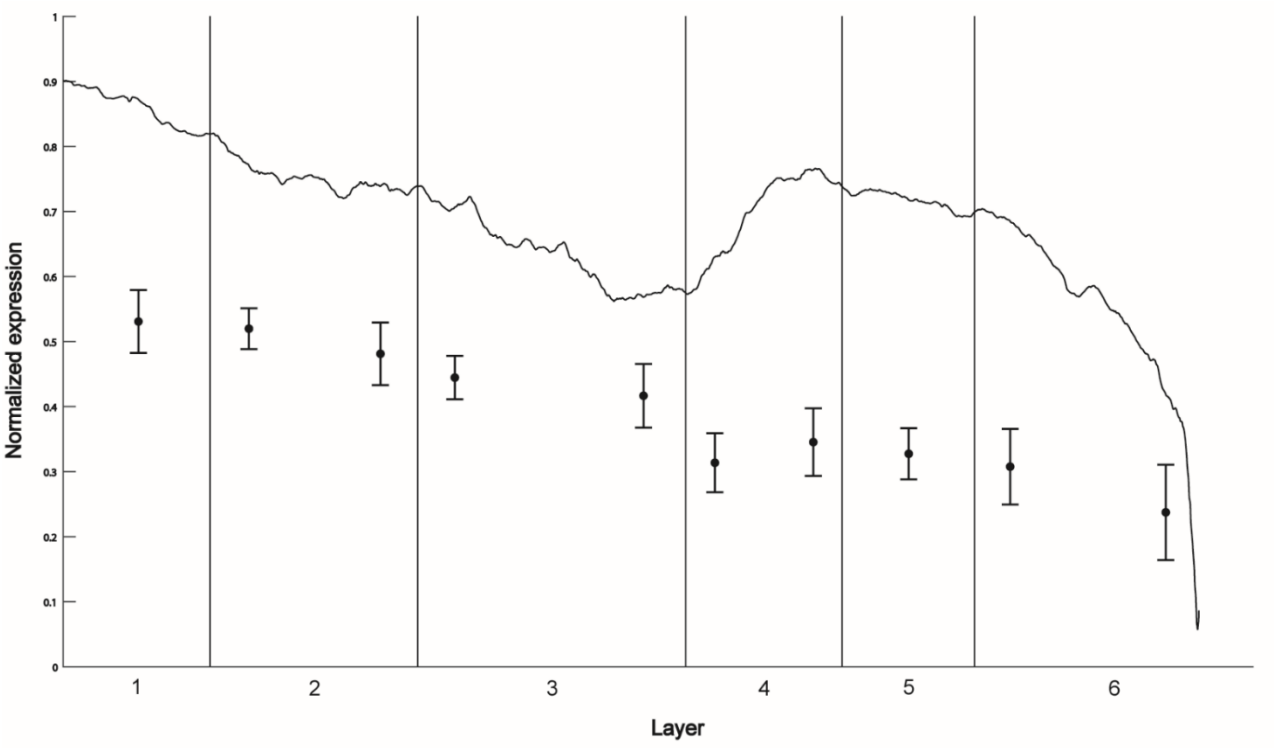

Figure 3-3: ChAT and AChE expression in LIPd
Y-axis are normalized values for ChAT density (points) and AChE expression (solid line) from 0-1. X-axis are cortical layers, with straight lines to make laminar boundaries. Error bars around circles = 2x standard error of the mean.

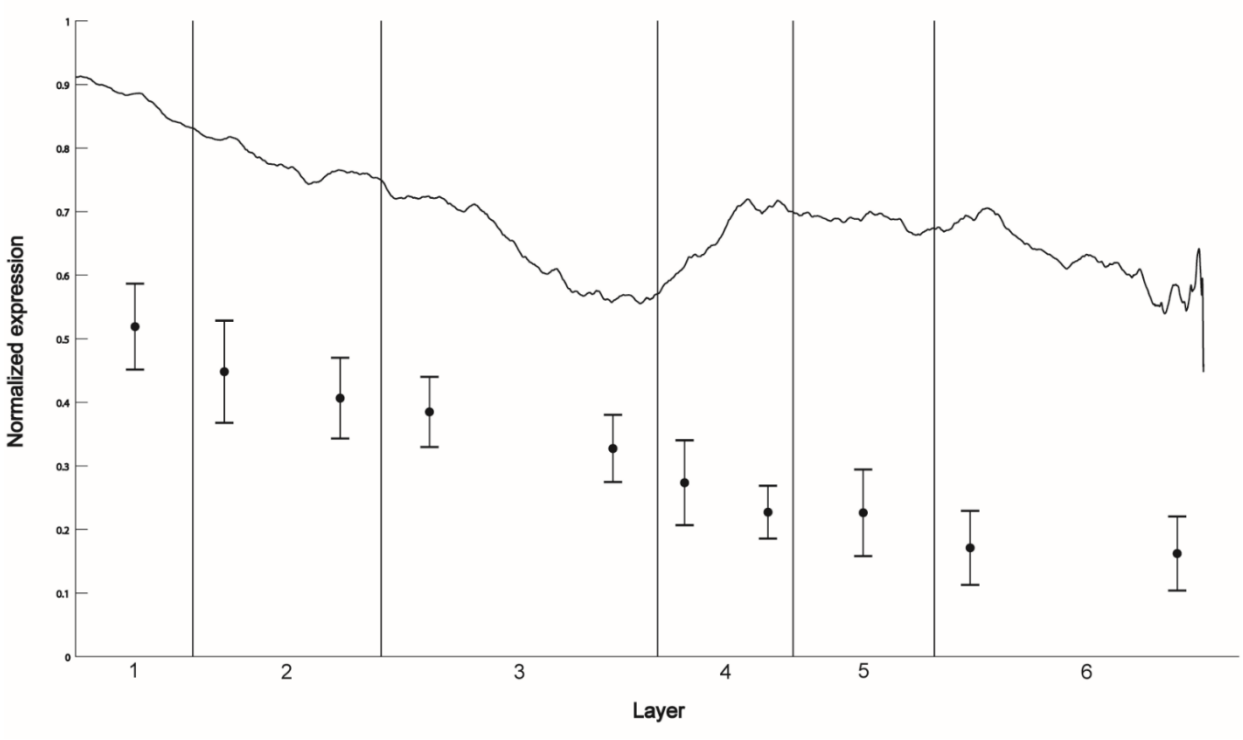

Figure 3-4: ChAT and AChE expression in LIPv
Y-axis are normalized values for ChAT density (points) and AChE expression (solid line) from 0-1. X-axis are cortical layers, with straight lines to make laminar boundaries. Error bars around circles = 2x standard error of the mean.

	Dorsal Average	Dorsal Minimum	Dorsal Maximum	Ventral Average	Ventral Minimum	Ventral Maximum
Layer 1: upper layer 2	1.004188	0.907884	1.066768	1.046633	0.878437	1.226687
Upper layer 2: lower layer 2	1.247377	1.040339	1.571909	1.178137	0.857627	1.567867
Upper layer 3: lower layer 3	1.035975	0.909801	1.181189	1.066567	0.835479	1.310746
Upper layer 4: lower layer 4	0.884142	0.54585	1.111818	0.953984	0.682557	1.153846
Lower layer 4: layer 5	1.02863	0.985101	1.128333	1.065215	1.00083	1.159946
Layer 5: upper layer 6	0.979516	0.915506	1.032492	1.114829	0.868669	1.348857
Upper layer 6: lower layer 6	1.251306	0.965651	1.589422	1.380466	1.140412	1.813165

Table 1: Acetylcholinesterase intensity ratios
Ratio values for acetylcholinesterase expression compared across or within layers for dorsal lateral intraparietal area and ventral intraparietal area.

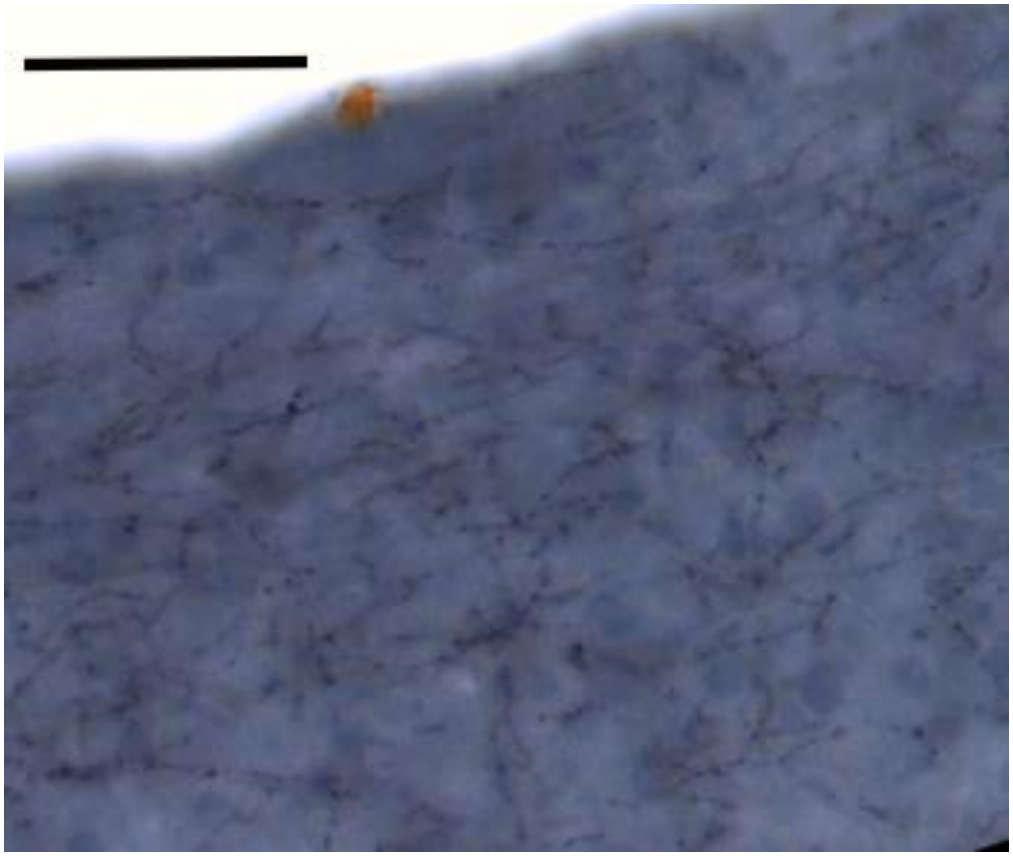

Figure 3-5: ChAT-ir axon density in layer 1
Cortical tissue stained to visual expression of choline acetyltransferase in layer 1 of ventral lateral intraparietal area. Axon orientation appears to be horizontal and matted. There is also punctate labeling likely representing varicosities. Scale bar = 100 µm.

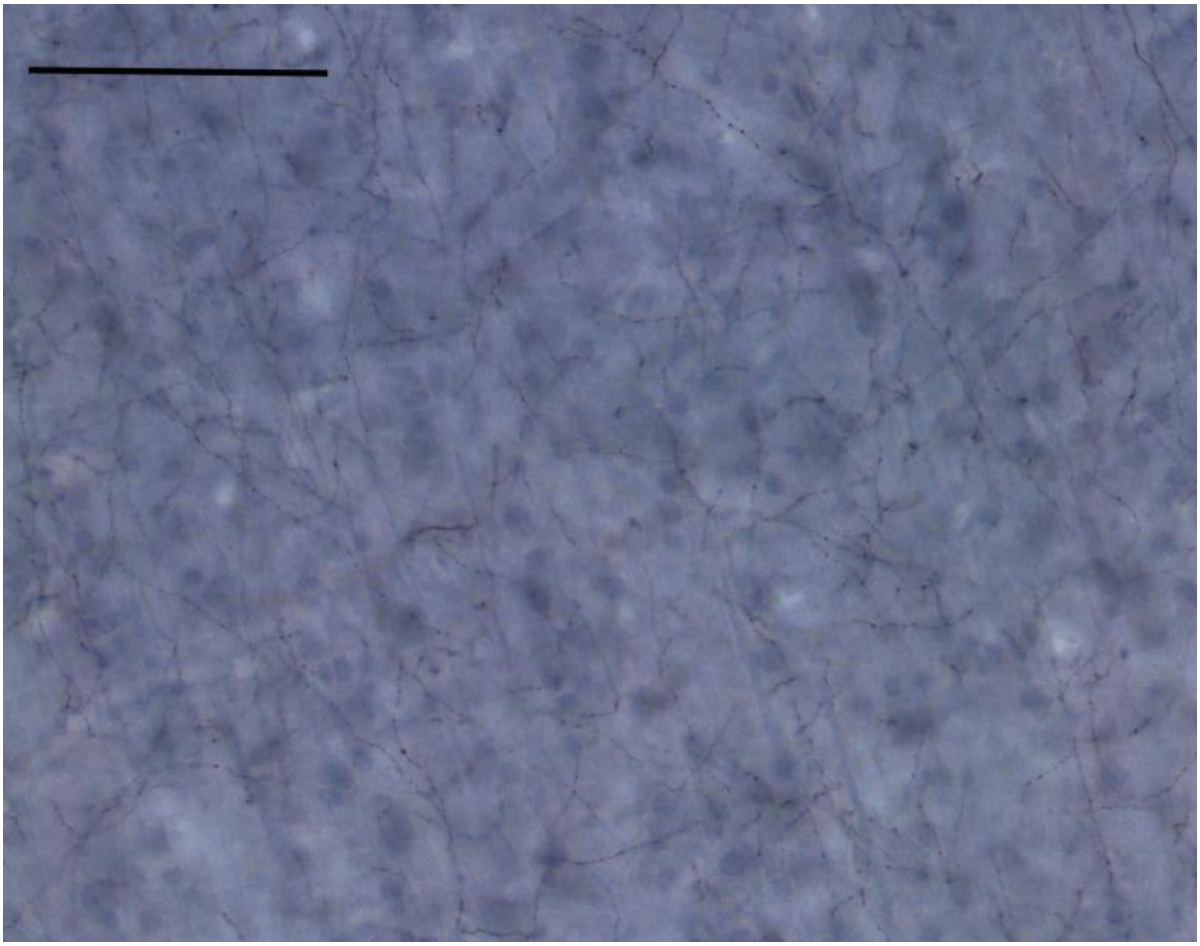

Figure 3-6: ChAT-ir axon density in layer 5
Cortical tissue stained to visual expression of choline acetyltransferase in layer 5 of ventral lateral intraparietal area. Axon orientation appears to be mostly vertical. Scale bar = 50 µm.

3.4 Discussion

Overall, I find that both AChE and ChAT levels are highest in the superficial layers, especially layers 1 and 2. For AChE, intensity declines from layer 1 to 2 to lower 3, where levels increase in 4 and 5 and finally decline in layer 6 toward white matter. For ChAT, I find that ChAT axons are densest in the superficial layers, with a more gradual decline from the pial surface toward white matter. For both AChE and ChAT, these trends are similar across dorsal and ventral subregions, however, in a number of cases, AChE and ChAT values are relatively lower in the ventral subregion compared to the dorsal subregion (although there were exceptions to this). Importantly, these two measures together provide insight to the capabilities of the cholinergic system to signal in LIP, serving as indicators of both transmitter release and transmitter clean up.

Projection neurons from the cholinergic basal forebrain innervate all of cortex, but the densities of these projections differ between and within cortical areas. This is a notable characteristic because a denser network of cholinergic axons is likely to yield a higher density of cholinergic release sites, potentially leading to more ACh being delivered. This is interesting given many studies have revealed differences in ChAT immunoreactivity across cortex, both across cortical areas and across layers within an area. In the human, for example, V1 is less densely innervated by cholinergic axons compared to other primary sensory and motor areas (Mesulam et al., 1992). In fact, occipital cortices in general are less densely innervated compared to the temporal or precentral regions (Lehmann et al., 1984). In human association cortex, layer 4 has one of the lowest densities of ChAT and layers 1, 2, and superficial 3 contain the highest (Mesulam and Geula, 1992). Cholinergic projections in the macaque also show clear differences between cortical areas, with macaque prefrontal area 4 (primary motor cortex M1) being more densely innervated than prefrontal areas 9 and 32 (Raghanti et al., 2008). As for laminar differences, in macaque primary auditory cortex A1, cholinergic axons are most dense in layers 1, 3, and 4 (Campbell et al., 1987). However, while layer 1 is also found to be densely labeled in macaque frontal cortex, layers 3 and 4 are least densely innervated (Lewis, 1991). In macaque frontal area 46, the supragranular layers 1, 2, and superficial 3 show denser networks of cholinergic axons than the infragranular layers (Mrzljak et al., 1995), again suggesting the supragranular layers will be exposed to higher levels of extracellular ACh. These studies provide evidence that while all ACh release across cortex is provided by a relatively small number of neurons in the basal forebrain, the signal received in a patch of cortex may vary as a result of differences in the density of cholinergic innervation. Tables 2 and 3 (Coppola and Disney, 2018a) provide a brief summarization of further species- and area-specific and laminar-specific patterns in cholinergic innervation. In LIP, I show that ChAT density is highest in layer 1 and upper layer 2, and declines toward the white matter, similar to what has been reported in macaque frontal area 46 (dorsolateral prefrontal cortex; Mrzljak et al., 1995) but different than what has been reported in many other cortical areas (e.g. macaque A1, frontal cortex).

In addition to measures of release (ChAT), the effective range (across the tissue) and temporal dynamics of the cholinergic signal are also limited by mechanisms that terminate that signal. Though it seems intuitive to expect areas with dense cholinergic innervation to exhibit high levels of AChE, and areas with sparse or no cholinergic innervation to exhibit low levels or an absence of AChE, this is not always the case (Kawaja et al., 1990; Dani and Bertrand, 2007). AChE intensity serves as an indicator of the efficacy of ACh degradation within a given compartment. Differential expression of AChE between regions of tissue will affect the spread of ACh molecules in both space and time (Figure 3-7A). When comparing between two regions of tissue, ACh will be able to move farther through tissue over a longer period of time in a region that expresses a lower level of AChE. In a region with higher levels, the movement of ACh molecules is expected to be more restricted in both space and time, as they will more readily be degraded. As with ChAT, there are many examples of AChE expression differences both across cortical areas and across layers within a cortical area. Density of AChE within primate A1, for example, differs sharply across the border between the core and belt cortical areas.

	Sensorimotor		Frontal		Primary auditory/visual		Parietal
Human	M1 (S1 n.d.)	>	32>9	>	A1>V1	<	39=40
Chimpanzee	M1 (S1 n.d.)	>	32=9	>	A1?V1	?	n.d
Macaque	M1?S1	>	9>32	>	A1?V1	?	n.d
Cat	M1=S1	>	n.d	>	A1>V1	?	n.d
Rat	M1=S1	=	4=8=10=11	>	A1=V1	>	5=7

Table 2: Relative degree of cholinergic innervation density across species and area
> indicates innervation density is greater than, < indicates innervation density is less than, = indicates innervation density is similar, n.d. indicates areas for which no data are available (to our knowledge), ? indicates the relationship between regions is unknown. M1: primary motor area; S1: primary somatosensory area; A1: primary auditory area; V1: primary visual area; frontal and parietal areas correspond to Brodmann's classification. Data for human: Mesulam et al., 1992, Raghanti et al., 2008; chimpanzee: Raghanti et al., 2008; macaque: Campbell et al., 1987, Lewis, 1991; Raghanti et al., 2008; cat: Avendaño et al., 1996; rat: Eckenstein et al., 1988, Lysakowski et al., 1989. Coppola and Disney, 2018a

	Layer I	Layer II	Layer III	Layer IV	Layer V	Layer VI
Macaque FC	++	+	-	-	-/+	-
Macaque A1	+	-	-/+	++	-	-
Rat A1	++	-	++	++*		-
Rat V1	++	-	-	++*		-
Cat V1	++	+	+	+	+	+
Cat M1	++	++	++/-	-	+/-	-

Table 3: Laminar variations in choline acetyltransferase fiber immunoreactivity across species and area ++ indicates densest innervation of cholinergic axons, + indicates moderate innervation, - indicates lightest innervation, * indicates the transition at the border between two layers, / indicates a transition within the superficial and deep portions of a layer. Data for rat: Lysakowski et al., 1989; cat: Avendaño et al., 1996; macaque: Campbell et al., 1987; Lewis, 1991. Coppola and Disney, 2018a

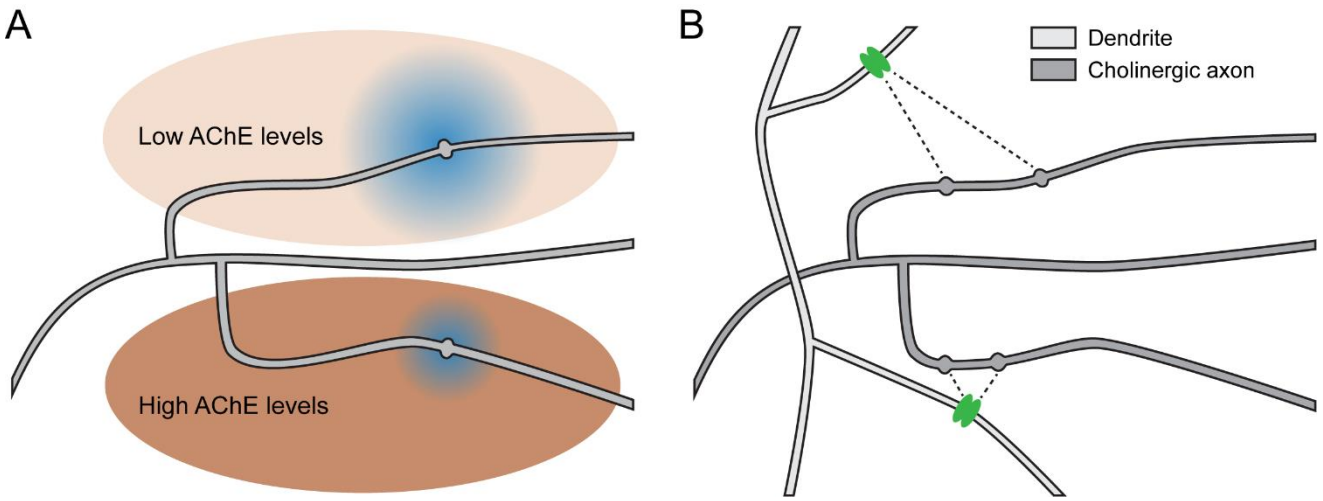

Figure 3-7: Acetylcholine diffusion, binding, and degradation
Examples show axonal varicosities releasing acetylcholine into a volume of tissue. A depicts the effect of acetylcholinesterase (AChE) levels on molecular diffusion. In regions of low AChE concentration (light brown), acetylcholine diffuses over a greater area whereas in regions of high AChE concentration (dark brown), acetylcholine has a more limited area of diffusion. Blue clouds depict the distance over which acetylcholine can diffuse in each region. B depicts the distance (dashed lines) between varicosities and receptors (green). Molecules are more likely to bind to nearby receptors than to distant receptors. Coppola et al., 2016

Furthermore, within these regions, AChE expression is highest in layers 3c and 4 (Kaas and Hackett, 2000). In association cortex of humans, layer 4 has lowest AChE expression and layer 1, 2, and superficial 3 contain the highest (Mesulam and Geula, 1992). In macaque V1, AChE fibers are most dense in layers 1, 4a, 4c, and 6b (Hedreen et al., 1984), however, another study reports similarly high levels of AChE in the deep layers but a less densely stained layer 1 (Mesulam et al., 1984). In this study, macaque V1 shows very similar expression to A1 and primary somatosensory cortex S1 as well (Mesulam et al., 1984). Interestingly, these studies in macaque show somewhat opposite results of what we see in LIP, in which the supragranular layers are more densely stained, especially in layer 1, compared to lower levels.

A particularly interesting location in LIP is the layer 3/4 border that exhibits a dip in AChE expression (sometimes the lowest point in all the layers) that then steeply increased in layer 4. At this location, it would seem that ACh molecules would be much more able to diffuse over time and through the space of the tissue, perhaps even diffusing across the laminar boundary into layer 4. This is interesting given that layer 4 is the thalamocortical recipient, granular layer and functionally distinct from other layers. It is also interesting that there is such a large difference in upper and lower layer 3, perhaps hinting at functional subdivisions within layer 3. This makes sense given how large this layer is in LIP.

Aside from comparing LIP AChE and ChAT levels to those described in other areas, an important comparison is that of AChE to ChAT within an area. This is because a neuromodulatory signal is reliant on at least two features of the local circuitry, the capability of ACh release in an area (ChAT) and the capability of ACh degradation in that area (AChE). Together, these two mechanisms shape the resulting cholinergic signal across layers and areas, and as we have seen, can vary independent of each other. In LIP, I find that both AChE and ChAT are highest in superficial layers. However, in the deeper layers, AChE levels remain high, while ChAT levels continue to decline. This means that, compared to superficial layers, the spread of the cholinergic signal in deeper layers will be more restricted, with less dense innervation to begin with, followed by a high capacity to break down the ACh that is released. As such, the cholinergic signal in the deeper layers may be more spatially and temporally precise. A functional difference between the upper and lower layers in LIP is their laminar connections. For example, the upper layers of LIP carry information between other cortical areas, such as the lateral prefrontal areas. The deeper layers, in contrast, send information to subcortical structures such as the intermediate and deep layers of the superior colliculus (Lynch et al., 1985). This subcortical pathway is thought to be activated in advance of saccade initiation, as a transitional step between sensory and motor processing (Paré and Wurtz, 2001). The upper layers, instead, maintain feedback connections with other cortical areas, for example, receiving projections from the frontal areas 46 and 8 to receive ongoing information about oculomotor commands and attentional processes (Stanton et al., 1995; Medalla and Barbas, 2006). Perhaps the information traveling from LIP to subcortical structures needs to be more precise (having less spatial and temporal flexibility) compared to the upper layers that communicate intracortically, mostly receiving feedback.

The degree to which ACh can be delivered to and cleared from an area is an important indicator of cholinergic tone. One way to measure actual cholinergic tone in cortex is through *in vivo* recordings of ACh in the macaque. This is the subject of the following chapter.

Chapter 4

Measures of the local cholinergic tone *in vivo* in macaque cortex

4.1 Introduction

The preceding anatomical experiments build upon literature detailing receptor expression and cholinergic innervation and clean up across cortical areas. These measures, together, provide information describing two critical points in signal transmission: release and signal termination (either through hydrolysis or through receptor binding). Still missing, however, is a description of the concentration dynamics of the signaling molecules themselves that transfer signal from axon to receptor. While data describing modulatory innervation to cortex is critical in understanding the capacity for synthesis and release, previous work investigating cortical innervation density of dopamine, serotonin, and noradrenaline can only partly (if at all) predict the respective molecule concentration within the tissue (Ward et al., 2018). As such, innervation patterns cannot be used as a proxy for molecular concentration as they traditionally have. Instead, the neurochemical environment itself must be studied. This is important especially considering neuromodulatory systems signal party through volume transmission. Because molecules, once released, may continue to diffuse through cortical tissue, the instantaneous extracellular concentration of signaling molecules represents a critical feature of cortical circuits. Importantly, extracellular modulatory levels have been shown to differ across cortex.

For example, baseline ACh levels in anesthetized rats are highest in the medial prefrontal cortex relative to visual cortex and somatosensory cortex (Fournier et al., 2004 but see Sarter and Bruno, 1997). Further, a recent study by Ward et al. (2018) suggests visual (occipital) and sensorimotor (parietal) areas comprise separate neurochemical groupings. Specifically, this study used cluster analysis to examine how similar cortical regions are to each other in terms of the dopaminergic, serotonergic, and noradrenergic chemical "signatures." The cluster analysis revealed that areas within in the parietal region represent a separate neurochemical cluster than areas within the occipital region, specifically with monoamine concentrations being lower in V1 compared to those in the parietal cortex. This study did not include ACh, but because there are already data to describe anatomical differences between the cholinergic systems in V1 and parietal areas (Chapters 2 and 3), it will be interesting to see how, if at all, their neurochemical environments differ. We can investigate cholinergic concentrations *in vivo* through microdialysis. This widely-used method samples and collects small molecules diffusing through the tissue. Because this method is based on molecular diffusion, in carefully designed experiments, the concentration in the sample will reflect the concentration in the tissue, thus providing information to describe concentration dynamics in the brain on slow timescales. Investigating the neurochemical environments across cortical areas using microdialysis can provide a measure of local neuromodulatory tone.

To obtain neurochemical data describing extracellular cholinergic levels in primate cortex, we performed concurrent microdialysis sampling from occipital and parietal cortices of an awake, behaving macaque. Detailed anatomical data in addition to *in vivo* microdialysis can provide better insight to the dynamical neurochemical environments across cortex.

4.2 Methods and materials

4.2a Animals

We used one male, macaque monkey (Animal 5, Appendix A) who was 9 years old at the time of recordings. We recorded from the right hemisphere. This animal also provided tissue that was used for anatomical studies in Chapters 2 and 3.

4.2b Defining regions of interest

To collect data from the posterior parietal cortex (where LIP is located), we placed a microdialysis probe through a cranial chamber previously implanted as part of an unrelated experiment for a brainstem nucleus. As a part of that experiment, we used MRI imaging to guide placement of the chamber and to predict the required point of insertion needed to reach the nucleus. Building upon this initial prediction, we systematically mapped white/gray matter boundaries beneath the chamber to a depth of 30 mm. We cross-referenced these measurements with macaque brain atlases in order to approximate the location of LIP (Paxinos et al., 2000b; Saleem and Logothetis, 2012). The atlas registration indicates our sampling region to most likely be at LIP or at neighboring medial intraparietal region MIP. For microdialysis recordings in V1, we used a second chamber placed over the opercular surface of cortex. The placement of this chamber was based on intraoperative estimations of the position of the lunate sulcus as intersecting the midline 2.7 cm anterior to the occipital ridge. The placement was confirmed by prior physiological recording and post mortem histological reconstruction, which together showed that the chamber was positioned entirely over V1. We concurrently measured ACh levels in chambers covering the parietal cortex and the occipital cortex (Figure 4-1).

4.2c Sample collection

In an awake, head fixed macaque, we used a hydraulic micromanipulator (Narishige; #MO-97A) outfitted with a custom-made adaptor (Figure 4-2) to position a microdialysis probe with a 2mm active surface (BASi; #MD-2200) in the center of each chamber. The adaptor consisted of a 6 mm tapered guide tube (designed to penetrate dura) attached to a 3D-printed plastic spacer that separated the large head of the microdialysis probe from the microdrive. The guide tube and probe were advanced together through the dura, the guide protecting the fragile active surface, and then, once in position, we retracted the guide tube 4 mm such that active surface of the microdialysis probe traversed the ~2 mm of cortex directly beneath the dura. We collected samples by infusing sterile artificial cerebrospinal fluid (aCSF) consisting of 90% sodium chloride, 5% calcium chloride dihyrdate, 3% magnesium chloride hexahydrate, and 2% potassium chloride (pH 6) at a flow rate of 1 µl/min. We collected samples in aliquots containing an antioxidant solution consisting of 10% glacial acetic acid, 3.5% L-cysteine, and 0.5% ethylenediaminetetraacetic acid (EDTA) in aCSF held in a container of dry ice. Each aliquot represented 20 minutes of sampling time. In order to investigate sensory-related release, the room illumination was cycled between “dark” and “light” periods (Table 4). During “dark” periods, the animal was in complete darkness. During “light” periods, the animal was free to watch the children’s cartoon Rolie Polie Olie (Nelvana and Sparx; Canada) on a projector screen. We collected samples on two days for 320 minutes each day. This included the initial 2 hours immediately following probe insertion. This is notable because our own pilot studies show that damage-related neurotransmitter release returns to baseline following this time period (Figure 4-3). As such, we tracked which samples occurred during and after this time. Following collection, we transported samples to a -80°C freezer for storage. We then submitted samples to Duke University’s Proteomics and Metabolomics Shared Resource (DPMSR) where liquid chromatography combined with mass spectrometry (LC-MS/MS) was used to analyze the chemical composition

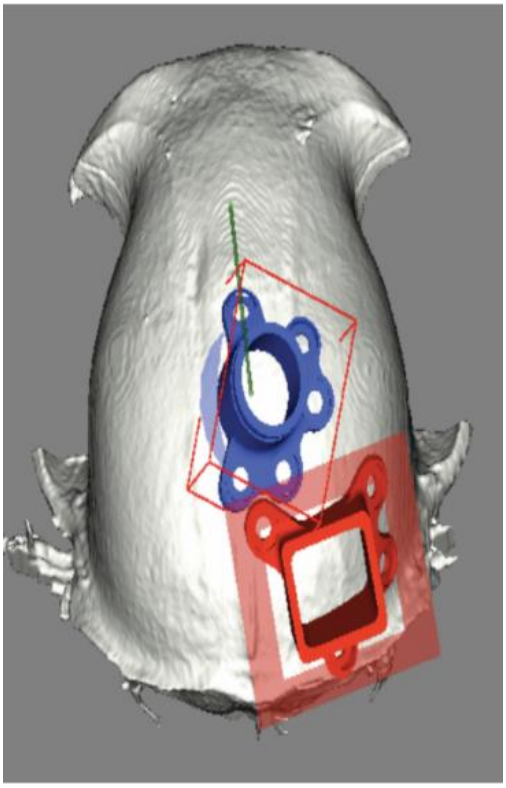

Figure 4-1: Microdialysis head chambers
Rendering of Animal 5's skull created using MRI data. The locations of the parietal chamber shown in blue and the occipital chamber shown in red.

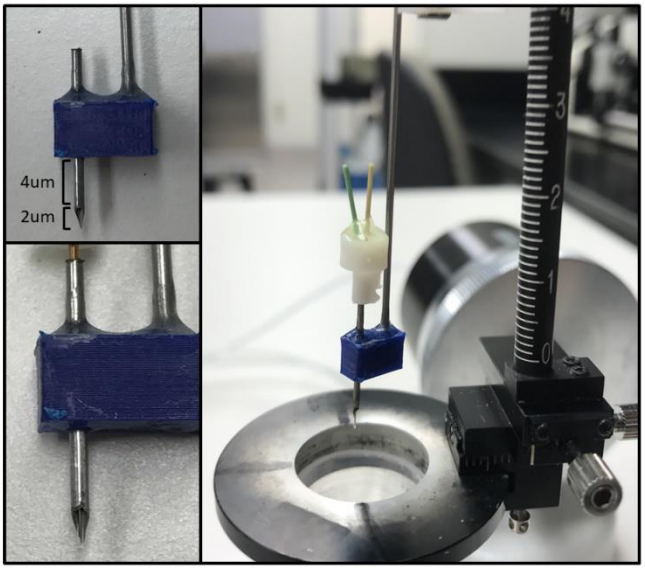

Figure 4-2: Microdialysis probe adaptor
Custom-made adaptor consisting of a 6 mm tapered guide tube attached to a plastic spacer.

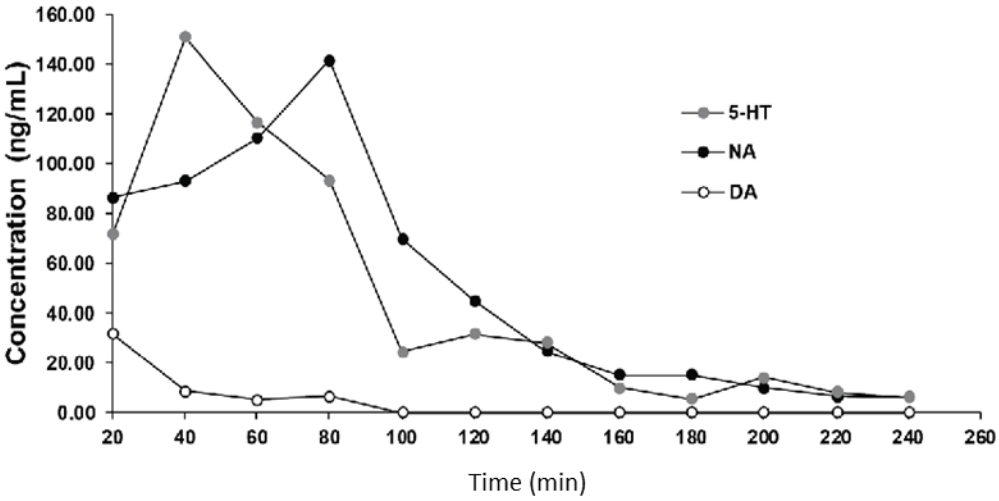

Figure 4-3: Neuromodulator concentrations *in vivo*
Mass spectroscopic measurement of *in vivo* monoamine (serotonin, noradrenaline, dopamine) samples collected by microdialysis in V1 of an awake rhesus macaque.

of the dialysates. As a control, standard samples containing known ACh levels (positive control) and samples containing only aCSF fluid (negative control) were also submitted for neurochemical analysis.

4.2d Sample analysis

aCSF and antioxidant mixture were prepared according to the recipe described above. Calibration matrix was prepared by mixing aCSF and antioxidant mixture 4/1 v/v (2 ml antioxidant to 8 ml aCSF). A calibration stock solution containing nominally 2 mM ACh was previously prepared and stored in small aliquots at -80°C. The calibration stock solution was thawed at 23°C and diluted with calibration matrix in two steps to yield a 400 nM concentration calibration solution. Serial dilutions of either 2x or 5x were performed to generate a 9-point calibration curve extending to 0.25 nM concentration. Calibration matrix was used as the blank samples.

Preparation of samples, calibration standards, and two blank samples proceeded in parallel following a benzoyl chloride derivatization protocol adapted from Wong et al. (2016). Samples were prepared and analyzed in a blinded manner, and only unblinded during data workup. The samples were stored at -80°C and thawed at 23°C. Each sample was vortexed and centrifuged briefly using a benchtop microfuge (Corning). Ten microliters from each sample, calibration solution, and blank was pipetted into a new, tube (Eppendorf, Hamburg, Germany). All samples were then vacuum-dried for 4 hours at 30°C in a Vacufuge (Eppendorf) and stored at 4°C overnight. Derivatization of samples was performed by mixing 3 volumes 0.167 M sodium carbonate (Sigma, pH>11) with 1 volume 200 nM stable-isotope labeled ACh in a mixture of 80/20 100 mM ammonium bicarbonate (Sigma)/acetonitrile (Fisher, LC-MS grade), and adding 20 µl of this reconstitution buffer (RB) to each sample, calibration standard, and blank.

The samples were vortexed to resuspend the analytes, and the liquid was settled in the bottom of the tubes by a brief centrifugation with a benchtop microfuge. Five microliters of 2% v/v benzoyl chloride (Sigma) in acetonitrile was then added to each sample. The derivatization reaction was allowed to proceed by incubating the samples in a Thermomixer (Eppendorf) for 30 minutes at 30°C and 600 rpm. The reaction was quenched by the addition of 1 µL 50% aqueous trifluoroacetic acid (Thermo, LC-MS grade ampule). The samples were then briefly centrifuged on the benchtop microfuge. Each sample was transferred to a labeled Total Recovery Vial (Waters) for LC-MS/MS analysis.

The analytical LC-MS/MS method was performed on an Acquity UPLC coupled to Xevo TQ-S mass spectrometer. Separation was optimized for speed of separation for four compounds (ACh, noradrenaline, serotonin, and dopamine), while maintaining analytical selectivity. The Wong et al. paper utilized a 20 minute separation, which was shortened to 3 minutes (6 minutes run total) for this analysis. Mobile phase A consists of 10 mM ammonium formate with 0.15% formic acid in water, while mobile phase B is acetonitrile. A 1 mm x 100 mm BEH C18 1.7 µm column (Waters) with a flow rate of 0.12 ml/min and column temperature of 27°C was utilized. The gradient was as follows: 3% B at 0 min, 20% B at 0.05 min, 95% B at 3 mins, 95% B at 3.5 min, 3% B at 3.6 min, and held at 3% B until 6 minutes. A 5 µl injection of sample was used for analysis, and introduced via ESI+ ionization for tandem mass spectrometry (3.0 kV, 400C desolvation, 400 L/hr N2 desolvation gas, 150 L/hr cone gas, 7 bar nebulizer). Collision energy was optimized for the Xevo TQ-S and MS/MS transitions were selected from Song et al. (2011) and verified for specificity. Data analysis was performed in Skyline -daily 19.0.9.149 (www.skyline.ms) using small molecule mode, including peak extraction and quantification. Each analyte was quantified versus a linear regression against a calibration curve with 1/x weighting.

4.2e Data analysis

To quantify and examine differences in magnitude of ACh levels *in vivo*, we first report raw ACh concentration data (nM). Then, to examine differences in the temporal profile of these concentrations, we baseline-subtracted and normalized the raw data separately for each cortical area and each recording day. This yields a scale from 0-1, 0 being the minimum ACh concentration observed for a given brain area on a given day (e.g. in occipital cortex on recording day 1) and 1 being the corresponding area and daily maximum concentration. Finally, to quantify differences between light and dark cycles, we averaged the normalize data during periods of light and during periods of darkness across both recording days. We did not include the initial 120 minutes of recording time in this averaging, as those data represent the "settle period" in which the room illumination was not being cycled and damage related release contaminates sample data (described above and in Table 4).

4.3 Results

In an awake, behaving, macaque monkey, we concurrently collected microdialysis samples from two areas: the occipital cortex and the parietal cortex. We measured extracellular ACh levels across 320 minutes for two days each. Our results indicate that ACh levels in the parietal cortex are higher in magnitude and differ in temporal profile compared to ACh levels in the occipital cortex.

4.3a ACh concentration in parietal cortex

Recordings from the parietal chamber show that ACh concentrations fluctuate between approximately 20 nM to 30 nM across day one and 20 nM to 35 nM across day two of sample collection (Figure 4-4) yielding a concentration dynamic range of 10-15 nM for cholinergic tone. For both days, ACh concentration is higher at the beginning of the recording sessions and decreases over time, although on day one, there is a spike in concentration near the end of the recording session. There are peaks in concentration levels at 80 minutes and 260 minutes (during a light period) on day one and 60 minutes and 140 minutes (during a dark period) on day two (but note that 0-120 minutes includes the settle period). On day one, the lowest concentration occurs between 220-240 minutes (a dark period); on day two, this occurs between 240-280 minutes (a light period). Our averaged light/dark analysis shows that ACh concentrations tend to be higher during periods of light (Figure 4-5). This study was designed to study differences between cortical areas, not behavioral conditions and so is under-powered for determining the statistical significance of the trend-level differences between light and dark periods.

4.3b ACh concentrations in occipital cortex

Recordings from the occipital cortex show that ACh concentrations are low (Figure 4-4). On day one, there is a notably high concentration between 20-40 minutes (during the settle period). Aside from this peak that reaches almost 10 nM, ACh levels range between 0.7-5 nM. On day two, ACh levels are consistently between 2-5 nM, yielding a dynamic range of 3-4 nM for cholinergic tone in V1. Our averaged light/dark analysis shows that ACh concentrations again tend to be higher during periods of light (Figure 4-5). The specific concentration dynamics differ between occipital and parietal cortex as well, such that the occipital data cannot obviously be predicted from knowledge of the parietal data. For example, the peaks and troughs in occipital cortex are at different time points than those observed in the parietal cortex on the same day (Figure 4-6). On recording day one, we can see a peak at ~160 minutes in the parietal cortex, but at this same time point, occipital cortex is

Time (min)	Experimental condition
0-120	Settle Period
120-140	dark
140-160	dark
160-180	light
180-200	light
200-220	dark
220-240	dark
240-260	light
260-280	light
280-300	dark
300-320	dark

Table 4: Light and dark periods during microdialysis sessions
A 120-minute settle period followed by cycles of light and dark phases. During dark phases, the animal was in complete darkness. During light phases, the animal watched a cartoon.

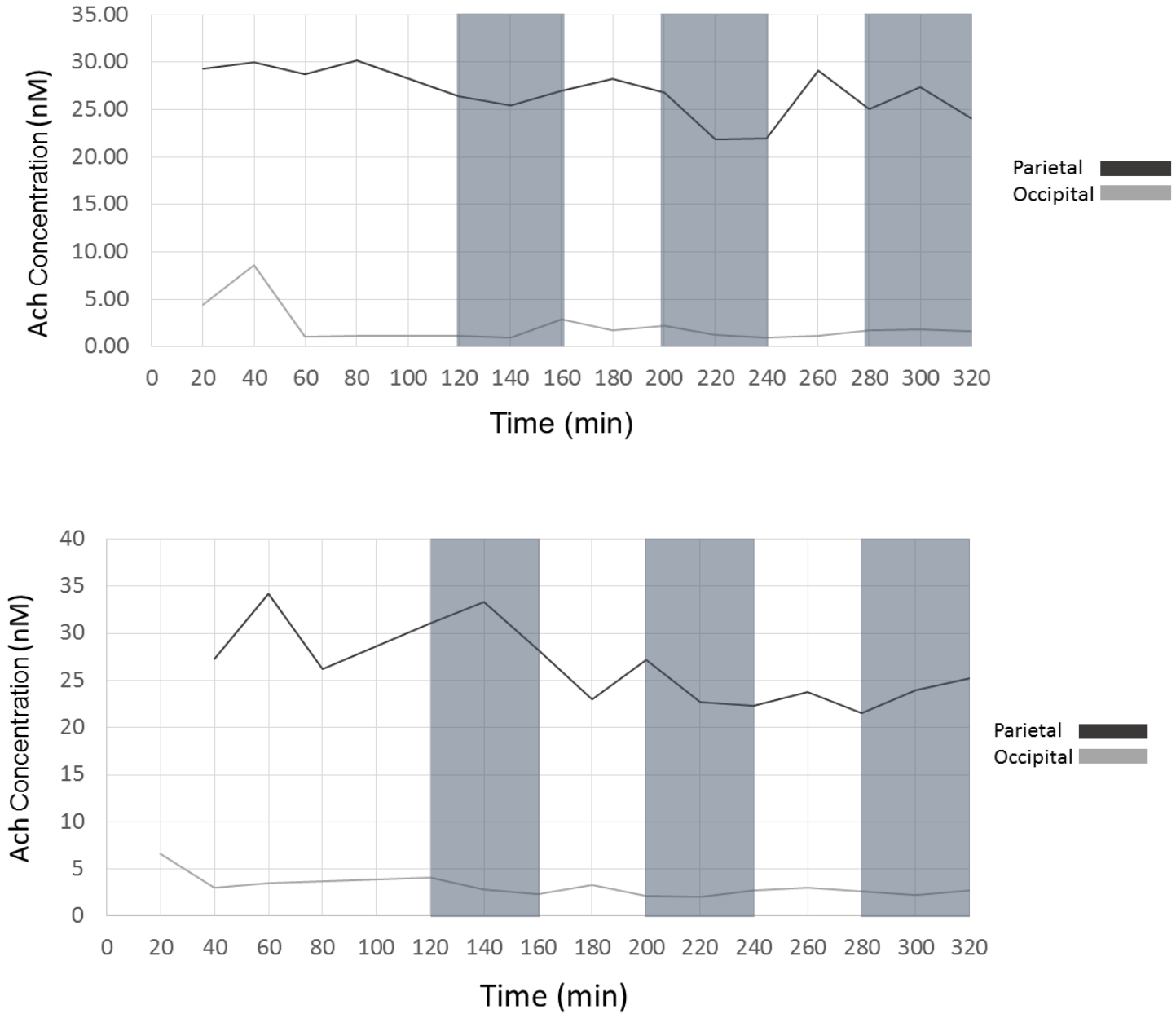

Figure 4-4: Acetylcholine concentrations
Acetylcholine concentration (nM) over time (minutes). Dark lines represent concentrations from parietal cortex, light lines represent concentrations from occipital cortex. Gray bars behind graphs mark times when the subject was in darkness. Recording day 1 (top), recording day 2 (bottom).

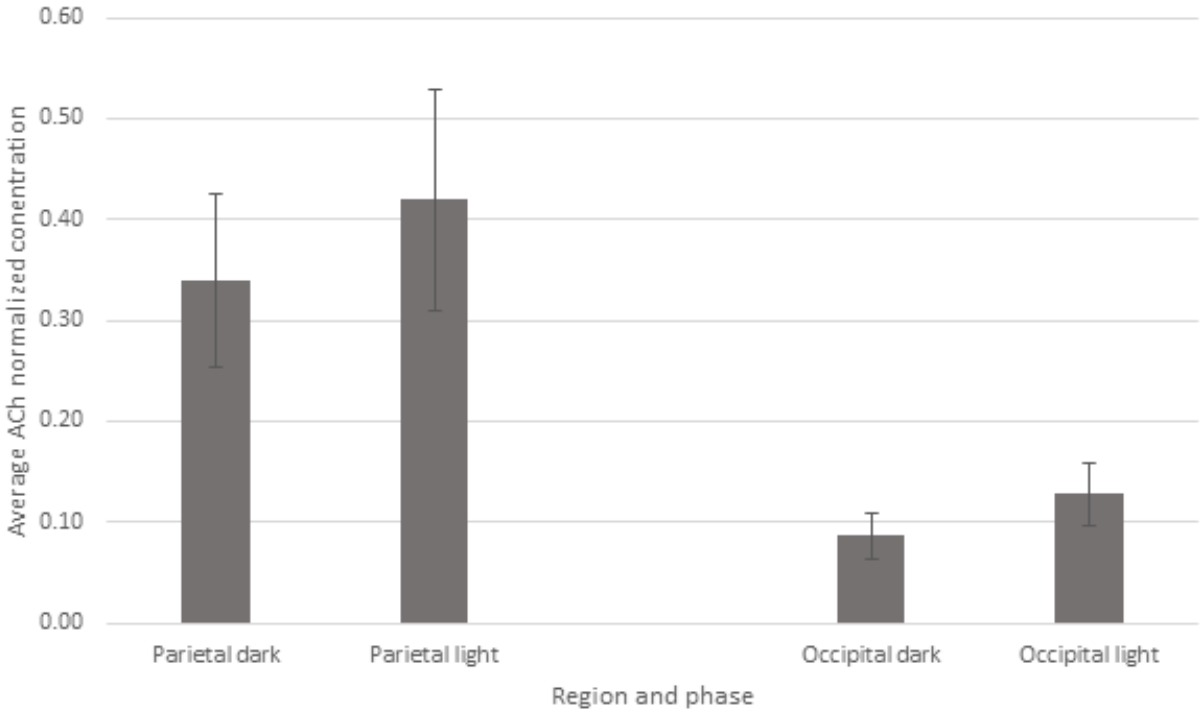

Figure 4-5: Acetylcholine concentrations in times of darkness and light
Averages of normalized acetylcholine concentrations across region (parietal versus occipital cortex) and phase (darkness versus light). Error bars = 2x standard error of the mean.

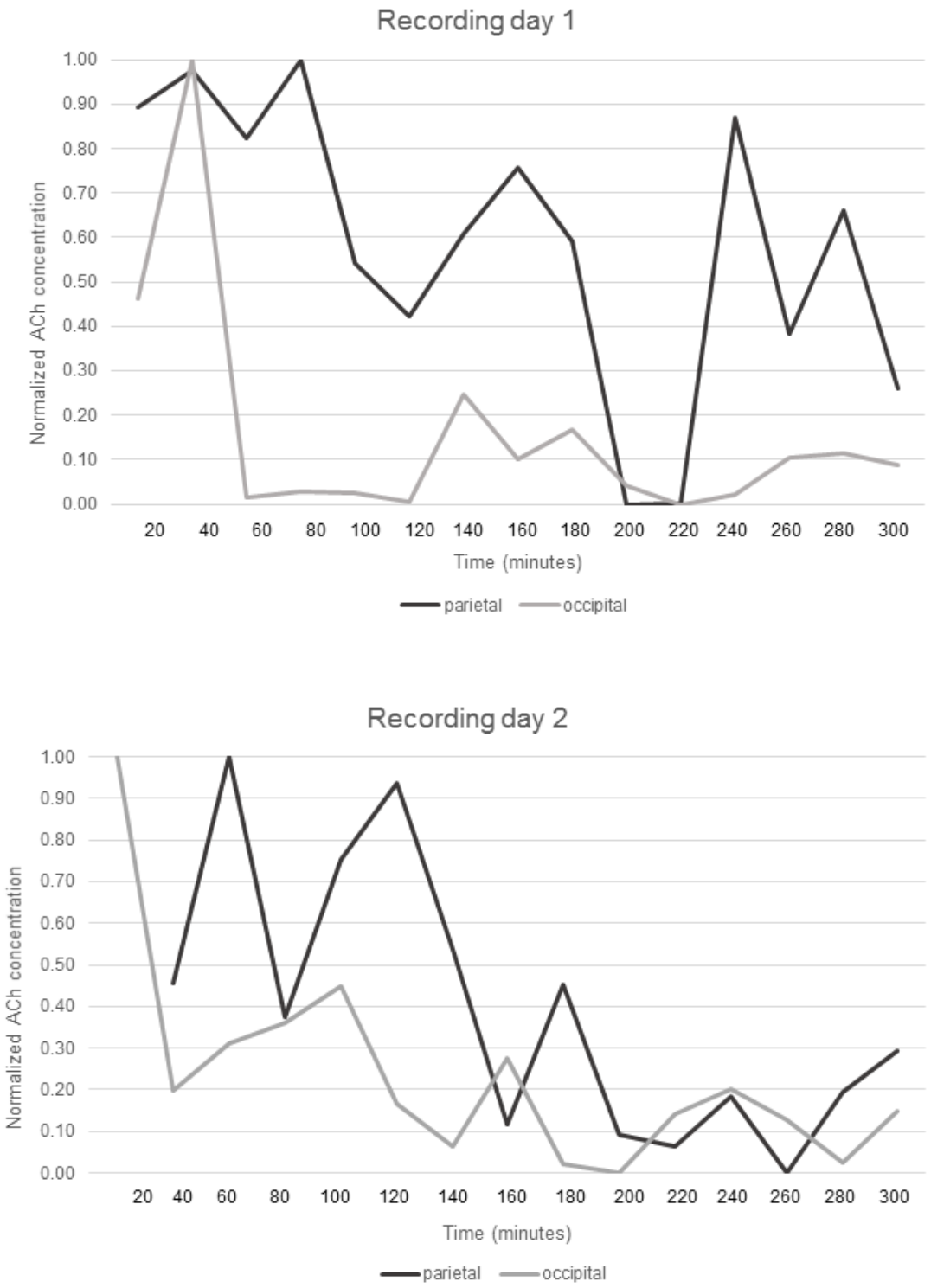

Figure 4-6: Normalized acetylcholine concentrations
Normalized acetylcholine concentration across time (minutes). Dark line represents concentrations from the parietal cortex, light line represents concentrations from the occipital cortex.

showing a trough. The same is true at ~160 minutes on recording day two, but with occipital cortex concentrations exhibiting a peak and parietal cortex exhibiting a trough. There are shared temporal features as well, however. For example, on day two, both parietal and occipital cortices exhibit a peak at 240 minutes. That peak is wider in occipital cortex than in parietal cortex (concentrations in the occipital cortex are remaining higher over a longer time compared to parietal cortex at that time point). Similarly, both areas exhibit a trough at 220 minutes on recording day 1, but with levels remaining low in the occipital cortex over a longer period than in the parietal cortex.

4.4 Discussion

Overall, I find that ACh concentrations are higher in the parietal cortex than they are in the occipital cortex (Figure 4-4). In terms of absolute magnitude, this holds true regardless of session duration, recording day, or periods of light/darkness. In fact, the maximum concentration observed in the occipital cortex, even immediately after probe insertion, is still half that of the lowest levels observed in the parietal cortex. This is notable given that upon probe insertion, cellular membranes are damaged, releasing their contents into the extracellular space. The settle period allows time for the tissue to repair itself and for extracellular levels to return to baseline. The reason we avoid interpreting concentrations at this time is because our results are contaminated by this large-scale molecular release that would not occur otherwise (if the cell membranes remained intact). In this context, it is worth noting that even during the settle period for the occipital cortex, ACh levels are so much lower than for the baseline period parietal ACh levels, indicating that even with a sudden damage-related event, the occipital cortex is not able to release nearly as much ACh as parietal cortex.

I also find that both occipital and parietal cortices show trends towards higher ACh concentrations during periods of light (and free viewing of a cartoon) compared to darkness (Figure 4-5). While we have too few data points to investigate this fully, a possible explanation for the higher averages in the parietal cortex could be due to a longer recovery time from probe insertion compared to recovery time in the occipital cortex. This is observable in the normalized data from recording day 2 (Figure 4-6) showing parietal values are still relatively high at 140 minutes (which occurs after the settle period) compared to occipital cortex, which recovers by that time point. While both recording days show occipital cortex recovering from initial spikes in concentration fairly early (40-60 minutes), it is difficult to determine without more data if this is a feature of occipital cortex or a sampling artifact. It would be interesting if occipital areas are able to recover more quickly from tissue damage compared to other cortical areas, although I am unaware of any data to support this.

Perhaps most interestingly, the two areas exhibit a difference in concentration dynamics (Figure 4-6). As we have seen from the normalized data, the temporal profiles of ACh concentration in occipital and parietal cortex are not the same. We can see peaks and troughs in one area that do not correspond (in timing or duration) to peaks and troughs in the other area. Importantly, the temporal profiles are also not simply a vertical translation or inverse of each other. For example, we do see some time points that show similar ACh dynamics in parietal and occipital cortices. That the temporal profiles are not the inverse of each other can be further supported by the differences in duration of peaks and troughs. Thus the temporal dynamics are such that the two cortical areas are not exposed to the same temporal signal, simply at different magnitude (i.e. we cannot obtain the parietal cortex data by applying a simple baseline offset to the occipital data).

Differences in magnitude alone could be explained by anatomical data regarding the cholinergic innervation and clean up for occipital versus parietal cortex. As we have discussed, there are data to show that in the occipital cortex, AChE levels are higher compared to other cortical areas, and that the occipital cortex has a less dense cholinergic innervation compared to other cortical areas (Mesulam et al., 1984; Mesulam et al., 1992). This means that in the occipital cortex, compared to the parietal cortex for example, there is less ACh being delivered and also a stronger capacity for ACh degradation once released. This would lead to the prediction that extracellular ACh levels in occipital cortex are lower in concentration compared to cortical

regions with more innervation and a lower capacity to terminate the signal (like in the parietal cortex). This is in line with our results that show ACh concentration is lower in the occipital cortex compared to parietal cortex.

Differences in temporal dynamics could partially be explained by differences in basal forebrain topography, which we know has broadly different innervating regions for occipital and parietal regions (Chapter 1). Our current data cannot distinguish between differences in dynamics that arise from basal forebrain topography or that arise from local cortical modification (or some combination of both). Our data do indicate, however, that there is no identifiably "global" signal such that two different cortical areas (in our case, parietal and occipital cortex) would maintain the same cholinergic signals (at least on the slow timescales observable using microdialysis). Another study reports microdialysis measurements in the cortex of an awake, rhesus macaque. This study shows a mean ACh concentration in prefrontal cortex of 10.3 nM +/- 3.0 (Zhang et al., 2007). This figure for prefrontal cortex is different from what we report here for both cortical areas: ~30 nM in parietal cortex and ~5 nM in occipital cortex. Previous theories regarding cholinergic actions in cortex have assumed a more global signal for ACh, for example, ambient ACh levels over large regions of cortex that support sleep/wake cycles, et cetera. (Descarries et al., 1997). Regardless of the origin of the differences in temporal dynamics (either basal forebrain topography, local modification, or something else), we can say based on our data that occipital and parietal cortices exhibit heterogeneous, non-global cholinergic signals.

Extracelluar differences in ACh concentration and its temporal profile are interesting because these differences can affect the way ACh interacts with the local circuitry. For example, modulatory signaling will depend partly upon the distance that separates a release site and a receptor (Muñoz and Rudy, 2014). Because signaling by ACh is usually not synaptic, increasing the distance between varicosities and receptors is expected to decrease the likelihood of a molecule binding to a receptor (Figure 3-7B). Thus, the extracellular concentrations of a molecule as it relates to distance from release site to nearest receptor can affect subsequent binding of ACh. Additionally, affinity for ACh differs across receptor subtypes, meaning that the instantaneous local ACh concentration may activate only certain subtypes of receptors. In the case of mAChRs, m2 and m4 receptors exhibit higher affinity for ACh than do m1, m3, and m5 receptors (Kuczewski et al., 2005). Similarly, the rate at which receptors desensitize will be related to extracellular ACh. For example, α7-containing nicotinic receptors become desensitized to ACh quickly, resulting in a decreased capacity for continuous cholinergic modulation at higher concentrations. Non-α7-containing nicotinic receptors, however, desensitize more slowly, which likely results in prolonged cholinergic modulation. As such, modulatory signaling can differ in type and can range from more rapid to more prolonged depending on the concentration-dependent recruitment of specific receptor subtypes.

However, it is difficult to predict what our observed differences mean for ACh's interaction with local cortex because microdialysis is limited in its spatial and temporal resolution (at the level of ~2 mm and over a course of 20 minutes). For example, at varicosities immediately following release, ACh concentration will be much higher compared to concentrations following diffusion. Further, we cannot know if there are any laminar differences or instances in time of more/less release. While these questions will require more finely resolved methods, we can show that the occipital and parietal cortices maintain unique cholinergic tones, not indicative of a completely global signal as has been traditionally ascribed of ACh.

In the previous chapters, I have characterized key anatomical features in the parietal cortex of the macaque (m1AChR expression by cell type, cholinergic innervation density and clean up capabilities, *in vivo* cholinergic tone). I have described how these features differ across cortical areas and across layers. Importantly, I have also discussed ways in which these varying anatomical characteristics might shape the resulting cholinergic tone. Given data such as these, we have recently proposed the existence of neuromodulatory compartments in cortex that can be defined by variation in structural features of the local receiving circuitry (Coppola et al., 2016). Further, we argue that these compartments are responsible for local regulation of neuromodulatory tone. This is the subject of the following chapter.

Chapter 5

Neuromodulatory compartments in cortex

5.1 Introduction

Chemical signaling between neurons is often viewed as a relatively simple relationship in which an action potential in one neuron leads to signal transduction in another neuron. In classical synaptic transmission, action potentials travel to the axon terminal, where signaling molecules are released into the synapse, across which they will diffuse and subsequently bind to postsynaptic receptors, thereby transmitting a neural signal. This type of "point-to-point" transmission generally results in a signal that is both temporally and spatially precise.

Synapses open signaling to local modification. We have proposed that in the case of diffuse communication by long-range neuromodulatory systems, there are many more opportunities to violate an assumption of a tightly coupled relationship between signal sent (by presynaptic neurons) and signal received (at postsynaptic neurons). In neuromodulatory systems signaling via non-synaptic transmission (such as the cholinergic system, described above), mechanisms exist that can alter the coupling between action potentials (spikes) at the soma and the resulting response in local cortical circuits. Features such as patterns of axonal innervation, tissue tortuosity and molecular diffusion, effectiveness of degradation and reuptake pathways, subcellular receptor localization, and patterns of receptor expression across the local receiving circuit can offer the capacity to locally modify long-range communication between neurons.

In much of the literature exploring the spatial and temporal scale of modulatory signaling, there is an implicit assumption that the number of neurons in the innervating modulatory structure defines an upper limit on the size of a uniquely modulated compartment in cortex. Here, I argue that local characteristics of cortical circuits can loosen spike-response coupling and introduce locally specific responses to broadcast modulatory signals, thereby creating small neuromodulatory compartments in cortex without increasing neuron numbers in subcortical structures. I further argue that the signaling between these compartments can vary considerably and that compartments have the ability to regulate their own modulatory input leading to a two-way, interactive communication. As such, the circuit itself can influence the modulatory signals that regulate its activity.

5.2 Evidence for compartments in cortex

A neuromodulatory compartment is a region of tissue, defined anatomically, within which modulatory conditions are predicted to be relatively uniform and between which modulatory conditions may differ profoundly. It is likely that the anatomical characteristics that define compartments shape the way ACh interacts with cortical circuitry and can provide a capacity for local modification of neuromodulatory inputs. In the following sections, I will provide evidence for differences in anatomical characteristics across cortex.

5.2a Axonal innervation

All chemical communication between cells provides an opportunity for a signal to be modified. In volume transmission, however, there is a greater opportunity for signal modification as a result of the time and distance over which the modulatory molecule is able to diffuse. That is, local features of the receiving circuit have the ability to influence cortical modulation, both across and within regions. As we have learned from Chapter 3, many regions exhibit areal and laminar differences in their density of ChAT-ir axons (Tables 2 and 3). This provides evidence that an early facet of the neuromodulatory process—the ability to deliver ACh to an area—differs across region, highlighting the degree to which each area can be exposed to ACh.

5.2b The extracellular space: diffusion and tortuosity

The region of tissue over which a neuromodulatory molecule, once released, can exert its influence is limited in part by features of the extracellular space (ECS). The ECS is composed of regions of tissue that separate one cell from another. Functionally, the ECS forms a channel for the movement of molecules, including neuromodulators. In the case of neuromodulators such as ACh, which participate in volume transmission, it is important to understand how these molecules move through the ECS. The ECS is estimated to compose between 20 and 25% of the normal adult brain volume *in vivo* (Syková and Vargová, 2008). ECS morphology likely varies within and across brain regions, imparting region-specific signaling potential upon molecules that communicate in a diffuse manner (McBain et al., 1990; Kinney et al., 2013). Characteristics of the ECS, therefore, partially define neuromodulatory compartments.

Once released into the ECS, the volume of tissue within which a neuromodulator can exert its effects is determined by a number of factors. The first is that movement of these neuromodulators through the ECS is by diffusion. This diffusion is influenced by the presence of structures such as cell membranes that serve as physical barriers to molecular movement. The degree to which physical features of the tissue impede diffusion of a molecule is referred to as the "tissue tortuosity." Similarly, local cellular topology influences characteristics of the ECS. For example, ECS domains can be classified as being sheet-like or tunnel-like (Figure 5-1A; (Kinney et al., 2013). These ECS domains are believed to differently influence molecular diffusion, with molecules diffusing more slowly through sheets than tunnels. Such sheet and tunnel characteristics are non-uniformly distributed throughout the ECS, and thus may also create unique neuromodulatory compartments. Neural tissue also requires the presence of biochemical components in the ECS that, among other functions, form a matrix that serves as a cellular scaffold. This matrix contains long-chain macromolecules that can either be tethered to the cell surface or float freely in the ECS (Bignami and Asher, 1992; Syková and Nicholson, 2008). In either case, the presence of these macromolecules can further hinder diffusion (Figure 5-1B). Altogether, variations in extracellular matrix composition and structure will contribute to differences in the ability of neuromodulators to diffuse throughout certain microenvironments, thereby altering local neuromodulation.

Given that the brain exhibits structural plasticity, it is unsurprising that ECS characteristics do not remain static across time. The extracellular volume fraction in the hippocampus decreases during early postnatal development until it reaches a value similar to that seen in adults (Fiala et al., 1998). Alterations of the brain due to pathology are also known to affect ECS parameters (Nicholson and Syková, 1998). ECS volume decreases in response to nerve stimulation (Svoboda and Syková, 1991), and the magnitude of this reduction in volume is related to the frequency and duration of stimulation. Thus, the tendency of a region of tissue toward activity may further influence the dynamics of neuromodulator diffusion.

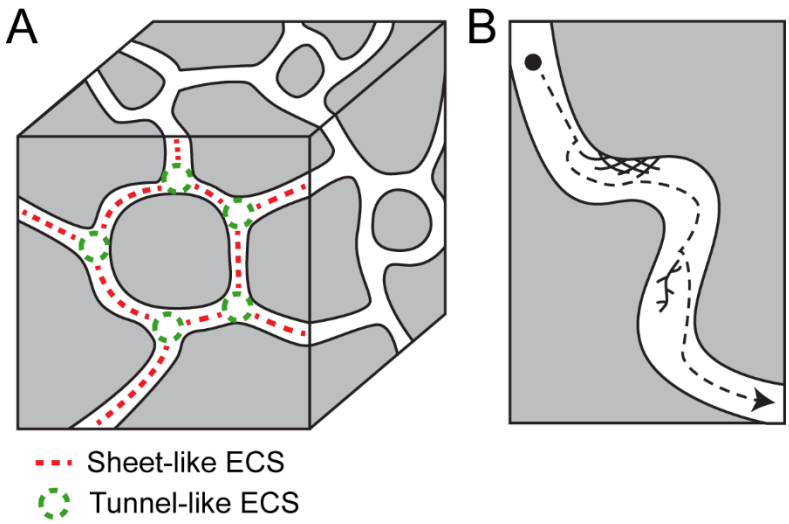

Figure 5-1: Physical characteristics of the extracellular space
A is a representation of neural tissue reconstructed from electron micrographs. Intracellular space is depicted in gray; extracellular space (ECS) is shown in white. Morphological features of the ECS are indicated by sheet-like features (red) and tunnel-like features (green). Molecular diffusion through sheet-like domains is predicted to occur more slowly than through tunnel-like domains. Figure adapted from Sykova & Nicholson 2008. B shows the path of diffusion (dashed line) of a neuromodulator (black circle) through the ECS. Diffusion along this path can be hindered by the presence of macromolecules attached the cellular membrane or floating freely through the ECS. Figure is adapted from Kinney et al., 2013. Coppola et al., 2016.

5.2c Signal termination

In Chapter 3, we discussed cholinergic signal termination via AChE. AChE, as discussed above, shows regional and laminar variations in its expression; a likely consequence of this variation being a more or less spatiotemporally precise signal due to the degree to which a molecule is able to diffuse across time and space. Especially paired with ChAT innervation, an area's ability to clear away the released ACh quickly and efficiently will almost certainly influence the cholinergic signal in that area.

5.2d Choline transporters

The local regulation of ACh synthesis can influence the capacity for cholinergic signaling to follow demands placed on it by the cortical circuits it serves. Choline, which is necessary for the synthesis of ACh, is taken up by cholinergic neurons via high affinity choline transporters (ChTs). These transporters are the rate-limiting factor in ACh synthesis (reviewed by Okuda and Haga, 2003). As such, ChT expression density at release sites may influence the dynamics of local ACh release. For example, when comparing across cortical regions, those areas with a higher density of ChT may have a greater capacity for ACh production, and therefore for sustained or high intensity cholinergic signaling. Similarly, cortical areas with a lower density of ChT may not be able to follow faithfully high and/or prolonged axonal firing. ChT expression density (which determines the ability to synthesize ACh in response to demand) combined with patterns of cholinergic innervation (which can partly influence the local extracellular ACh concentration, and therefore the "load" placed on local ChTs), ultimately provides an opportunity for more finely tuned local regulation of ACh release. This interplay between release and reuptake is very likely dynamic, potentially offering greater temporal precision under conditions of high demand. It has been shown, for example, that ChTs can be moved from cytosolic pools to the cell membrane in response to local demands on ACh signaling that result from varying activity-relevance of local cortical circuits (Ferguson et al., 2003). Further, the distribution of ChTs in primate cortex shows laminar differences, with a lower density of ChT-positive fibers in layer 1 compared to other layers (Kus et al., 2003). Overall, such variation could lead to local constraints on dynamic ACh signaling.

5.2e Receptor expression

As discussed in Chapter 1, ACh receptor subtypes are expressed differently across the receiving circuits of the cortex. Receptor autoradiography in human indicates that, within a cortical area, both muscarinic (mAChRs) and nicotinic (nAChRs) exhibit differences in density when examined across layers (Zilles et al., 2004). Across cortical areas, mAChR autoradiography reveals differences in mean binding site concentration and laminar receptor distribution (Eickhoff et al., 2007). For example, when comparing between visual areas, binding site densities for the m2 receptor are highest in V1 and decrease with the progression to V2 and to V3 (Eickhoff et al., 2008). Even within a cortical area, modulatory compartments can be defined based on receptor expression. For example, Zilles et al. (2004) reported differences in regional distribution of cholinergic receptors within human secondary somatosensory cortex. Likewise, when comparing between ventral and dorsal regions of both V2 and V3, binding site densities for m1 and m3 receptors exhibit significant differences (Eickhoff et al. 2008).

Functionally, differences in cholinergic receptor expression can affect the receipt of ACh. For example, a compartment more predominantly expressing the low affinity, α7-containing nAChRs will become desensitized to ACh more quickly, resulting in a decreased capacity for continuous cholinergic modulation. The high affinity nAChRs, however, desensitize more slowly, likely resulting in prolonged modulation by ACh. Therefore, based on the specific expression of receptor subtypes, modulatory signaling can range from more temporally precise to more prolonged. This variability in receptor expression across and within cortical areas highlights the ability of the receiving circuit itself to respond to signals in a locally-specific fashion. Receipt of a signaling molecule may result in widely different signals depending on the local receptor expression.

5.2f Subcellular receptor localization

When a signaling molecule is bound by a receptor, the localization of that receptor can significantly determine the resulting impact on the receiving neuron. In addition to expression by traditionally understood postsynaptic circuit elements (dendrites, spines, and cell bodies), receptors are also expressed by neuromodulatory axons. These presynaptic receptors can be broadly classified as autoreceptors or as heteroreceptors. Autoreceptors respond to the molecules released by the same axons that express them and act as an inhibitory feedback mechanism, reducing further release (Figure 5-2A and B). Conversely, heteroreceptors are activated by ligands released by neighboring cells and thereby allow one signaling molecule to modulate the release of another (Figure 5-2C and D; Gilsbach and Hein, 2008). Heteroreceptor activation thus depends on action potentials in other neurons and regulates local release by the neurons upon which the heteroreceptors are expressed. Currently, most of the pharmacological evidence for the function of heteroreceptors comes from rodent model systems. For example, noradrenaline release in the rat cortex, while dependent upon firing in the locus coeruleus, is also locally facilitated by axonally-expressed receptors for GABA (Bonanno and Raiteri, 1987). Similarly, Mohebi et al. (2018) have shown that rat forebrain dopamine levels—specifically in the nucleus accumbens—related to reward expectation arise independently from midbrain dopamine firing in the ventral tegmental area. They conclude this to be the result of local modulation over forebrain dopamine varicosities, likely through cholinergic actions.

There are well-documented examples of cholinergic receptors implicated as heteroreceptors. The m2 receptor is expressed by non-cholinergic terminals, allowing ACh to regulate release of other transmitters (Mrzljak et al., 1993). Furthermore, activation of nicotinic receptors can enhance noradrenaline release in hippocampal synaptosomes (Wonnacott, 1997). Activation of cholinergic heteroreceptors has in fact been shown to elicit neurotransmitter release independent of axonal action potentials in the receiving neuron's axon. For example, Cachope et al. (2012) report that stimulation of nicotinic receptors is sufficient to elicit dopamine release in the nucleus accumbens of mice, without the occurrence of a spike in the dopaminergic cell. Similarly, glutamate release from hippocampal mossy fiber synapses has been shown to increase, again independent of a somatic action potential, through activation of axonal nicotinic receptors (Sharma et al., 2008).

Finally, cholinergic tone can be regulated by other modulatory systems as well. Altering local levels of serotonin (Hirano et al., 1995) or glutamate receptor activation (Parikh et al., 2008) modulates local ACh release in rodent prefrontal cortex. These studies indicate the importance of receptor expression in receiving cortical circuits. Appropriately localized receptors can modify feedforward signaling via postsynaptic receptors, inhibit further release via an autoreceptor, or regulate (bi-directionally) axonal release via an axonal heteroreceptor. As such, receptor localization is an important aspect of signal receipt and response by the local circuitry.

5.2g Microvascular regulation

Many studies have linked cortical microvessel dilation to stimulation of the basal forebrain, implicating the cholinergic system in regulating vascular tone (reviewed by Hamel, 2004). Increases in cortical blood flow—as well as ACh—in the parietal cortex of rats proportionally follows the intensity and frequency of nucleus basalis stimulation (Kurosawa et al., 1989). Further, administration of both muscarinic and nicotinic antagonists has been shown to reduce cortical blood flow in the frontal and parietal cortices of rats (Biesold et al., 1989; Dauphin et al., 1991). The cholinergic system can directly regulate vasculature through cholinergic projections onto cortical microvessels expressing cholinergic receptors. Indirectly, ACh can regulate vasculature through interaction with interneuron populations that communicate with neighboring microvessels (Hamel, 2004). Receptor densities and interneuron populations exhibit significant variation throughout cortex (Disney and Aoki, 2008; Disney and Reynolds, 2014; Coppola and Disney, 2018b). Thus, both direct and

indirect cholinergic modulation of blood flow may vary across areas. This is important considering the tight coupling between blood flow and neuronal activity (reviewed by (Lou et al., 1987). As such, the interaction of ACh with local cortical microvessels may represent a significant feature of neuromodulatory compartments.

5.2h Astrocytic regulation

Astrocytes have the capacity to communicate with neurons in a number of ways, and they express neuromodulatory receptors (cholinergic and noradrenergic; reviewed by Lopez-Hidalgo and Schummers, 2014). As such, these glial cells act as neuromodulatory targets within cortical circuits. For example, muscarinic receptors are expressed by astrocytes—the most abundant glial cell in the brain—in rodent cortex (Van Der Zee et al., 1993). Cholinergic actions through these glial-expressed modulatory receptors have important functional implications, as astrocytes have been shown to act as effectors for cholinergic modulation in the cortex. Specifically, the binding of ACh to receptors expressed by astrocytes can result in "gliotransmission" in which the receiving glial cell releases a signaling molecule—such as glutamate—that in turn exerts modulatory effects on neighboring cells within the local circuit (Lopez-Hidalgo and Schummers, 2014). Further, in rodent visual cortex, nucleus basalis stimulation paired with a visual stimulus induces potentiation. This stimulus-specific potentiation is mediated through astrocytes expressing muscarinic receptors (Chen et al., 2012). As discussed above, muscarinic receptor expression by neurons varies, resulting in modulatory differences across cortex. It may be posited, then, that glial expression of receptors may also be subject to variation, in which case modulatory actions through astrocytes may differ across areas.

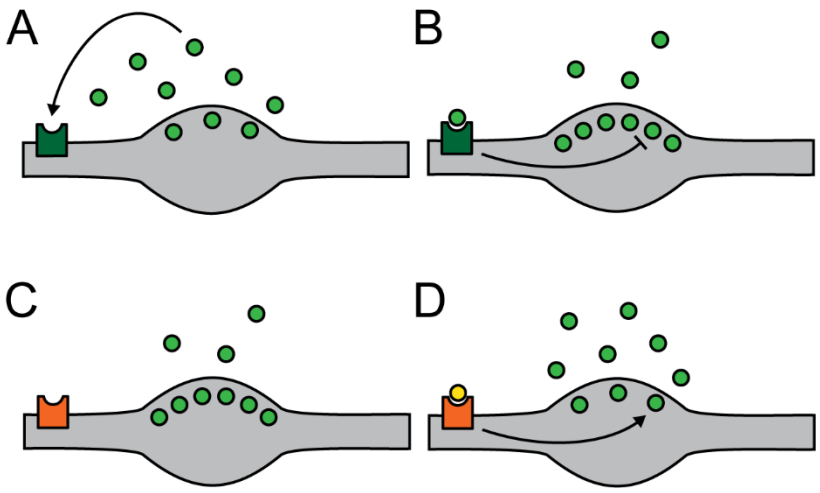

Figure 5-2: Autoreceptor- and heteroreceptor-mediated release of acetylcholine
A-B are examples of a cholinergic autoreceptor expressed on a cholinergic axon. A depicts acetylcholine (light green) release in the absence of activation of the cholinergic autoreceptor (dark green). In B, released acetylcholine binds to the autoreceptor and inhibits further acetylcholine release. C-D are examples of a serotonergic heteroreceptor expressed on a cholinergic axon. C demonstrates the release of acetylcholine from a varicosity in the absence of serotonin (yellow) binding to the serotonergic heteroreceptor (orange). In D, serotonin binds to the heteroreceptor, which mediates a greater output of acetylcholine release from the varicosity. Coppola et al., 2016.

5.3 Conclusion

The studies described above suggest a complexity to modulatory signaling throughout cortex. In diffuse communication, in which there is no point-to-point connection, the relationship between signal sent and signal received can be readily weakened. Each stage of diffuse signal transmission offers the opportunity to modify the modulatory signal, from differences in axonal innervation, through control of release and diffusion, to the response by the local circuit. Neuromodulatory compartments encompass a multidimensional space in which signaling can vary considerably based on features of the local circuit.

This structural inhomogeneity makes it essential to understand specific signaling conditions in any local cortical circuit of interest; without such data it becomes difficult to infer mechanisms of cholinergic modulation in cortex. For example, in order understand the role of ACh release in a task that is known to be dependent upon cholinergic innervation (such as a sustained vigilance task in a rodent; Himmelheber et al., 2000), recording electrophysiological activity in the basal forebrain will provide valuable insight. Further, because the signal sent from the basal forebrain does not necessarily equate to signal received in the cortex, additionally measuring local levels of released ACh across cortical areas will provide a second layer of valuable information regarding ACh's role in task performance. Beyond this, describing features of the local circuit and the local response to ACh release will help to characterize the transformation from signal sent to signal received (Figure 5-3). First, understanding the tissue tortuosity will describe the movement of molecules through the tissue once released. Second, some limits on the capacity for spatial and temporal precision of the signal can be determined by quantifying the local levels of AChE. Next, understanding the types of neurons that express ACh receptors (i.e. inhibitory, excitatory), as well as the subcellular localization of those receptors (e.g. autoreceptor, heteroreceptor; somatic versus dendritic) will help to describe the effects of ACh binding in a given area. Finally, measuring the resulting neuronal responses will reveal the effect of the locally transformed ACh signal on the local computation and spiking output of the cortical area of interest. Altogether, these data will help us to understand the transformation from signal sent in a diffuse modulatory system to signal received in cortex. An understanding of modulatory compartments as dynamic features of cortical circuits will allow us to better characterize the many points along the circuit where signal modification is possible. This offers opportunities to understand, and perhaps correct, signal modifications that lead to pathological states—a critical step given that the majority of medications prescribed for neuropathological states target modulatory systems that signal diffusely in cortex.

In the context of neuromodulatory compartments, the data presented in Chapters 2-4 can be viewed as foundational steps in understanding ACh's functional roles throughout cortex and specifically in area LIP. The final chapter will further contextualize these findings and buttress the importance of having structural and neurochemical data to better understand the complex mechanisms involved in the neuromodulation of primate cortex.

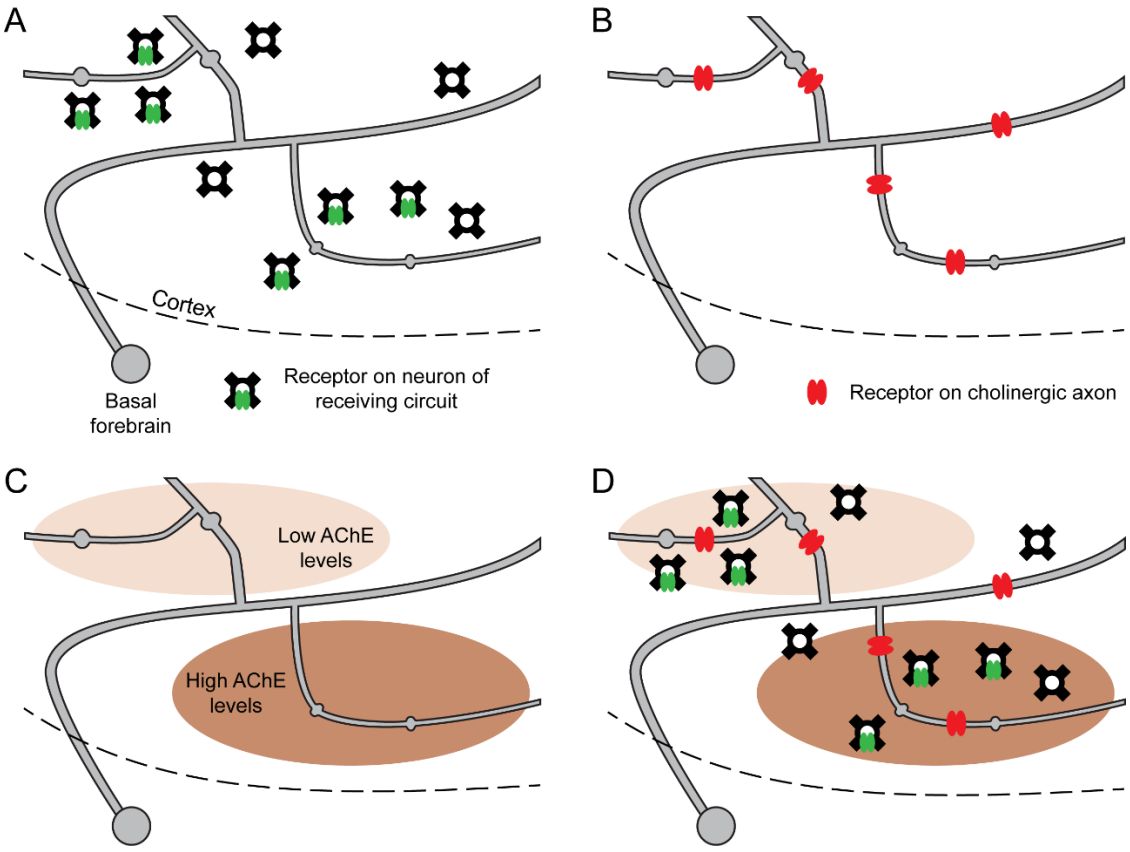

Figure 5-3: Features of the local circuit in cortex
Cholinergic projections originating in the basal forebrain innervate two different cortical compartments. A illustrates differences in receptor expression among neurons in the receiving circuit. B shows the presence of receptors along cholinergic axons that may influence local output of acetylcholine. C depicts regions with low and high concentrations of acetylcholinesterase. D demonstrates that together, these features create a multidimensional space in which modulatory signals can be modified at many points. Coppola et al., 2016.

Chapter 6

Discussion

6.1 Introduction

The goals of this dissertation were to quantify ACh receptor expression and distribution, to characterize the expression of cholinergic synthesizing and degradation enzymes, and to measure the local cholinergic tone *in vivo* in macaque LIP. Further, there was an emphasis on anatomical comparison between these data and those from other cortical regions in the primate. In Chapter 2, we learned that in LIP, approximately 75% of inhibitory neurons expresses m1AChR and that approximately 50% of m1AChR-expressing neurons is inhibitory. As discussed in Chapter 2, this means that of all neurons in LIP, roughly 40% express the m1AChR, with half being inhibitory and half being excitatory. In Chapter 3, we learned that both AChE and ChAT levels are highest in the superficial layers, especially layers 1 and 2. For AChE specifically, expression declines from layer 1 to 2 to lower 3, where levels increase in layers 4 and 5 and decline in layer 6 toward the white matter. For ChAT, immunoreactive axons are densest in the superficial layers, with a steadier decline from the pial surface toward the white matter. Finally in Chapter 4, we learned that parietal cortex maintains a higher ACh concentration than does the occipital cortex, and that this is preserved over session duration, recording day, and periods of light/darkness. We also found that for both occipital and parietal cortex, ACh concentration was highest in times of light compared to darkness. Finally we learned that the temporal profile of ACh concentration differs in each area, indicating they maintain unique concentration dynamics. In the discussion of each of the preceding chapters, I emphasized the differences observed between these data in LIP (parietal cortex) compared to other primate cortices (notably V1) and related these differences to hypotheses of functional specialization within the cholinergic system. Under this framework, in Chapter 5, I introduced the concept of neuromodulatory compartments in cortex and provided anatomical evidence for their existence. In the following sections, I will describe area LIP as a distinct compartment (given the features designated in this dissertation) and compare it with V1 as a separate cortical compartment. I will also discuss potential caveats, implications of cortical compartments, future directions, and the broader impacts of this work.

6.2 Potential caveats

In anatomical studies such as these, it is imperative to know that the antibodies used to bind antigens of interest are specific and offer a high probability of detection. Detection failure is a problem whereby the antibody is binding to the antigen of interest but that a reliably high proportion of those antigens is not detected. This would lead to an underreporting of the data. For example, if our m1AChR antibody is exhibiting detection failure, there would be more receptor-expressing cells than we would be able to quantify. Importantly, though, even detection failure and non-specific binding should have little effect on the interpretation of our data. This is because we are not interested in the absolute number of neurons or axons that expresses our antigens of interest (either the m1 receptor, GABA, or ChAT). Instead, we are interested in the proportional data to describe percentages and relative differences of these populations. Because I are unaware of any data to suggest, for example, that there would be a GABA detection failure with a bias toward cells that do or do not express m1, it is likely that our results would not change even if detection failure were present. We are also uninterested in the absolute number of ChAT-immunoreactive axons; we are instead interested in the relative degree to which cortical layers are innervated by the cholinergic system. Similarly, I am unaware of any data that suggest there would be a laminar bias in ChAT antibody detection such that one layer would be more prone to detection than another. Based on this information, I consider our anatomical findings to be reasonably accurate.

Another point to consider is that AChE may not actually terminate the cholinergic signal in cortex. For example, it has been proposed that following degradation of ACh, some portion of the extracellular choline that results from hydrolysis may act as a ligand at some nicotinic receptors (Alkonon & Albuquerque, 2006). If this

is the case, it follows, then, that AChE might not be a strong indicator of cholinergic tone because the cholinergic signal can persist to some extent regardless of the presence of AChE. While it has been shown that extracellular choline does act as a full agonist at α7 nicotinic receptors, it fails to activate the α4β2 nicotinic receptors, which are the principle β-containing subtype in cortex (Alkondon et al., 1997; Gotti et al., 2006). Further, choline cannot activate any of the muscarinic receptor subtypes. Thus, in cortex, the primary target for choline would be the α7 nicotinic receptors. However, it is unclear if choline is an effective agonist at these receptors at the concentrations likely to be found *in vivo*, since the agonistic effects have been observed at choline concentrations higher than the mean extracellular concentration of choline in the brain. Further, α7 receptors recover from desensitization more quickly when activated by choline than by ACh, and choline dissociates from the receptors more quickly than does ACh, indicating that if choline does act as a functional ligand *in vivo*, its results are lesser compared to ACh (Mike et al., 2000). As such, I consider AChE a direct indicator of cholinergic tone based on its ability to limit the cholinergic signal through the breakdown of ACh and the limited functional role of choline *in vivo*. Moreover, regardless of the degree to which choline acts as a functional ligand, there is still evidence that AChE expression differs across regions and areas, highlighting its designation as a feature of neuromodulatory compartments.

Similarly, it is possible that ChAT does not provide a sufficient measure of ACh release in cortex. While it is the case that ChAT synthesizes ACh, and it follows that the ability to create ACh should correlate with the amount of ACh delivered to an area, it is possible that the presence of ChAT does not predict the amount of ACh that is released. Instead, ChAT levels may just represent the capacity to create ACh. Two other—albeit less commonly used—cholinergic markers perhaps may be more directly predictive of the quantity of ACh synthesis. They are the choline transporter (ChT) and the vesicular ACh transporter (VAChT). Described in Chapter 5, ChTs are considered the rate-limiting step in ACh synthesis. They are located on the presynaptic cell membrane and their job is to take up choline from the extracellular space into the cell where it will be used to produce new ACh. Somewhat surprisingly, the laminar patterns of ChT expression in cortex do not match those for ChAT. Notably, in primate cortex, ChT expression is lowest in layer 1 while ChAT density is highest in layer 1. Additionally, ChT expression was found to be more comparable across cortical regions than ChAT expression (which differs substantially), again highlighting a difference between ChT and ChAT densities (Kus et al., 2003). Similarly, the VAChT, another molecular marker specific to cholinergic cells can provide an indication of cholinergic tone in an area. VAChT is responsible for accumulating newly created ACh into synaptic vesicles. However, ChAT and VAChT have been described as being invariably co-expressed across all mammals. This is because the complimentary DNA (cDNA) for VAChT is contained entirely within the first segment of the ChAT gene locus (i.e. a "nested" fashion; Erickson et al., 1994). As such, ChAT and VAChT expression across cortex within a species are likely the same. Taken together, it is probably reasonable to explore two indicators of ACh innervation: ChAT and ChT, which likely overlap in many cases but do provide different measures (ACh synthesis and choline reuptake, respectively). At this time, though, ChAT does serve as an interesting marker given its differences across and within cortices, and pairing these data with ChT expression would provide a clearer picture of an area's ability to synthesize ACh. Further, as discussed in Chapter 4, the innervation density of an area should not be used as a proxy for extracellular molecular concentration; neurochemical environment itself should be studied. Instead, ChAT density, ChT expression, and the local concentration together would provide a more holistic view of cholinergic tone in an area.

Regarding our *in vivo* data, as discussed in Chapter 4, a noteworthy caveat is the limitation of microdialysis as a method to describe ACh concentrations at specific times and locations. Because the probe is large, the smallest unit of tissue we can measure is ~2 mm. Similarly, because of the volume of sample that needs to be collected for analysis is large, the smallest unit of time we measured across is ~20 minutes. These robust measures leave open the possibility that finer scale actions could be occurring. As previously noted, we know that at the time of release, ACh concentration will be much higher near the release site than farther from it. We also do not know if our recorded concentration values (5 nM of ACh in occipital cortex, for example) are the result of steady release across the 20 minute sample, or some more instantaneous, higher volume release that

was able to diffuse in the probe over time. It is also possible that one layer is exhibiting higher/lower concentrations compared to another layer within the 2 mm probe depth. While these data are obscured in our samples, our goal was to address lobe level differences in cholinergic tone. We now have neurochemical data to show that there exists a non-homogenous, non-global cholinergic signal across two cortices of the primate brain.

Finally, two critical assumptions we make in evaluating cortical compartments are that there are no local cholinergic neurons in the cortex of adult non-human primates and that ACh is dispatched via volume transmission. Regarding the former point, numerous studies investigating the anatomy of the cholinergic system have described an absence of local neurons immunoreactive for any of the cholinergic markers described here (ChAT, ChT, and VAChT) (Hedreen et al., 1983; Mesulam et al., 1983; Everitt and Robbins, 1997; Lehmann et al., 1984; Erickson et al., 1994; Kus et al., 2003; Raghanti et al., 2008). Similarly, results from Chapter 3 show that I did not find any neurons immunoreactive for ChAT in LIP. Most of the reports that show intrinsic cholinergic cortical neurons seem to be restricted to rat models, although one report describes a small number of weakly stained ChAT-ir neurons in the human layers 3 and 5 of secondary sensory and motor areas but not in primary sensory areas (Kasashima et al., 1999). This population has never been observed in non-human primates. As such, I consider the assumption that there are no intrinsic cholinergic neurons in the cortex of adult non-human primates to be reasonable.

Next, the significance of cortical compartments is most notable in a system that uses volume transmission. Indeed, any space in which a signaling molecule is freely floating (even the synapse) makes the signal vulnerable to local modification. In the case of volume transmission, the capacity for local modification becomes much greater (see Chapter 5). As such, a critical assumption of cholinergic neuromodulatory compartments is that ACh participates to some degree in volume transmission, and many anatomical studies indicate that it does. For example, an electron microscopy study characterizing three-dimensional reconstructions of axons in their entirety provides evidence that the majority of cholinergic varicosities (56%) do not form synapses in macaque prefrontal cortex (Mrzljak et al., 1995). In fact, in rodent prefrontal cortex, only about 15% of cholinergic varicosities was found to form synapses (Umbriaco et al., 1994), and a number of other studies describe diffuse cholinergic signaling (Descarries et al., 1997; Mechawar et al., 2000 but see Smiley et al., 1997; Turrini et al., 2001). Other evidence comes from receptor expression; cholinergic receptors have been observed at non-cholinergic synapses (Mrzljak et al., 1993). Regarding AChE expression, my own results indicate that the laminar pattern for AChE expression differs from that of ChAT expression, and indeed, just the fact that AChE is not considered to be a cholinergic marker as it is found at non-cholinergic sites (described above) provides evidence that at least some degree of ACh diffusion through the extracellular space is a common feature of the cholinergic system. There are also numerous studies from other systems (serotonergic and noradrenergic) that indicate similarly diffuse transmission. Taken together, the most detailed anatomical data we have provides evidence that ACh participates in volume transmission.

6.3 Neuromodulatory compartments in cortex

In the context of a cortical compartment, I have provided evidence that LIP has distinct cholinergic circuitry compared to other cortical areas, namely V1. In LIP, we see that approximately 75% of inhibitory neurons and approximately 25% of excitatory neurons express the m1 receptor. In V1, the m1 receptor is expressed by approximately 60% of inhibitory neurons and by less than 10% of excitatory neurons (Disney et al., 2006). This increase in cholinoceptivity through both inhibitory and excitatory cell types in LIP compared to V1 is a clear indication of compartmentalization. It may also provide evidence of a mechanism for increases in attentional modulation that has been shown moving up through the visual hierarchy (discussed in Chapter 2). We know from existing literature that AChE expression is higher in V1 than in LIP, and that ChAT innervation is lower in V1 than in LIP (discussed in Chapter 3). This also supports compartmentalization between the two areas and provides evidence to suggest the cholinergic signaling is more spatially and temporally precise in V1

compared to LIP. This is especially true for the superficial layers in LIP whose ratio of AChE expression to ChAT innervation is such that molecules are likely able to diffuse more freely compared to the deeper layers of LIP. Finally, parietal cortex (where LIP is located) maintains a higher concentration of ACh than does V1 and along a different timescale. This finding alone provides evidence that LIP and V1 comprise separate compartments, but especially within the context of the anatomical data we just summarized, it is clear that the cholinergic circuitry in LIP is different from the cholinergic circuitry in V1.

Overall, a likely prediction is that the cholinergic signaling is more limited and thus more precise in V1 compared to LIP (with more targeted receptor binding through less cholinoceptivity, lower innervation with higher clean up capabilities, and a lower concentration of molecules diffusing through the extracellular space). This idea seems compatible with the status of V1 as a primary receiver of incoming sensory data from which most other visual sensory processing occurs. Perhaps at this level of processing, a signal that is too flexible would be problematic compared to an area at the status of LIP. LIP does use bottom-up sensory information, and it does provide saccade related signals to areas that generate motor commands, but it seems reasonable that an area that is also responsible for monitoring top-down information and ongoing motor and attentional needs could afford more flexibility in its signaling dynamics compared to a primary sensory region. This prediction may also be in line with the fact that other neuromodulatory molecules (dopamine, noradrenaline, serotonin) in V1 maintain lower concentrations *in vivo* than do most downstream cortical areas (Ward et al., 2018). The idea that V1 requires a different cholinergic signal than LIP is also supported by the differences in concentration dynamics (temporal profile) reveled by the mircrodialysis data. While anatomical data from other neuromodulatory systems is outside the scope of this dissertation, it would be interesting to see if similar trends are observed when investigating anatomical data for those systems. This work is underway in the Disney lab.

Interestingly, I did not find evidence for compartmentalization at the level of LIP subregions. Between LIPd and LIPv, I did not observe clear indications that the two regions differ based on receptor expression or innervation/clean up capacity, and as discussed, our methods do not allow us to observe differences in neurochemical environment at this resolution. It could be the case that while anatomically and functionally distinct, LIPd and LIPv have similar processing needs regarding the cholinergic system. It would be helpful to know the cholinergic anatomical characteristics of other regions in the parietal cortex. In this case, it becomes interesting to consider how spatially large a compartment is. For example, it could be the case that all cortical areas at the level of LIP maintain similar receptor expression patterns. Perhaps a compartment defined by receptor expression is relatively large in cortical space. However, since we have already seen that ChAT density and AChE expression differ on a laminar scale, perhaps compartments defined by those characteristics are spatially quite small (at least as small as a single layer). I have defined a cortical compartment as a region of tissue within which modulatory conditions are predicted to be relatively uniform and between which modulatory conditions may differ profoundly. This likely describes relatively small units of cortex, but that does not mean that each anatomical characteristic involved in delineating a compartment will also differ across a similarly small scale. It is possible that the rate of variation for any of the characteristics that define compartments could be different, but that together they comprise unique cortical areas that recruit unique modulatory signals. Whatever the case, it is clear that anatomical data such as these are necessary in describing neuromodulatory actions throughout cortex.

6.4 Implications of compartments

Based on the data and concepts discussed in this dissertation, it becomes apparent that neuromodulation and its actions throughout cortex are dynamical. By this I mean that through neuromodulatory compartments, neuromodulation can vary across at least three dimensions: space (cortical area), time (temporal dynamics/development/aging), and "cross-modulation" (one or many neuromodulatory systems influencing another). Most of the data presented here concern the dimension of space. As we have seen, the anatomical features of the cholinergic system differ, sometimes subtly but often significantly, across cortex. Even

considering space alone, many functional implications are borne out of these differences (see Discussion from Chapters 2 and 3). Extracellular concentration of ACh *in vivo* is likely related to both the dimensions of space and time. For example, local levels of ACh will recruit different receptors types (discussed above), which encompasses the anatomy of receptor expression and distance from release site—anatomical features in space. However, as we have seen from microdialysis data, ACh levels differ across time as well (a difference in the temporal profiles). Theoretically, even cholinergic compartments that are the same spatially can be activated differently across time based on the instantaneous ACh levels that result from or contribute to brain state. These types of differences can exist on a small scale, (minutes, hours), but more long-term differences can exist as well. For example, perhaps receptor expression can also differ in time (in addition to across cortex), but across a much longer period. This highlights the importance of development, which is beyond the scope of my dissertation but is almost surely a significant feature in shaping neuromodulation. For a review of ChAT, AChE, and cholinergic receptor expression across embryonic and perinatal development using data from different species, see Semba (2004). Briefly, different aspects of cholinergic anatomy reach adult-like levels at different times throughout development. On the other end of the spectrum, neuromodulatory changes related to aging are also known to occur. For example, muscarinic receptors are known to be depleted in aged humans who do not have any evidence of dementias (White et al., 1977). In aged rats, the number of cholinergic neurons in the basal forebrain decreases by 30% compared to young rats (Smith and Booze, 1995). These studies highlight changes in the cholinergic system that occur perhaps over a lifetime, although the timespan may be shorter because the groups being compared are "young" and "aged" with no data points in between. Whatever the case, we know that these systems are not static over time or space. Finally, an interesting dimension of compartments is what I have referred to as cross-modulation.

Cross-modulation occurs when one or more neuromodulatory system influences the actions of another. This can occur in at least two ways. First, one modulatory system can impact another by sending projections from its own subcortical innervating nucleus to another innervating nucleus. For example, we know that the basal forebrain of the cholinergic system receives projections from the innervating bodies of the other neuromodulators (Chapter 1). In this case, cholinergic activity originating in the basal forebrain could be modulated by noradrenergic activity originating in the locus coeruleus, for example. The second way for cross-modulation to occur is through the presence of heteroreceptors expressed on neuromodulatory axons (Chapter 5). It is possible that two areas neighboring each other with the exact same receiving circuitry and extracellular environment could exist as two different compartments if, for example, heteroreceptors expressed on axons differed. This is especially interesting given we know that local heteroreceptors can drive neurotransmitter release independent of spiking in the innervating subcortical nuclei. For example, one cholinergic compartment could be overlapped by two separate noradrenergic compartments. If the cholinergic axons express noradrenergic receptors, with some portion of those receptors making up the different noradrenergic compartments, then perhaps the cholinergic compartment itself will become two different compartments, based on the local influence from the noradrenaline compartments. Altogether, it becomes clear that neuromodulatory systems are far from static, and that cortical compartments are multidimensional and dynamical. They can vary across either cortical space, time, their degree of cross-modulation, or some combination of the three to create highly compartmentalized areas of circuitry.

6.5 Future directions

Because neuromodulatory signaling is dynamical as opposed to static, a likely future path is through dynamical systems modeling. However, this view challenges the more commonly held belief that computational models can use static neuromodulatory data to describe the role of neuromodulators in cortical function such as attention and memory. For example, a model of cognition describing the mechanisms underlying cholinergic modulation in the prefrontal cortex focuses on neurophysiological data regarding cholinergic receptors but does not include anatomical data regarding their expression by cell type, innervation and clean up patterns, or extracellular concentrations of ACh (Hasselmo and Sarter, 2011). This is problematic as we have seen all of

these features can differ and work together to delineate discrete areas of cholinergic function. A dynamical model, especially that accounts for release and signal termination (which, importantly, can function independent of each other) of a diffuse modulator will likely be more efficient at describing cortical modulatory phenomena.

To create dynamical models of function, extensive anatomical data, similar to what is described here, would be needed across each cortical area of interest as well as across each neuromodulatory system. Additionally, it would be helpful to know the proportion of synaptic versus non-synaptic transmission that occurs in each area. Studies using electron microscopy can investigate where varicosities are located and how many of them allow for the diffusion of ACh beyond confines of a synapse through the extracellular space. Further, knowing the degree to which cross-neuromodulation occurs would be beneficial. This would involve studying anatomy from all neuromodulatory systems in an area, especially through heteroreceptor expression. Having these data to input into dynamical models of function would provide a solid foundation for investigations of function and intervention, as opposed to models that simply use neuromodulators as static components within a circuit.

Beyond anatomy and modeling, we can perform functional experiments as well, specifically in investigating mechanisms related to ACh concentration *in vivo*. For example, our data could not resolve finer scale differences that might be present in the cholinergic signal, however, microdialysis methods on shorter timescales do exist. Our LC-MS/MS analyses can use sample volumes much smaller than the ones described in Chapter 4, resulting in samples representing many fewer minutes than 20. Concentration analyses on a shorter times scale would provide a clearer snapshot into instantaneous cholinergic release. During experiments using such methods, there are a number of ways to probe the cholinergic system. For example, to see how critical AChE expression is to degrading the cholinergic signal, administration of the AChE inhibitor donepezil (described in Chapter 1) could be utilized. Perhaps AChE expression contributes significantly to cholinergic tone only immediately after release, but not during diffusion. Or, perhaps in areas with relatively low AChE expression, AChE is not significant at all in limiting the signal—and instead the innervation density is the main contributor in cholinergic tone for that area. To investigate the degree to which cross-modulation affects cholinergic tone, noradrenaline (or any neuromodulator) iontophoresis could be applied locally in cortex. The locus coeruleus (that provides noradrenergic innervation) could be stimulated as well to see how release of noradrenaline across the brain impacts cholinergic compartments. Perhaps we would find that noradrenaline does little to affect the cholinergic signal in one area but is quite influential in other. Or, perhaps we find that it is dopamine that mainly impacts ACh, and not noradrenaline. In either case, measuring the resulting cholinergic tone across cortex could reveal the level of interaction between these two (or other) systems.

In any case, the more we can observe about neuromodulatory compartments, the more we can begin to study them in a dynamical context. This is especially important in appreciating differences in tonic versus phasic signaling. The tonic signal refers to the ambient levels of ACh, broadly responsible for brain states like sleep, waking, arousal, et cetera. These would be in line with a more "global" view of the cholinergic signal. The phasic signal refers to a transient signal, perhaps in response to a specific stimuli. The phasic signal would be responsible for more fine-tuned types of cognition, perhaps focal attention in one particular sensory cortex. This would be more in line with a compartmentalized view of the cholinergic signal, in which precise, local functions could be carried out. The data described in these sections can provide insight to the degree to which both tonic and phasic (i.e. global and precise) mechanisms are accomplished.

6.6 Broader impacts

ACh is implicated in a number of neurological disease states. These notably include Alzheimer's Disease, schizophrenia (Martin and Freedman, 2007; Jones et al., 2012), Autism Spectrum Disorder (Lippiello, 2006; Deutsch et al., 2015), and attention deficit disorder (Beane and Marrocco, 2004). For example, a major aspect of advanced Alzheimer's Disease is substantial loss of cholinergic innervation to cortex with nearly 80%

of cholinergic axons being depleted along with a reduction in the number of expressed cholinergic receptors (Mash et al., 1985; Whitehouse et al., 1986; Geula and Mesulam, 1989; Mesulam, 2004b). Further, in many of the disease states that involve ACh, selective antagonism specifically of the α7 nicotinic receptors has shown to be a promising treatment option (Lloyd and Williams, 2000). Beyond ACh, neuromodulatory systems more broadly are implicated in disease states. In fact, eight of the 10 drugs that are most often prescribed by psychiatrists target neuromodulatory systems, and yet, we know very little about mechanisms of their circuitry for neuromodulatory actions. This is especially concerning given that therapies often involve systemic delivery of drug, and as has been demonstrated in this dissertation, neuromodulatory compartments are such that different cortical areas interact with modulatory molecules differently. Further, we describe neuromodulatory actions using static modeling principles, again missing many nuanced changes in cortical neuromodulation. However, if we are to use the data from studies of cholinergic structure and function to drive improvements in human health and treatments of disease, the precise mechanisms by which neuromodulatory computations are achieved matters, and thus is a critical consideration for future work.

References

Aigner T, Mitchell S, Aggleton J, DeLong M, Struble R, Price DL, Wenk G, Pettigrew K, Mishkin M. 1991. Transient impairment of recognition memory following ibotenic-acid lesions of the basal forebrain in macaques. Experimental Brain Research 86(1):18-26.

Albanese A, Butcher LL. 1979. Locus ceruleus somata contain both acetylcholin esterase and norepinephrine: direct histochemical demonstration on the same tissue section. Neuroscience letters 14(1):101-104.

Albuquerque EX, Pereira EF, Alkondon M, Rogers SW. 2009. Mammalian nicotinic acetylcholine receptors: from structure to function. Physiological reviews 89(1):73-120.

Alkondon M, Pereira EF, Cartes WS, Maelicke A, Albuquerque EX. 1997. Choline is a selective agonist of α7 nicotinic acetylcholine receptors in the rat brain neurons. European Journal of Neuroscience 9(12):2734-2742.

Angelucci A, Bressloff PC. 2006. Contribution of feedforward, lateral and feedback connections to the classical receptive field center and extra-classical receptive field surround of primate V1 neurons. Progress in brain research 154:93-120.

Arendt T, Bigl V, Tennstedt A, Arendt A. 1985. Neuronal loss in different parts of the nucleus basalis is related to neuritic plaque formation in cortical target areas in Alzheimer's disease. Neuroscience 14(1):1-14.

Avendano C, Umbriaco D, Dykes RW, Descarries L. 1996. Acetylcholine innervation of sensory and motor neocortical areas in adult cat: a choline acetyltransferase immunohistochemical study. J Chem Neuroanat 11(2):113-130.

Beane M, Marrocco R. 2004. Norepinephrine and acetylcholine mediation of the components of reflexive attention: implications for attention deficit disorders. Progress in neurobiology 74(3):167-181.

Berger-Sweeney J, Heckers S, Mesulam M-M, Wiley RG, Lappi DA, Sharma M. 1994. Differential effects on spatial navigation of immunotoxin-induced cholinergic lesions of the medial septal area and nucleus basalis magnocellularis. Journal of Neuroscience 14(7):4507-4519.

Biesold D, Inanami O, Sato A, Sato Y. 1989. Stimulation of the nucleus basalis of Meynert increases cerebral cortical blood flow in rats. Neuroscience letters 98(1):39-44.

Bignami A, Asher R. 1992. Some observations on the localization of hyaluronic acid in adult, newborn and embryonal rat brain. International journal of developmental neuroscience 10(1):45-57.

Blatt GJ, Andersen RA, Stoner GR. 1990. Visual receptive field organization and cortico-cortical connections of the lateral intraparietal area (area LIP) in the macaque. Journal of Comparative Neurology 299(4):421-445.

Bonanno G, Raiteri M. 1987. Release-regulating GABAA receptors are present on noradrenergic nerve terminals in selective areas of the rat brain. Synapse 1(3):254-257.

Bonner TI, Young AC, Bran MR, Buckley NJ. 1988. Cloning and expression of the human and rat m5 muscarinic acetylcholine receptor genes. Neuron 1(5):403-410.

Boucart M, Bubbico G, Defoort S, Ponchel A, Waucquier N, Deplanque D, Deguil J, Bordet R. 2015. Donepezil increases contrast sensitivity for the detection of objects in scenes. Behavioural brain research 292:443-447.

Browning PG, Gaffan D, Croxson PL, Baxter MG. 2009. Severe scene learning impairment, but intact recognition memory, after cholinergic depletion of inferotemporal cortex followed by fornix transection. Cerebral cortex 20(2):282-293.

Bucci DJ, Holland PC, Gallagher M. 1998. Removal of cholinergic input to rat posterior parietal cortex disrupts incremental processing of conditioned stimuli. The Journal of neuroscience : the official journal of the Society for Neuroscience 18(19):8038-8046.

Butcher L, Talbot K, Bilezikjian L. 1975. Acetylcholinesterase neurons in dopamine-containing regions of the brain. Journal of neural transmission 37(2):127-153.

Butcher LL, Semba K. 1989. Reassessing the cholinergic basal forebrain: nomenclature schemata and concepts. Trends in neurosciences 12(12):483-485.

Cachope R, Mateo Y, Mathur BN, Irving J, Wang H-L, Morales M, Lovinger DM, Cheer JF. 2012. Selective activation of cholinergic interneurons enhances accumbal phasic dopamine release: setting the tone for reward processing. Cell reports 2(1):33-41.
Campbell MJ, Lewis DA, Foote SL, Morrison JH. 1987. Distribution of choline acetyltransferase-, serotonin-, dopamine-β-hydroxylase-, tyrosine hydroxylase-immunoreactive fibers in monkey primary auditory cortex. Journal of Comparative Neurology 261(2):209-220.
Chen N, Sugihara H, Sharma J, Perea G, Petravicz J, Le C, Sur M. 2012. Nucleus basalis-enabled stimulus-specific plasticity in the visual cortex is mediated by astrocytes. Proceedings of the National Academy of Sciences 109(41):E2832-E2841.
Clarke PB, Pert CB, Pert A. 1984. Autoradiographic distribution of nicotine receptors in rat brain. Brain research 323(2):390-395.
Cooper JR, Bloom FE, Roth RH. 2003. The biochemical basis of neuropharmacology: Oxford University Press, USA.
Coppola J, Disney A. 2018a. Is there a canonical cortical circuit for the cholinergic system? Anatomical differences across common model systems. Frontiers in neural circuits 12:8.
Coppola JJ, Disney AA. 2018b. Most calbindin-immunoreactive neurons, but few calretinin-immunoreactive neurons, express the m1 acetylcholine receptor in the middle temporal visual area of the macaque monkey. Brain and behavior 8(9):e01071.
Coppola JJ, Ward NJ, Jadi MP, Disney AA. 2016. Modulatory compartments in cortex and local regulation of cholinergic tone. Journal of Physiology-Paris 110(1):3-9.
Croxson PL, Kyriazis DA, Baxter MG. 2011. Cholinergic modulation of a specific memory function of prefrontal cortex. Nature neuroscience 14(12):1510.
Dani JA, Bertrand D. 2007. Nicotinic acetylcholine receptors and nicotinic cholinergic mechanisms of the central nervous system. Annu Rev Pharmacol Toxicol 47:699-729.
Dauphin F, Lacombe P, Sercombe R, Hamel E, Seylaz J. 1991. Hypercapnia and stimulation of the substantia innominata increase rat frontal cortical blood flow by different cholinergic mechanisms. Brain research 553(1):75-83.
DeFelipe J. 1993. Neocortical neuronal diversity: chemical heterogeneity revealed by colocalization studies of classic neurotransmitters, neuropeptides, calcium-binding proteins, and cell surface molecules. Cerebral cortex 3(4):273-289.
Descarries L, Gisiger V, Steriade M. 1997. Diffuse transmission by acetylcholine in the CNS. Progress in neurobiology 53(5):603-625.
Deutsch SI, Burket JA, Urbano MR, Benson AD. 2015. The α7 nicotinic acetylcholine receptor: A mediator of pathogenesis and therapeutic target in autism spectrum disorders and Down syndrome. Biochemical Pharmacology 97(4):363-377.
Disney AA, Alasady HA, Reynolds JH. 2014. Muscarinic acetylcholine receptors are expressed by most parvalbumin-immunoreactive neurons in area MT of the macaque. Brain and behavior 4(3):431-445.
Disney AA, Aoki C. 2008. Muscarinic acetylcholine receptors in macaque V1 are most frequently expressed by parvalbumin-immunoreactive neurons. The Journal of comparative neurology 507(5):1748-1762.
Disney AA, Aoki C, Hawken MJ. 2007. Gain modulation by nicotine in macaque v1. Neuron 56(4):701-713.
Disney AA, Aoki C, Hawken MJ. 2012. Cholinergic suppression of visual responses in primate V1 is mediated by GABAergic inhibition. J Neurophysiol.
Disney AA, Domakonda K, Aoki C. 2006. Differential expression of muscarinic acetylcholine receptors across excitatory and inhibitory cells in visual cortical areas V1 and V2 of the macaque monkey. Journal of Comparative Neurology 499(1):49-63.
Disney AA, Reynolds JH. 2014. Expression of m1-type muscarinic acetylcholine receptors by parvalbumin-immunoreactive neurons in the primary visual cortex: a comparative study of rat, guinea pig, ferret, macaque and human. The Journal of comparative neurology 522:986-1003.

Dubois B, Mayo W, Agid Y, Le Moal M, Simon H. 1985. Profound disturbances of spontaneous and learned behaviors following lesions of the nucleus basalis magnocellularis in the rat. Brain research 338(2):249-258.
Eickhoff SB, Rottschy C, Kujovic M, Palomero-Gallagher N, Zilles K. 2008. Organizational principles of human visual cortex revealed by receptor mapping. Cerebral cortex 18(11):2637-2645.
Eickhoff SB, Rottschy C, Zilles K. 2007. Laminar distribution and co-distribution of neurotransmitter receptors in early human visual cortex. Brain Structure and Function 212(3-4):255-267.
Erickson JD, Varoqui H, Schäfer M, Modi W, Diebler M-F, Weihe E, Rand J, Eiden LE, Bonner TI, Usdin TB. 1994. Functional identification of a vesicular acetylcholine transporter and its expression from a" cholinergic" gene locus. Journal of Biological Chemistry 269(35):21929-21932.
Everitt BJ, Robbins TW. 1997. Central cholinergic systems and cognition. Annu Rev Psychol 48:649-684.
Ferguson SM, Savchenko V, Apparsundaram S, Zwick M, Wright J, Heilman CJ, Yi H, Levey AI, Blakely RD. 2003. Vesicular localization and activity-dependent trafficking of presynaptic choline transporters. Journal of Neuroscience 23(30):9697-9709.
Fiala JC, Feinberg M, Popov V, Harris KM. 1998. Synaptogenesis via dendritic filopodia in developing hippocampal area CA1. Journal of Neuroscience 18(21):8900-8911.
Fine A, Hoyle C, Maclean C, Levatte T, Baker H, Ridley R. 1997. Learning impairments following injection of a selective cholinergic immunotoxin, ME20. 4 IgG-saporin, into the basal nucleus of Meynert in monkeys. Neuroscience 81(2):331-343.
Flynn DD, Ferrari-DiLeo G, Mash DC, Levey AI. 1995. Differential regulation of molecular subtypes of muscarinic receptors in Alzheimer's disease. Journal of neurochemistry 64(4):1888-1891.
Fournier G, Semba K, Rasmusson D. 2004. Modality-and region-specific acetylcholine release in the rat neocortex. Neuroscience 126(2):257-262.
Fuxe K, Agnati LF. 1991. Volume transmission in the brain: novel mechanisms for neural transmission: Raven Press.
Gallyas F. 1970. Silver staining of micro- and oligodendroglia by means of physical development. Acta Neuropathol 16(1):35-38.
Geneser-Jensen FA, Blackstad TW. 1971. Distribution of acetyl cholinesterase in the hippocampal region of the guinea pig. Cell and Tissue Research 114(4):460-481.
Geula C, Mesulam M-M. 1989. Cortical cholinergic fibers in aging and Alzheimer's disease: a morphometric study. Neuroscience 33(3):469-481.
Gil Z, Connors BW, Amitai Y. 1997. Differential regulation of neocortical synapses by neuromodulators and activity. Neuron 19(3):679-686.
Gilsbach R, Hein L. 2008. Presynaptic metabotropic receptors for acetylcholine and adrenaline/noradrenaline. Pharmacology of neurotransmitter release: Springer. p 261-288.
Gorry JD. 1963. Studies on the comparative anatomy of the ganglion basale of Meynert. Acta anatomica 55:51.
Gotti C, Zoli M, Clementi F. 2006. Brain nicotinic acetylcholine receptors: native subtypes and their relevance. Trends in pharmacological sciences 27(9):482-491.
Gottlieb J, Snyder LH. 2010. Spatial and non-spatial functions of the parietal cortex. Current opinion in neurobiology 20(6):731-740.
Gritti I, Henny P, Galloni F, Mainville L, Mariotti M, Jones B. 2006. Stereological estimates of the basal forebrain cell population in the rat, including neurons containing choline acetyltransferase, glutamic acid decarboxylase or phosphate-activated glutaminase and colocalizing vesicular glutamate transporters. Neuroscience 143(4):1051-1064.
Gritti I, Mainville L, Mancia M, Jones BE. 1997. GABAergic and other noncholinergic basal forebrain neurons, together with cholinergic neurons, project to the mesocortex and isocortex in the rat. The Journal of comparative neurology 383(2):163-177.
Hackett TA, Preuss TM, Kaas JH. 2001. Architectonic identification of the core region in auditory cortex of macaques, chimpanzees, and humans. Journal of Comparative Neurology 441(3):197-222.

Hamed SB, Duhamel J-R, Bremmer F, Graf W. 2001. Representation of the visual field in the lateral intraparietal area of macaque monkeys: a quantitative receptive field analysis. Experimental brain research 140(2):127-144.
Hamel E. 2004. Cholinergic modulation of the cortical microvascular bed. Progress in brain research 145:171-178.
Hardy SP, Lynch JC. 1992. The spatial distribution of pulvinar neurons that project to two subregions of the inferior parietal lobule in the macaque. Cerebral cortex 2(3):217-230.
Hasselmo M, Giocomo L. 2006. Cholinergic modulation of cortical function. Journal of Molecular Neuroscience 30(1):133-135.
Hasselmo ME, Bower JM. 1992. Cholinergic suppression specific to intrinsic not afferent fiber synapses in rat piriform (olfactory) cortex. J Neurophysiol 67(5):1222-1229.
Hasselmo ME, McGaughy J. 2004. High acetylcholine levels set circuit dynamics for attention and encoding and low acetylcholine levels set dynamics for consolidation. Progress in brain research 145:207-231.
Hasselmo ME, Sarter M. 2011. Modes and models of forebrain cholinergic neuromodulation of cognition. Neuropsychopharmacology : official publication of the American College of Neuropsychopharmacology 36(1):52.
Hedreen JC, Bacon SJ, Cork LC, Kitt CA, Crawford GD, Salvterra PM, Price DL. 1983. Immunocytochemical identification of cholinergic neurons in the monkey central nervous system using monoclonal antibodies against choline acetyltransferase. Neuroscience letters 43(2-3):173-177.
Hedreen JC, Uhl GR, Bacon SJ, Fambrough DM, Price DL. 1984. Acetylcholinesterase-immunoreactive axonal network in monkey visual cortex. Journal of Comparative Neurology 226(2):246-254.
Hendry SH, Schwark HD, Jones EG, Yan J. 1987. Numbers and proportions of GABA-immunoreactive neurons in different areas of monkey cerebral cortex. The Journal of neuroscience : the official journal of the Society for Neuroscience 7(5):1503-1519.
Hepler DJ, Wenk GL, Cribbs BL, Olton DS, Coyle JT. 1985. Memory impairments following basal forebrain lesions. Brain research 346(1):8-14.
Herrero JL, Roberts MJ, Delicato LS, Gieselmann MA, Dayan P, Thiele A. 2008. Acetylcholine contributes through muscarinic receptors to attentional modulation in V1. Nature 454(7208):1110-1114.
Himmelheber AM, Sarter M, Bruno JP. 2000. Increases in cortical acetylcholine release during sustained attention performance in rats. Brain Res Cogn Brain Res 9(3):313-325.
Hirano H, Day J, Fibiger HC. 1995. Serotonergic regulation of acetylcholine release in rat frontal cortex. Journal of neurochemistry 65(3):1139-1145.
Houser CR, Hendry SH, Jones EG, Vaughn JE. 1983. Morphological diversity of immunocytochemically identified GABA neurons in the monkey sensory-motor cortex. J Neurocytol 12(4):617-638.
Hsieh CY, Cruikshank SJ, Metherate R. 2000. Differential modulation of auditory thalamocortical and intracortical synaptic transmission by cholinergic agonist. Brain research 880(1-2):51-64.
Ichikawa T, Hirata Y. 1986. Organization of choline acetyltransferase-containing structures in the forebrain of the rat. Journal of Neuroscience 6(1):281-292.
Ipata AE, Gee AL, Bisley JW, Goldberg ME. 2009. Neurons in the lateral intraparietal area create a priority map by the combination of disparate signals. Experimental brain research 192(3):479-488.
Jasper HH, Tessier J. 1971. Acetylcholine liberation from cerebral cortex during paradoxical (REM) sleep. Science 172(983):601-602.
Jones CK, Byun N, Bubser M. 2012. Muscarinic and nicotinic acetylcholine receptor agonists and allosteric modulators for the treatment of schizophrenia. Neuropsychopharmacology : official publication of the American College of Neuropsychopharmacology 37(1):16.
Kaas JH, Hackett TA. 2000. Subdivisions of auditory cortex and processing streams in primates. Proceedings of the National Academy of Sciences 97(22):11793-11799.
Kasashima S, Kawashima A, Muroishi Y, Futakuchi H, Nakanishi I, Oda Y. 1999. Neurons with choline acetyltransferase immunoreactivity and mRNA are present in the human cerebral cortex. Histochemistry and cell biology 111(3):197-207.

Katz B. 1969. The release of neural transmitter substances. Liverpool University Press:5-39.
Katz P, Edwards D. 1999. Beyond neurotransmission: Oxford University Press New York.
Kawaja M, Flumerfelt B, Hrycyshyn A. 1990. A comparison of the subnuclear and ultrastructural distribution of acetycholinesterase and choline acetyltransferase in the rat interpeduncular nucleus. Brain research bulletin 24(3):517-523.
Kimura F, Fukuda M, Tsumoto T. 1999. Acetylcholine suppresses the spread of excitation in the visual cortex revealed by optical recording: possible differential effect depending on the source of input. Eur J Neurosci 11(10):3597-3609.
Kinney JP, Spacek J, Bartol TM, Bajaj CL, Harris KM, Sejnowski TJ. 2013. Extracellular sheets and tunnels modulate glutamate diffusion in hippocampal neuropil. Journal of Comparative Neurology 521(2):448-464.
Kitt CA, Mitchell SJ, DeLong MR, Wainer BH, Price DL. 1987. Fiber pathways of basal forebrain cholinergic neurons in monkeys. Brain research 406(1-2):192-206.
Kuczewski N, Aztiria E, Gautam D, Wess J, Domenici L. 2005. Acetylcholine modulates cortical synaptic transmission via different muscarinic receptors, as studied with receptor knockout mice. J Physiol 566(Pt 3):907-919.
Kurosawa M, Sato A, Sato Y. 1989. Well-maintained responses of acetylcholine release and blood flow in the cerebral cortex to focal electrical stimulation of the nucleus basalis of Meynert in aged rats. Neuroscience letters 100(1-3):198-202.
Kus L, Borys E, Ping Chu Y, Ferguson SM, Blakely RD, Emborg ME, Kordower JH, Levey AI, Mufson EJ. 2003. Distribution of high affinity choline transporter immunoreactivity in the primate central nervous system. Journal of Comparative Neurology 463(3):341-357.
Lavine N, Reuben M, Clarke PB. 1997. A population of nicotinic receptors is associated with thalamocortical afferents in the adult rat: laminal and areal analysis. The Journal of comparative neurology 380(2):175-190.
Lawler HC. 1961. Turnover time of acetylcholinesterase. Journal of Biological Chemistry 236(8):2296-2301.
Lehmann J, Struble RG, Antuono PG, Coyle JT, Cork LC, Price DL. 1984. Regional heterogeneity of choline acetyltransferase activity in primate neocortex. Brain research 322(2):361-364.
Lewis DA. 1991. Distribution of choline acetyltransferase-immunoreactive axons in monkey frontal cortex. Neuroscience 40(2):363-374.
Lewis JW, Van Essen DC. 2000a. Corticocortical connections of visual, sensorimotor, and multimodal processing areas in the parietal lobe of the macaque monkey. The Journal of comparative neurology 428(1):112-137.
Lewis JW, Van Essen DC. 2000b. Mapping of architectonic subdivisions in the macaque monkey, with emphasis on parieto-occipital cortex. The Journal of comparative neurology 428(1):79-111.
Lidow MS, Gallager DW, Rakic P, Goldman-Rakic PS. 1989. Regional differences in the distribution of muscarinic cholinergic receptors in the macaque cerebral cortex. Journal of Comparative Neurology 289(2):247-259.
Lippiello P. 2006. Nicotinic cholinergic antagonists: a novel approach for the treatment of autism. Medical hypotheses 66(5):985-990.
Liu Y, Yttri EA, Snyder LH. 2010. Intention and attention: different functional roles for LIPd and LIPv. Nature neuroscience 13(4):495-500.
Lloyd GK, Williams M. 2000. Neuronal nicotinic acetylcholine receptors as novel drug targets. Journal of Pharmacology and Experimental Therapeutics 292(2):461-467.
London ED, Waller SB, Wamsley JK. 1985. Autoradiographic localization of [3H] nicotine binding sites in the rat brain. Neuroscience letters 53(2):179-184.
Lopez-Hidalgo M, Schummers J. 2014. Cortical maps: a role for astrocytes? Current opinion in neurobiology 24:176-189.

Lou HC, Edvinsson L, MacKenzie ET. 1987. The concept of coupling blood flow to brain function: revision required? Annals of Neurology: Official Journal of the American Neurological Association and the Child Neurology Society 22(3):289-297.
Lynch J, Graybiel A, Lobeck L. 1985. The differential projection of two cytoarchitectonic subregions of the inferior parietal lobule of macaque upon the deep layers of the superior colliculus. Journal of Comparative Neurology 235(2):241-254.
MacIntosh F. 1984. Subtypes of muscarinic receptors-A summary with comments. ELSEVIER SCI LTD THE BOULEVARD, LANGFORD LANE, KIDLINGTON, OXFORD, OXON ….
Marder E. 2012. Neuromodulation of neuronal circuits: back to the future. Neuron 76(1):1-11.
Martin LF, Freedman R. 2007. Schizophrenia and the α7 nicotinic acetylcholine receptor. International review of neurobiology 78:225-246.
Mash DC, Flynn DD, Potter LT. 1985. Loss of M2 muscarine receptors in the cerebral cortex in Alzheimer's disease and experimental cholinergic denervation. Science 228(4703):1115-1117.
Mash DC, White WF, Mesulam MM. 1988. Distribution of muscarinic receptor subtypes within architectonic subregions of the primate cerebral cortex. Journal of Comparative Neurology 278(2):265-274.
Maskos U, Molles BE, Pons S, Besson M, Guiard BP, Guilloux JP, Evrard A, Cazala P, Cormier A, Mameli-Engvall M, Dufour N, Cloez-Tayarani I, Bemelmans AP, Mallet J, Gardier AM, David V, Faure P, Granon S, Changeux JP. 2005. Nicotine reinforcement and cognition restored by targeted expression of nicotinic receptors. Nature 436(7047):103-107.
McBain CJ, Traynelis SF, Dingledine R. 1990. Regional variation of extracellular space in the hippocampus. Science 249(4969):674-677.
McGaughy J, Dalley JW, Morrison CH, Everitt BJ, Robbins TW. 2002. Selective behavioral and neurochemical effects of cholinergic lesions produced by intrabasalis infusions of 192 IgG-saporin on attentional performance in a five-choice serial reaction time task. The Journal of neuroscience : the official journal of the Society for Neuroscience 22(5):1905-1913.
McGaughy J, Everitt BJ, Robbins TW, Sarter M. 2000. The role of cortical cholinergic afferent projections in cognition: impact of new selective immunotoxins. Behavioural brain research 115(2):251-263.
McGaughy J, Sarter M. 1998. Sustained attention performance in rats with intracortical infusions of 192 IgG-saporin-induced cortical cholinergic deafferentation: effects of physostigmine and FG 7142. Behav Neurosci 112(6):1519-1525.
Mechawar N, Cozzari C, Descarries L. 2000. Cholinergic innervation in adult rat cerebral cortex: a quantitative immunocytochemical description. Journal of Comparative Neurology 428(2):305-318.
Medalla M, Barbas H. 2006. Diversity of laminar connections linking periarcuate and lateral intraparietal areas depends on cortical structure. European Journal of Neuroscience 23(1):161-179.
Mesulam M-M. 2004a. The cholinergic innervation of the human cerebral cortex. Progress in brain research 145:67-78.
Mesulam M-M, Geula C. 1992. Overlap between acetylcholinesterase-rich and choline acetyltransferase-positive (cholinergic) axons in human cerebral cortex. Brain research 577(1):112-120.
Mesulam M. 2004b. The cholinergic lesion of Alzheimer's disease: pivotal factor or side show? Learning & memory 11(1):43-49.
Mesulam MM, Geula C. 1988. Nucleus basalis (Ch4) and cortical cholinergic innervation in the human brain: observations based on the distribution of acetylcholinesterase and choline acetyltransferase. Journal of Comparative Neurology 275(2):216-240.
Mesulam MM, Hersh LB, Mash DC, Geula C. 1992. Differential cholinergic innervation within functional subdivisions of the human cerebral cortex: a choline acetyltransferase study. The Journal of comparative neurology 318(3):316-328.
Mesulam MM, Mufson EJ. 1984. Neural inputs into the nucleus basalis of the substantia innominata (Ch4) in the rhesus monkey. Brain 107 (Pt 1):253-274.
Mesulam MM, Mufson EJ, Levey AI, Wainer BH. 1983. Cholinergic innervation of cortex by the basal forebrain: cytochemistry and cortical connections of the septal area, diagonal band nuclei, nucleus

basalis (substantia innominata), and hypothalamus in the rhesus monkey. The Journal of comparative neurology 214(2):170-197.
Mesulam MM, Rosen AD, Mufson EJ. 1984. Regional variations in cortical cholinergic innervation: chemoarchitectonics of acetylcholinesterase-containing fibers in the macaque brain. Brain research 311(2):245-258.
Mesulam MM, Volicer L, Marquis JK, Mufson EJ, Green RC. 1986. Systematic regional differences in the cholinergic innervation of the primate cerebral cortex: distribution of enzyme activities and some behavioral implications. Ann Neurol 19(2):144-151.
Mohebi A, Pettibone J, Hamid A, Wong J-M, Kennedy R, Berke J. 2018. Forebrain dopamine value signals arise independently from midbrain dopamine cell firing. BioRxiv:334060.
Mrzljak L, Levey AI, Goldman-Rakic PS. 1993. Association of m1 and m2 muscarinic receptor proteins with asymmetric synapses in the primate cerebral cortex: morphological evidence for cholinergic modulation of excitatory neurotransmission. Proceedings of the National Academy of Sciences of the United States of America 90(11):5194-5198.
Mrzljak L, Pappy M, Leranth C, Goldman-Rakic PS. 1995. Cholinergic synaptic circuitry in the macaque prefrontal cortex. The Journal of comparative neurology 357(4):603-617.
Muller CM, Singer W. 1989. Acetylcholine-induced inhibition in the cat visual cortex is mediated by a GABAergic mechanism. Brain research 487(2):335-342.
Muñoz W, Rudy B. 2014. Spatiotemporal specificity in cholinergic control of neocortical function. Current opinion in neurobiology 26:149-160.
Murphy PC, Sillito AM. 1991. Cholinergic enhancement of direction selectivity in the visual cortex of the cat. Neuroscience 40(1):13-20.
Nicholson C, Syková E. 1998. Extracellular space structure revealed by diffusion analysis. Trends in neurosciences 21(5):207-215.
Okuda T, Haga T. 2003. High-affinity choline transporter. Neurochemical research 28(3-4):483-488.
Pandya DN, Seltzer B. 1980. Cortical connections and the functional organization of posterior parietal cortex. Behavioral and Brain Sciences 3(4):511-513.
Paré M, Wurtz RH. 2001. Progression in neuronal processing for saccadic eye movements from parietal cortex area lip to superior colliculus. Journal of Neurophysiology 85(6):2545-2562.
Parikh V, Man K, Decker MW, Sarter M. 2008. Glutamatergic contributions to nicotinic acetylcholine receptor agonist-evoked cholinergic transients in the prefrontal cortex. Journal of Neuroscience 28(14):3769-3780.
Paxinos G, Huang XF, Toga AW. 2000a. The rhesus monkey brain in stereotaxic coordinates: Academic Press.
Paxinos G, Huang XF, Toga AW. 2000b. The rhesus monkey brain in stereotaxic coordinates/; George Paxinos, Xu-Feng Huang, Arthur Toga.
Pearson RC, Gatter KC, Brodal P, Powell TP. 1983. The projection of the basal nucleus of Meynert upon the neocortex in the monkey. Brain research 259(1):132-136.
Price J, Amaral DG. 1981. An autoradiographic study of the projections of the central nucleus of the monkey amygdala. Journal of Neuroscience 1(11):1242-1259.
Price JL, Stern R. 1983. Individual cells in the nucleus basalis--diagonal band complex have restricted axonal projections to the cerebral cortex in the rat. Brain research 269(2):352-356.
Prusky GT, Shaw C, Cynader MS. 1987. Nicotine receptors are located on lateral geniculate nucleus terminals in cat visual cortex. Brain research 412(1):131-138.
Raghanti M-A, Simic G, Watson S, Stimpson CD, Hof PR, Sherwood CC. 2011. Comparative analysis of the nucleus basalis of Meynert among primates. Neuroscience 184:1-15.
Raghanti MA, Stimpson CD, Marcinkiewicz JL, Erwin JM, Hof PR, Sherwood CC. 2008. Cholinergic innervation of the frontal cortex: differences among humans, chimpanzees, and macaque monkeys. The Journal of comparative neurology 506(3):409-424.
Ridley R, Murray T, Johnson J, Baker H. 1986. Learning impairment following lesion of the basal nucleus of Meynert in the marmoset: modification by cholinergic drugs. Brain research 376(1):108-116.

Roberts MJ, Zinke W, Guo K, Robertson R, McDonald JS, Thiele A. 2005. Acetylcholine dynamically controls spatial integration in marmoset primary visual cortex. J Neurophysiol 93(4):2062-2072.
Rye DB, Wainer BH, Mesulam MM, Mufson EJ, Saper CB. 1984. Cortical projections arising from the basal forebrain: a study of cholinergic and noncholinergic components employing combined retrograde tracing and immunohistochemical localization of choline acetyltransferase. Neuroscience 13(3):627-643.
Saleem KS, Logothetis NK. 2012. A combined MRI and histology atlas of the rhesus monkey brain in stereotaxic coordinates: Academic Press.
Sarter M, Bruno JP. 1997. Cognitive functions of cortical acetylcholine: toward a unifying hypothesis. Brain Res Brain Res Rev 23(1-2):28-46.
Sarter M, Hasselmo ME, Bruno JP, Givens B. 2005. Unraveling the attentional functions of cortical cholinergic inputs: interactions between signal-driven and cognitive modulation of signal detection. Brain Res Brain Res Rev 48(1):98-111.
Sato H, Hata Y, Masui H, Tsumoto T. 1987. A functional role of cholinergic innervation to neurons in the cat visual cortex. J Neurophysiol 58(4):765-780.
Schmahmann JD, Pandya DN. 1990. Anatomical investigation of projections from thalamus to posterior parietal cortex in the rhesus monkey: A WGA-HRP and fluorescent tracer study. Journal of Comparative Neurology 295(2):299-326.
Semba K. 2004. Phylogenetic and ontogenetic aspects of the basal forebrain cholinergic neurons and their innervation of the cerebral cortex. Progress in brain research 145:3-43.
Sharma G, Grybko M, Vijayaraghavan S. 2008. Action potential-independent and nicotinic receptor-mediated concerted release of multiple quanta at hippocampal CA3–mossy fiber synapses. Journal of Neuroscience 28(10):2563-2575.
Sillito AM, Kemp JA. 1983. Cholinergic modulation of the functional organization of the cat visual cortex. Brain research 289(1-2):143-155.
Silver MA, Shenhav A, D'Esposito M. 2008. Cholinergic enhancement reduces spatial spread of visual responses in human early visual cortex. Neuron 60(5):904-914.
Smiley JF, Morrell F, Mesulam MM. 1997. Cholinergic synapses in human cerebral cortex: an ultrastructural study in serial sections. Exp Neurol 144(2):361-368.
Smith M, Booze R. 1995. Cholinergic and GABAergic neurons in the nucleus basalis region of young and aged rats. Neuroscience 67(3):679-688.
Soma S, Shimegi S, Osaki H, Sato H. 2012. Cholinergic modulation of response gain in the primary visual cortex of the macaque. J Neurophysiol 107(1):283-291.
Song P, Mabrouk OS, Hershey ND, Kennedy RT. 2011. *In vivo* neurochemical monitoring using benzoyl chloride derivatization and liquid chromatography–mass spectrometry. Analytical chemistry 84(1):412-419.
Stanton GB, Bruce CJ, Goldberg ME. 1995. Topography of projections to posterior cortical areas from the macaque frontal eye fields. The Journal of comparative neurology 353(2):291-305.
Stephenson AR, Edler MK, Erwin JM, Jacobs B, Hopkins WD, Hof PR, Sherwood CC, Raghanti MA. 2017. Cholinergic innervation of the basal ganglia in humans and other anthropoid primates. Journal of Comparative Neurology 525(2):319-332.
Stepniewska I, Preuss TM, Kaas JH. 1994. Architectonic subdivisions of the motor thalamus of owl monkeys: Nissl, acetylcholinesterase, and cytochrome oxidase patterns. Journal of Comparative Neurology 349(4):536-557.
Svoboda J, Syková E. 1991. Extracellular space volume changes in the rat spinal cord produced by nerve stimulation and peripheral injury. Brain research 560(1-2):216-224.
Syková E, Nicholson C. 2008. Diffusion in brain extracellular space. Physiological reviews 88(4):1277-1340.
Syková E, Vargová L. 2008. Extrasynaptic transmission and the diffusion parameters of the extracellular space. Neurochemistry international 52(1-2):5-13.
Tootell RB, Hadjikhani N, Hall EK, Marrett S, Vanduffel W, Vaughan JT, Dale AM. 1998. The retinotopy of visual spatial attention. Neuron 21(6):1409-1422.

Turchi J, Sarter M. 1997. Cortical acetylcholine and processing capacity: effects of cortical cholinergic deafferentation on crossmodal divided attention in rats. Brain Res Cogn Brain Res 6(2):147-158.
Turchi J, Saunders RC, Mishkin M. 2005. Effects of cholinergic deafferentation of the rhinal cortex on visual recognition memory in monkeys. Proceedings of the National Academy of Sciences 102(6):2158-2161.
Turrini P, Casu MA, Wong TP, De Koninck Y, Ribeiro-da-Silva A, Cuello AC. 2001. Cholinergic nerve terminals establish classical synapses in the rat cerebral cortex: synaptic pattern and age-related atrophy. Neuroscience 105(2):277-285.
Umbriaco D, Watkins KC, Descarries L, Cozzari C, Hartman BK. 1994. Ultrastructural and morphometric features of the acetylcholine innervation in adult rat parietal cortex: an electron microscopic study in serial sections. The Journal of comparative neurology 348(3):351-373.
Van Der Zee E, De Jong G, Strosberg A, Luiten P. 1993. Muscarinic acetylcholine receptor-expression in astrocytes in the cortex of young and aged rats. Glia 8(1):42-50.
Volpicelli LA, Levey AI. 2004. Muscarinic acetylcholine receptor subtypes in cerebral cortex and hippocampus. Progress in brain research 145:59-66.
Waite JJ, Wardlow ML, Power AE. 1999. Deficit in selective and divided attention associated with cholinergic basal forebrain immunotoxic lesion produced by 192-saporin; motoric/sensory deficit associated with Purkinje cell immunotoxic lesion produced by OX7-saporin. Neurobiology of learning and memory 71(3):325-352.
Ward NJ, Zinke W, Coppola JJ, Disney AA. 2018. Variations in neuromodulatory chemical signatures define compartments in macaque cortex. bioRxiv:272849.
Wenk GL, Stoehr JD, Quintana G, Mobley S, Wiley RG. 1994. Behavioral, biochemical, histological, and electrophysiological effects of 192 IgG-saporin injections into the basal forebrain of rats. Journal of Neuroscience 14(10):5986-5995.
White P, Goodhardt M, Keet J, Hiley C, Carrasco L, Williams I, Bowen DM. 1977. Neocortical cholinergic neurons in elderly people. The Lancet 309(8013):668-671.
Whitehouse PJ, Martino AM, Antuono PG, Lowenstein PR, Coyle JT, Price DL, Kellar KJ. 1986. Nicotinic acetylcholine binding sites in Alzheimer's disease. Brain research 371(1):146-151.
Wiley RG, Oeltmann TN, Lappi DA. 1991. Immunolesioning: selective destruction of neurons using immunotoxin to rat NGF receptor. Brain research 562(1):149-153.
Wong J-MT, Malec PA, Mabrouk OS, Ro J, Dus M, Kennedy RT. 2016. Benzoyl chloride derivatization with liquid chromatography–mass spectrometry for targeted metabolomics of neurochemicals in biological samples. Journal of Chromatography A 1446:78-90.
Wonnacott S. 1997. Presynaptic nicotinic ACh receptors. Trends in neurosciences 20(2):92-98.
Wouterlood FG, Jorritsma-Byham B. 1993. The anterograde neuroanatomical tracer biotinylated dextran-amine: comparison with the tracer Phaseolus vulgaris-leucoagglutinin in preparations for electron microscopy. J Neurosci Methods 48(1-2):75-87.
Zhang X, Rauch A, Lee H, Xiao H, Rainer G, Logothetis NK. 2007. Capillary hydrophilic interaction chromatography/mass spectrometry for simultaneous determination of multiple neurotransmitters in primate cerebral cortex. Rapid Commun Mass Spectrom 21(22):3621-3628.
Zilles K, Palomero-Gallagher N, Schleicher A. 2004. Transmitter receptors and functional anatomy of the cerebral cortex. Journal of anatomy 205(6):417-432.
Zilles K, Schlaug G, Matelli M, Luppino G, Schleicher A, Qü M, Dabringhaus A, Seitz R, Roland P. 1995. Mapping of human and macaque sensorimotor areas by integrating architectonic, transmitter receptor, MRI and PET data. Journal of Anatomy 187(Pt 3):515.
Zinke W, Roberts MJ, Guo K, McDonald JS, Robertson R, Thiele A. 2006. Cholinergic modulation of response properties and orientation tuning of neurons in primary visual cortex of anaesthetized Marmoset monkeys. Eur J Neurosci 24(1):314-328.

Appendices

Appendix A: Animal information

Animal	Species	Sex	Hemisphere	Fixative	Experiment
1	*Macaca mulatta*	Male	Right	4% paraformaldehyde	Chapter 3
2	*Macaca mulatta*	Male	Right	4% paraformaldehyde + 0.15% glutaraldehyde	Chapter 2 Chapter 3
3	*Macaca mulatta*	Female	Left	4% paraformaldehyde	Chapter 3
4	*Macaca mulatta*	Male	Right	4% paraformaldehyde + 0.15% glutaraldehyde	Chapter 2 Chapter 3
5	*Macaca mulatta*	Male	Left (anatomy) Right (microdialysis)	4% paraformaldehyde + 0.15% glutaraldehyde	Chapter 2 Chapter 3 Chapter 4

Appendix B: Antibody information

Antibody name	Immunogen	Manufacturer details	Dilution	Experiment
Primary antibodies				
Anti-GABA	Serum-free ascitic fluids	Swant Mouse monoclonal Catalog# 3A12 Lot# ps2 RRID:AB_2721208	1:5000	Chapter 2
Anti-m1 Acetylcholine Receptor	GST fusion protein and part of i3 intercellular loop of human m1 muscarinic acetylcholine receptor (amino acids 227-353) (Accession P11229)	Millipore Rabbit polyclonal Catalog# AB5164 Lot# JC1682904 RRID:AB_2260554	1:1000	Chapter 2
Anti-Choline Acetyltransferase	Human placental enzyme	Millipore Goat polyclonal Catalog # AB144P Lot# 3029486 RRID:AB_2079751	1:500	Chapter 3
Secondary antibodies				
Alexa Fluor 647 AffiniPure F(ab')$_2$ Fragments Donkey Anti-Mouse IgG (H+L)	Mouse IgG	Jackson ImmunoResearch Laboratories Polyclonal Cat # 715-606-150 Lot# 140554 RRID:AB_2340865	1:16,000	Chapter 2
DyLight 405 AffiniPure Donkey Anti-Rabbit IgG (H+L)	Rabbit IgG	Jackson ImmunoResearch Laboratories Polyclonal Cat # 711-475-152 Lot# 142329 RRID:AB_2340616	1:16,000	Chapter 2
Biotin-SP (long spacer) AffiniPure F(ab')$_2$ Fragment Donkey Anti-Goat IgG (H+L)	Goat IgG	Jackson ImmunoResearch Laboratories Polyclonal Cat # 705-066-147 Lot# 136390 RRID:AB_2340398	1:800	Chapter 3